OOFEM.ORG

Material Model Library Manual

Bořek Patzák

Czech Technical University
Faculty of Civil Engineering
Department of Structural Mechanics
Thákurova 7, 166 29 Prague, Czech Republic

March 19, 2019

Contents

List of Tables

1 Material Models for Structural Analysis

1.1 Elastic materials

1.1.1 Isotropic linear elastic material - IsoLE

Linear isotropic material model. The model parameters are summarized in Tab. 1.

Description	Linear isotropic elastic material
Record Format	**IsoLE** num$_{\text{(in)}}$ # d$_{\text{(rn)}}$ # E$_{\text{(rn)}}$ # n$_{\text{(rn)}}$ # tAlpha$_{\text{(rn)}}$ #
Parameters	- *num* material model number - *d* material density - *E* Young modulus - *n* Poisson ratio - *tAlpha* thermal dilatation coefficient
Supported modes	3dMat, PlaneStress, PlaneStrain, 1dMat, 2dPlateLayer, 2dBeamLayer, 3dShellLayer, 2dPlate, 2dBeam, 3dShell, 3dBeam, PlaneStressRot
Features	Adaptivity support

Table 1: Linear Isotropic Material - summary.

1.1.2 Orthotropic linear elastic material - OrthoLE

Orthotropic, linear elastic material model. The model parameters are summarized in Tab. 2. Local coordinate system, which determines axes of material orthotrophy can by specified using *lcs* array. This array contains six numbers, where the first three numbers represent directional vector of a local x-axis, and next three numbers represent directional vector of a local y-axis. The local z-axis is determined using the vector product. The right-hand coordinate system is assumed.

Local coordinate system can also be specified using *scs* parameter. Then local coordinate system is specified in so called "shell" coordinate system, which is defined locally on each particular element and its definition is as follows: principal z-axis is perpendicular to shell mid-section, x-axis is perpendicular to z-axis and normal to user specified vector (so x-axis is parallel to plane, with being normal to this plane) and y-axis is perpendicular both to x and z axes. This definition of coordinate system can be used only with plates and shells elements. When vector is parallel to z-axis an error occurs. The *scs* array contain three numbers defining direction vector . If no local coordinate system is specified, by default a global coordinate system is used.

For 3D case the material compliance matrix has the following form

$$\boldsymbol{C} = \begin{bmatrix} 1/E_X & -\nu_{xy}/E_x & -\nu_{xz}/E_x & 0 & 0 & 0 \\ -\nu_{yx}/E_y & 1/E_y & -\nu_{yz}/E_y & 0 & 0 & 0 \\ -\nu_{zx}/E_z & -\nu_{zy}/E_z & 1/E_z & 0 & 0 & 0 \\ 0 & 0 & 0 & 1/G_{yz} & 0 & 0 \\ 0 & 0 & 0 & 0 & 1/G_{xz} & 0 \\ 0 & 0 & 0 & 0 & 0 & 1/G_{xy} \end{bmatrix} \tag{1}$$

By inversion, the material stiffness matrix has the form

$$
\boldsymbol{D} = \begin{bmatrix} d_{xx} & d_{xy} & d_{xz} & 0 & 0 & 0 \\ & d_{yy} & d_{yz} & 0 & 0 & 0 \\ \text{sym} & & d_{zz} & 0 & 0 & 0 \\ 0 & 0 & 0 & G_{yz} & 0 & 0 \\ 0 & 0 & 0 & 0 & G_{xz} & 0 \\ 0 & 0 & 0 & 0 & 0 & G_{xy} \end{bmatrix} \tag{2}
$$

where $\xi = 1 - (\nu_{xy} * \nu_{yx} + \nu_{yz} * \nu_{zy} + \nu_{zx} * \nu_{xz}) - (\nu_{xy} * \nu_{yz} * \nu_{zx} + \nu_{yx} * \nu_{zy} * \nu_{xz})$ and

$$
\begin{aligned}
d_{xx} &= E_X(1 - \nu_{yz} * \nu_{zy})/\xi, && (3)\\
d_{xy} &= E_y * (\nu_{xy} + \nu_{xz} * \nu_{zy})/\xi, && (4)\\
d_{xz} &= E_z * (\nu_{xz} + \nu_{yz} * \nu_{xy})/\xi, && (5)\\
d_{yy} &= E_y * (1 - \nu_{xz} * \nu_{zx})/\xi, && (6)\\
d_{yz} &= E_z * (\nu_{yz} + \nu_{yx} * \nu_{xz})/\xi, && (7)\\
d_{zz} &= E_z * (1 - \nu_{yx} * \nu_{xy})/\xi. && (8)
\end{aligned}
$$

E_i is Young's modulus in the i-th direction, G_{ij} is the shear modulus in ij plane, ν_{ij} is the major Poisson ratio, and ν_{ji} is the minor Poisson ratio. Assuming that $E_x > E_y > E_z$, $\nu_{xy} > \nu_{yx}$ etc., then ν_{xy} is referred to as the major Poisson ratio, while ν_{yx} is referred as the minor Poisson ratio. Note that there are only nine independent material parameters, because of symmetry conditions. The symmetry condition yields

$$
\nu_{xy}E_y = \nu_{yx}E_x, \quad \nu_{yz}E_z = \nu_{zy}E_y, \quad \nu_{zx}E_x = \nu_{xz}E_z
$$

The model description and parameters are summarized in Tab. 2.

1.1.3 General anisotropic linear elastic material - AnisoLE

Linear elastic material model with completely general material stiffness (21 independent elastic constants). The model parameters are summarized in Tab. 3. The material stiffness matrix is a completely arbitrary symmetric 6×6 matrix. The input line must contain an array with the upper triangle of this matrix. This array has length 21 and the stiffness coefficients are listed in each row from the diagonal to the last column.

1.1.4 Hyperelastic material - HyperMat

This material model can describe elastic behavior at large strains. A hyperelastic model postulates the existence of free energy potential. Existence of the potential implies reversibility of deformations and no energy dissipation during loading process. Here we use the free energy function introduced in [20]

$$
\rho_0\psi = \frac{1}{4}\left(K - \frac{2}{3}G\right)\left(J^2 - 2\mathrm{lnJ} - 1\right) + G\left(\boldsymbol{E} : \boldsymbol{I} - \mathrm{lnJ}\right) \tag{9}
$$

where K is the bulk modulus, G is the shear modulus, J is the Jacobian (determinant of the deformation gradient, corresponding to the ratio of the current

Description	Orthotropic, linear elastic material
Record Format	**OrthoLE** num(in) # d(rn) # Ex(rn) # Ey(rn) # Ez(rn) # NYyz(rn) # NYxz(rn) # NYxy(rn) # Gyz(rn) # Gxz(rn) # Gxy(rn) # tAlphax(rn) # tAlphay(rn) # tAlphaz(rn) # [lcs(ra) #] [scs(ra) #]
Parameters	- *num* material model number - *d* material density - *Ex*, *Ey*, *Ez* Young moduli for x,y, and z directions - *NYyz*, *NYxz*, *NYxy* major Poisson's ratio coefficients - *Gyz*, *Gxz*, *Gxy* shear moduli - *tAlphax*, *tAlphay*, *tAlphaz* thermal dilatation coefficients in x,y,z directions - *lcs* Array defining local material x and y axes of orthotrophy - *scs* Array defining a normal vector n. The local x axis is parallel to plane with n being plane normal. The material local z-axis is perpendicular to shell mid-section.
Supported modes	3dMat, PlaneStress, PlaneStrain, 1dMat, 2dPlateLayer, 2dBeamLayer, 3dShellLayer, 2dPlate, 2dBeam, 3dShell, 3dBeam, PlaneStressRot

Table 2: Orthotropic, linear elastic material – summary.

Description	Anisotropic, linear elastic material
Record Format	**OrthoLE** num(in) # d(rn) # stiff(ra) # tAlphax(ra) #
Parameters	- *num* material model number - *d* material density - *stiff* real array of length 21 with stiffness coefficients D_{11}, D_{12}, $D_{13} \ldots D_{66}$ - *tAlpha* real array of length 0 or 3 with thermal dilatation coefficients in x,y,z directions
Supported modes	3dMat, PlaneStress, PlaneStrain, 1dMat

Table 3: Anisotropic, linear elastic material – summary.

and initial volume) and $\boldsymbol{E}$ is the Green-Lagrange strain. Then stress-strain law can be derived from (9) as

$$\boldsymbol{S} = \rho_0 \frac{\partial \psi}{\partial \boldsymbol{E}} = \frac{1}{2}\left(K - \frac{2}{3}G\right)\left(J^2 - 1\right)\boldsymbol{C}^{-1} + G\left(\boldsymbol{I} - \boldsymbol{C}^{-1}\right) \tag{10}$$

where $\boldsymbol{S}$ is the second Piola-Kirchhoff stress, $\boldsymbol{E}$ is the Green-Lagrange strain and $\boldsymbol{C}$ is the right Cauchy-Green tensor. The model description and parameters are summarized in Tab. 4.

1.1.5 Hyperelastic material - Compressible Mooney-Rivlin

The Mooney-Rivlin strain energy function is expressed by

$$\rho_0 \psi = C_1(\bar{I}_1 - 3) + C_2(\bar{I}_2 - 3) + \frac{1}{2}K(\ln J)^2 \tag{11}$$

Description	Hyperelastic material
Record Format	**HyperMat** (in) # d(rn) # K(rn) # G(rn) #
Parameters	- material number
	- d material density
	- K bulk modulus
	- G shear modulus
Supported modes	3dMat

Table 4: Hyperelastic material - summary.

where C_1 and C_2 are material constants, K is the bulk modulus, J is the Jacobian (determinant of the deformation gradient, corresponding to the ratio of the current and initial volume), $\bar{I}_1 = J^{-\frac{2}{3}} I_1$, $\bar{I}_2 = J^{-\frac{2}{3}} I_2$, where I_1 and I_2 are the first and the second principal invariants of the right Cauchy-Green deformation tensor $\boldsymbol{C}$. Compressible neo-Hookean material model is obtained by setting $C_2 = 0$. Then stress-strain law can be derived from (11) as

$$\boldsymbol{P} = \rho_0 \frac{\partial \psi}{\partial \boldsymbol{F}} = C_1 \frac{\partial \bar{I}_1}{\partial \boldsymbol{F}} + C_2 \frac{\partial \bar{I}_2}{\partial \boldsymbol{F}} + K \ln J \boldsymbol{F}^{-T} \tag{12}$$

where $\boldsymbol{P}$ is the first Piola-Kirchhoff stress,

$$\frac{\partial \bar{I}_1}{\partial \boldsymbol{F}} = \frac{2}{J^{\frac{2}{3}}} \boldsymbol{F} - \frac{2}{3} \bar{I}_1 \boldsymbol{F}^{-T} \tag{13}$$

and

$$\frac{\partial \bar{I}_2}{\partial \boldsymbol{F}} = 2 \bar{I}_1 \boldsymbol{F} - \frac{4}{3} \bar{I}_2 \boldsymbol{F}^{-T} - \frac{2}{J^{\frac{4}{3}}} \boldsymbol{F} \cdot \boldsymbol{C} \tag{14}$$

The first elasticity tensor is derived as

$$A_{ijkl} = \frac{\partial P_{ij}}{\partial F_{kl}} = C_1 A^1_{ijkl} + C_2 A^2_{ijkl} + K (F^{-1}_{ji} F^{-1}_{lk} - \ln J F^{-1}_{jk} F^{-1}_{li}) \tag{15}$$

where

$$A^1_{ijkl} = \frac{2}{3} J^{-\frac{2}{3}} \left[3\delta_{ik}\delta_{jl} + I_1 F^{-1}_{jk} F^{-1}_{li} - 2F^{-1}_{lk} F_{ij} + \frac{2}{3} I_1 F^{-1}_{ji} F^{-1}_{lk} - 2F^{-1}_{ji} F_{kl} \right] \tag{16}$$

and

$$A^2_{ijkl} = 2J^{-\frac{4}{3}} \left[I_1 \delta_{ik}\delta_{jl} + 2F_{ij}F_{kl} - \frac{4}{3} I_1 F_{ij} F^{-1}_{lk} - \frac{8}{9} I_2 F^{-1}_{ji} F^{-1}_{lk} - \frac{4}{3} I_1 F^{-1}_{ji} F_{kl} \right.$$
$$\left. + \frac{4}{3} F_{kn} C_{nl} F^{-1}_{ji} + \frac{2}{3} I_2 F^{-1}_{li} F^{-1}_{jk} + \frac{4}{3} F^{-1}_{kl} F_{im} C_{mj} - \delta_{ik} C_{lj} - F_{il} F_{kj} + F_{km} F_{im} \delta_{jl} \right] \tag{17}$$

The model description and parameters are summarized in Tab. 5.

1.2 Winkler-Pasternak model

Implementation of 2D winkler-pasternak model for plate (and potentially beam) subsoil model.

Description	Mooney-Rivlin
Record Format	**MooneyRivlin** (in) # d(rn) # K(rn) # C1(rn) # C2(rn) #
Parameters	- material number - *d* material density - *K* bulk modulus - *C1* material constant - *C2* material constant
Supported modes	3dMat, PlaneStrain

Table 5: Compressible Mooney-Rivlin - summary.

Description	Winkler Pasternak isotropic material for subsoil interaction
Record Format	**winklerpasternak** (in) # d(rn) # c1(rn) # c2(rn) #
Parameters	- material number - *d* material density - *c1* C1 Winkler parameter (foundation modulus) - *c2* C2 shear interaction modulus
Supported modes	2dPlateSubSoil

Table 6: Winkler Pasternak material - summary.

1.3 Large-strain master material

In this section, a large-strain master model based on generalized stress-strain measures is described. In the first step, strain measure is computed from equation (18).

$$\boldsymbol{E}^{(m)} = \begin{cases} \dfrac{1}{2m}\left(\boldsymbol{C}^m - \boldsymbol{I}\right), & \text{if } m \neq 0 \\[2ex] \dfrac{1}{2}\ln \boldsymbol{C}, & \text{if } m = 0 \end{cases} \tag{18}$$

where $\boldsymbol{I}$ is the second-order unit tensor and $\boldsymbol{C} = \boldsymbol{F}^T\boldsymbol{F}$ is Cauchy-Green strain tensor. In the special cases when $m = 0$ and $m = 0.5$ we obtain the so-called Hencky (logarithmic) and Biot tensor, while for $m = 1$ we obtain the right Green-Lagrange strain tensor. In the second step, this strain measure enters a constitutive law of slave material and the stress measure conjugated to the strain measure defined in step one and appropriate stiffness matrix are computed. In the third step, the generalized stress tensor and stiffness matrix are transformed into the second Piola-Kirchhoff stress and the appropriate stiffness tensor. The model description and parameters are summarized in Tab. 7.

1.4 Plasticity-based material models

1.4.1 Drucker-Prager model - DruckerPrager

The Drucker-Prager plasticity model[1] is an isotropic elasto-plastic model based on a yield function

$$f\left(\boldsymbol{\sigma}, \tau_{\mathrm{Y}}\right) = F\left(\boldsymbol{\sigma}\right) - \tau_{\mathrm{Y}} \tag{19}$$

[1]Contributed by Simon Rolshoven, LSC, FENAC, EPFL.

Description	Large-strain master material material
Record Format	**LSmasterMat** $_{\text{(in)}}$ # m$_{\text{(rn)}}$ # slavemat$_{\text{(in)}}$ #
Parameters	- material number
	- m parameter defining the strain measure
	- *slavemat* number of slave material
Supported modes	3dMatF

Table 7: Large-strain master material material - summary.

with the pressure-dependent equivalent stress

$$F(\boldsymbol{\sigma}) = \alpha I_1 + \sqrt{J_2} \tag{20}$$

As usual, $\boldsymbol{\sigma}$ is the stress tensor, $\tau_{\rm Y}$ is the yield stress under pure shear, and I_1 and J_2 are the first invariant and second deviatoric invariant of the stress tensor. The friction coefficient α is a positive parameter that controls the influence of the pressure on the yield limit, important for cohesive-frictional materials such as concrete, soils or other geomaterials. Regarding Mohr-Coulomb plasticity, relation to cohesion, c, and the angle of friction, θ, exists for the Drucker-Prager model

$$\alpha = \frac{2\sin\theta}{(3-\sin\theta)\sqrt{3}} \tag{21}$$

$$\tau_{\rm Y} = \frac{6c\cos\theta}{(3-\sin\theta)\sqrt{3}} \tag{22}$$

The flow rule is derived from the plastic potential

$$g(\boldsymbol{\sigma}) = \alpha_\psi I_1 + \sqrt{J_2} \tag{23}$$

where α_ψ is the dilatancy coefficient. An associated model with $\alpha_\psi = \alpha$ would overestimate the dilatancy of concrete, so the dilatancy coefficient is usually chosen smaller than the friction coefficient. The model is described by the equations

$$\boldsymbol{\sigma} = \boldsymbol{D} : (\boldsymbol{\varepsilon} - \boldsymbol{\varepsilon}_{\rm p}) \tag{24}$$

$$\tau_{\rm Y} = h(\kappa) \tag{25}$$

$$\dot{\boldsymbol{\varepsilon}}_{\rm p} = \dot{\lambda}\frac{\partial g}{\partial \boldsymbol{\sigma}} = \dot{\lambda}\left(\alpha_\psi \boldsymbol{\delta} + \frac{\boldsymbol{s}}{2\sqrt{J_2}}\right) \tag{26}$$

$$\dot{\kappa} = \sqrt{\frac{2}{3}}\,\|\dot{\boldsymbol{\varepsilon}}_{\rm p}\| \tag{27}$$

$$\dot{\lambda} \geq 0, \quad f(\boldsymbol{\sigma}, \tau_{\rm Y}) \leq 0, \quad \dot{\lambda}\, f(\boldsymbol{\sigma}, \tau_{\rm Y}) = 0 \tag{28}$$

which represent the linear elastic law, hardening law, evolution laws for plastic strain and hardening variable, and the loading-unloading conditions. In the above, $\boldsymbol{D}$ is the elastic stiffness tensor, $\boldsymbol{\varepsilon}$ is the strain tensor, $\boldsymbol{\varepsilon}_{\rm p}$ is the plastic strain tensor, λ is the plastic multiplier, $\boldsymbol{\delta}$ is the unit second-order tensor, $\boldsymbol{s}$ is the deviatoric stress tensor, κ is the hardening variable, and a superior dot marks the derivative with respect to time. The flow rule has the form given in Eq. (26) at all points of the conical yield surface with the exception of its vertex, located on the hydrostatic axis.

For the present model, the evolution of the hardening variable can be explicitly linked to the plastic multiplier. Substituting the flow rule (26) into Eq. (27) and computing the norm leads to

$$\dot{\kappa} = k\dot{\lambda} \tag{29}$$

with a constant parameter $k = \sqrt{1/3 + 2\alpha_\psi^2}$, so the hardening variable is proportional to the plastic multiplier. For $\alpha = \alpha_\psi = 0$, the associated J_2-plasticity model is recovered as a special case.

In the simplest case of linear hardening, the hardening function is a linear function of κ, given by

$$h(\kappa) = \tau_0 + HE\kappa \tag{30}$$

where τ_0 is the initial yield stress, and H is the hardening modulus normalized with the elastic modulus. Alternatively, an exponential hardening function

$$h(\kappa) = \tau_{\text{limit}} + (\tau_0 - \tau_{\text{limit}})\,\mathrm{e}^{-\kappa/\kappa_{\mathrm{c}}} \tag{31}$$

can be used for a more realistic description of hardening.

The stress-return algorithm is based on the Newton-iteration. In plasticity, this is commonly called Closest-Point-Projection (CPP), and it generally leads to quadratic convergence. The implemented algorithm is convergent in any stress case, but in the vicinity of the vertex region, quadratic convergence might be lost because of insufficient regularity of the yield function.

The algorithmic tangent stiffness matrix is implemented for both the regular case and the vertex region. Generally, the error decreases quadratically (of course only asymptotically). Again, in the vicinity of the vertex region, quadratic convergence might be lost due to insufficient regularity. Furthermore, the tangent stiffness matrix does not always exist for the vertex case. In these cases, the elastic stiffness is used instead. It is generally safer (but slower) to use the elastic stiffness if you encounter any convergence problems, especially if your problem is tension-dominated.

1.4.2 Drucker-Prager model with tension cut-off and isotropic damage - DruckerPragerCut

The Drucker-Prager plasticity model with tension cut-off is a multisurface model, appropriate for cohesive-frictional materials such as concrete loaded both in compression and tension. The plasticity model is formulated for isotropic hardening and enhanced by isotropic damage, which is driven by the cumulative plastic strain. The model can be used only in the small-strain context, with additive split of the strain tensor into the elastic and plastic parts.

The basic equations include the additive decomposition of strain into elastic and plastic parts,

$$\boldsymbol{\varepsilon} = \boldsymbol{\varepsilon}_{\mathrm{e}} + \boldsymbol{\varepsilon}_{\mathrm{p}}, \tag{32}$$

the stress strain law

$$\boldsymbol{\sigma} = (1-\omega)\bar{\boldsymbol{\sigma}} = (1-\omega)\boldsymbol{D} : (\boldsymbol{\varepsilon} - \boldsymbol{\varepsilon}_{\mathrm{p}}), \tag{33}$$

Description	DP material
Record Format	**DruckerPrager** num$_{(in)}$ # d$_{(rn)}$ # tAlpha$_{(rn)}$ # E$_{(rn)}$ # n$_{(rn)}$ # alpha$_{(rn)}$ # alphaPsi$_{(rn)}$ # ht$_{(in)}$ # iys$_{(rn)}$ # lys$_{(rn)}$ # hm$_{(rn)}$ # kc$_{(rn)}$ # [yieldtol$_{(rn)}$ #]
Parameters	- *num* material model number - *d* material density - *tAlpha* thermal dilatation coefficient - *E* Young modulus - *n* Poisson ratio - *alpha* friction coefficient - *alphaPsi* dilatancy coefficient - *ht* hardening type, 1: linear hardening, 2: exponential hardening - *iys* initial yield stress in shear, τ_0 - *lys* limit yield stress for exponential hardening, τ_{limit} - *hm* hardening modulus normalized with E-modulus (!) - *kc* κ_c for the exponential softening law - *yieldtol* tolerance of the error in the yield criterion, default value 1.e-14 - *newtonIter* maximum number of iterations in λ search, default value 30
Supported modes	3dMat, PlaneStrain, 3dRotContinuum

Table 8: DP material - summary.

the definition of the yield function in terms of the effective stress,

$$f(\bar{\boldsymbol{\sigma}}, \kappa) = \alpha I_1 + \sqrt{J_2} - \tau_Y, \tag{34}$$

the flow rule

$$g(\bar{\boldsymbol{\sigma}}) = \alpha_\psi I_1 + \sqrt{J_2}, \tag{35}$$

the linear hardening law

$$\tau_Y(\kappa) = \tau_0 + H\kappa, \tag{36}$$

where τ_0 represents the initial yield stress under pure shear, the damage law

$$\omega(\kappa) = \omega_c(1 - \mathrm{e}^{-a\kappa}), \tag{37}$$

where ω_c is critical damage and a is a positive dimensionless parameter. More detailed descriptioin of some parameters is in Section 1.4.1.

The dilatancy coefficient α_ψ controls flow associativeness; if $\alpha_\psi = \alpha$, an associate model is recovered, which overestimates the dilatancy of concrete. Hence, the dilatancy coefficient is usually chosen smaller, $\alpha_\psi \leq \alpha$, and the non-associated model is formulated.

Description	Drucker Prager material with tension cut-off
Record Format	**DruckerPragerCut** num(in) # d(rn) # tAlpha(rn) # E(rn) # n(rn) # tau0(rn) # alpha(rn) # [alphaPsi(rn) #] [H(rn) #] [omega_crit(rn) #] [a(rn) #] [yieldtol(rn) #] [NewtonIter(in) #]
Parameters	- *num* material model number - *d* material density - *tAlpha* thermal dilatation coefficient - *E* Young modulus - *n* Poisson ratio - *tau0* initial yield stress in shear τ_0 - *alpha* friction coefficient - *alphaPsi* dilatancy coefficient, equals to *alpha* by default - *H* hardening modulus (can be negative in the case of plastic softening), 0 by default - *omega_crit* critical damage in damage law (37), 0 by default - *a* exponent in damage law (37), 0 by default - *yieldtol* tolerance of the error in the yield criterion, default value 1.e-14 - *newtonIter* maximum number of iterations in λ search, default value 30
Supported modes	1dMat, 3dMat, PlaneStrain

Table 9: Drucker Prager material with tension cut-off - summary.

1.4.3 Mises plasticity model with isotropic damage - MisesMat

This model is appropriate for the description of plastic yielding in ductile material such as metals, and it can also cover the effects of void growth. The model uses the Mises yield condition (in terms of the second deviatoric invariant, J_2), associated flow rule, linear isotropic hardening driven by the cumulative plastic strain, and isotropic damage, also driven by the cumulative plastic strain. The model can be used in the small-strain context, with additive split of the strain tensor into the elastic and plastic parts, or in the large-strain context, with multiplicative split of the deformation gradient and with yield condition formulated in terms of Kirchhoff stress (which is the true Cauchy stress multiplied by the Jacobian).

Small-strain formulation: The small-strain version of hardening Mises plasticity can be combined with isotropic damage. The basic equations include the additive decomposition of strain into elastic and plastic parts,

$$\boldsymbol{\varepsilon} = \boldsymbol{\varepsilon}_{\mathrm{e}} + \boldsymbol{\varepsilon}_{\mathrm{p}}, \tag{38}$$

the stress strain law

$$\boldsymbol{\sigma} = (1-\omega)\bar{\boldsymbol{\sigma}} = (1-\omega)\boldsymbol{D} : (\boldsymbol{\varepsilon} - \boldsymbol{\varepsilon}_{\mathrm{p}}), \tag{39}$$

the definition of the yield function in terms of the effective stress,

$$f(\bar{\boldsymbol{s}}, \kappa) = \sqrt{\frac{3}{2}\bar{\boldsymbol{s}} : \bar{\boldsymbol{s}}} - \sigma_Y(\kappa) = \sqrt{3J_2(\bar{\boldsymbol{\sigma}})} - \sigma_Y(\kappa), \tag{40}$$

the incremental definition of cumulative plastic strain

$$\dot{\kappa} = \|\dot{\boldsymbol{\varepsilon}}_{\mathrm{p}}\|, \tag{41}$$

the linear hardening law

$$\sigma_Y(\kappa) = \sigma_0 + H\kappa, \tag{42}$$

the evolution law for the plastic strain

$$\dot{\boldsymbol{\varepsilon}}_{\mathrm{p}} = \dot{\lambda}\frac{\partial f}{\partial \bar{\boldsymbol{s}}}, \tag{43}$$

the loading-unloading conditions

$$\dot{\lambda} > 0 \qquad f(\bar{\boldsymbol{s}}, \kappa) \leq 0 \qquad \dot{\lambda} f(\bar{\boldsymbol{s}}, \kappa) = 0. \tag{44}$$

and the damage law

$$\omega(\kappa) = \omega_c(1 - \mathrm{e}^{-a\kappa}), \tag{45}$$

In the equations above, $\boldsymbol{\varepsilon}$ is the strain tensor, $\boldsymbol{\varepsilon}_{\mathrm{e}}$ is the elastic strain tensor, $\boldsymbol{\varepsilon}_p$ is the plastic strain tensor, $\boldsymbol{D}$ is the elastic stiffness tensor, $\boldsymbol{\sigma}$ is the nominal stress tensor, $\bar{\boldsymbol{\sigma}}$ is the effective stress tensor, $\bar{\boldsymbol{s}}$ is the effective deviatoric stress tensor, σ_Y is the magnitude of stress at yielding under uniaxial tension (or compression), κ is the cumulated plastic strain, H is the hardening modulus, λ is the plastic multiplier, ω is the damage variable, ω_c is critical damage and a is a positive dimensionless parameter.

Large-strain formulation is based on the introduction of an intermediate local configuration, with respect to which the elastic response is characterized. This concept leads to a multiplicative decomposition of deformation gradient into elastic and plastic parts:

$$\boldsymbol{F} = \boldsymbol{F}^e \boldsymbol{F}^p. \tag{46}$$

The stress-evaluation algorithm can be based on the classical radial return mapping; see [20] for more details. Damage is not yet implemented in the large-strain version of the model.

The model description and parameters are summarized in Tab. 10.

Description	Mises plasticity model with isotropic hardening
Record Format	**MisesMat** (in) # d(rn) # E(rn) # n(rn) # sig0(rn) # H(rn) # omega_crit(rn) #a(rn) #
Parameters	- material number - *d* material density - *E* Young's modulus - *n* Poisson's ratio - *sig0* initial yield stress in uniaxial tension (compression) - *H* hardening modulus (can be negative in the case of plastic softening) - *omega_crit* critical damage in damage law (45) - *a* exponent in damage law (45)
Supported modes	1dMat, PlaneStrain, 3dMat, 3dMatF

Table 10: Mises plasticity – summary.

VTKxml output can report Mises stress, which equals to $\sqrt{3J_2}$. When no hardening/softening exists, Mises stress reaches values up to given uniaxial yield stress *sig0*.

1.4.4 Mises plasticity model with isotropic damage, nonlocal - MisesMatNl, MisesMatGrad

The small-strain version of the model is regularized by the over-nonlocal formulation with damage driven by a combination of local and nonlocal cumulated plastic strain,

$$\hat{\kappa} = (1-m)\kappa + m\bar{\kappa}, \tag{47}$$

where m is a dimensionless material parameter (typically $m > 1$) and $\bar{\kappa}$ is the nonlocal cumulated plastic strain, which is evaluated either using the integral approach, or using the implicit gradient approach.

Integral nonlocal formulation One possible regularization technique is based on the integral definition of nonlocal cumulated plastic strain

$$\bar{\kappa}(x) = \int_V \alpha(x,s)\kappa(s)\,\mathrm{d}s \tag{48}$$

The nonlocal weight function is usually defined as

$$\alpha(x,s) = \frac{\alpha_0(\|x-s\|)}{\int\limits_V \alpha_0(\|x-t\|)\,\mathrm{d}t} \tag{49}$$

where

$$\alpha_0(r) = \begin{cases} \left(1 - \frac{r^2}{R^2}\right)^2 & \text{if } r < R \\ \\ 0 & \text{if } r \geq R \end{cases} \tag{50}$$

is a nonnegative function, for $r < R$ monotonically decreasing with increasing distance $r = \|x - s\|$, and V denotes the domain occupied by the investigated material body. The key idea is that the damage evolution at a certain point depends not only on the cumulated plastic strain at that point, but also on points at distances smaller than the interaction radius R, considered as a new material parameter.

Implicit gradient formulation The gradient formulation can be conceived as the differential counterpart to the integral formulation. The nonlocal cumulated plastic strain is computed from a Helmholtz-type differential equation

$$\bar{\kappa} - l^2\nabla^2\bar{\kappa} = \kappa \tag{51}$$

with homogeneous Neumann boundary condition

$$\frac{\partial\bar{\kappa}}{\partial n} = 0. \tag{52}$$

In (51), l is the length scale parameter and ∇ is the Laplace operator.

The model description and parameters are summarized in Tabs. 11 and 12. Note that the internal length parameter r has the meaning of the radius of interaction R for the integral version (and thus has the dimension of length) but for the gradient version it has the meaning of the coefficient l^2 multiplying the Laplacean in (51), and thus has the dimension of length squared.

1.4.5 Rankine plasticity model with isotropic damage and its nonlocal formulations - RankMat, RankMatNl, RankMatGrad

This model has a very similar structure to the model described in Section 1.4.3, but is based on the Rankine yield condition. It is available in the small-strain version only, and so far exclusively for plane stress analysis. The basic equations (38)–(39) and (41)–(45) remain valid, and the yield function (40) is redefined as

$$f(\bar{\boldsymbol{\sigma}},\kappa) = \max_I \bar{\sigma_I} - \sigma_Y(\kappa) \tag{53}$$

where $\bar{\sigma_I}$ are the principal values of the effective stress tensor $\bar{\boldsymbol{\sigma}}$. The hardening law can have either the linear form (42), or the exponential form

$$\sigma_Y(\kappa) = \sigma_0 + \Delta\sigma_Y\left(1 - \exp(-H\kappa/\Delta\sigma_Y)\right), \tag{54}$$

where H is now the initial plastic modulus and $\Delta\sigma_Y$ is the value of yield stress increment asymptotically approached as $\kappa \to \infty$. In damage law (45), parameter ω_c is always set to 1. If the plastic hardening is linear, the user can specify

Description	Nonlocal Mises plasticity with isotropic hardening
Record Format	**MisesMatNl** $_{\rm (in)}$ # d$_{\rm (rn)}$ # E$_{\rm (rn)}$ # n$_{\rm (rn)}$ # sig0$_{\rm (rn)}$ # H$_{\rm (rn)}$ # omega_crit$_{\rm (rn)}$ #a$_{\rm (rn)}$ #r$_{\rm (rn)}$ #m$_{\rm (rn)}$ #[wft$_{\rm (in)}$ #][scalingType$_{\rm (in)}$ #]
Parameters	- material number - *d* material density - *E* Young's modulus - *n* Poisson's ratio - *sig0* initial yield stress in uniaxial tension (compression) - *H* hardening modulus - *omega_crit* critical damage - *a* exponent in damage law - *r* nonlocal interaction radius R from eq. (50) - *m* over-nonlocal parameter - *wft* selects the type of nonlocal weight function (see Section 1.5.7): 1 - default, quartic spline (bell-shaped function with bounded support) 2 - Gaussian function 3 - exponential function (Green function in 1D) 4 - uniform averaging up to distance R 5 - uniform averaging over one finite element 6 - special function obtained by reducing the 2D exponential function to 1D (by numerical integration) - *scalingType* selects the type of scaling of the weight function (e.g. near a boundary; see Section 1.5.7): 1 - default, standard scaling with integral of weight function in the denominator 2 - no scaling (the weight function normalized in an infinite body is used even near a boundary) 3 - Borino scaling (local complement)
Supported modes	1dMat, PlaneStrain, 3dMat

Table 11: Nonlocal integral Mises plasticity – summary.

either the exponent a from (45), or the dissipation per unit volume, g_f, which represents the area under the stress-strain diagram (and parameter a is then determined automatically such that the area under the diagram has the prescribed value). For exponential plastic hardening, the evaluation of a from g_f is not properly implemented and it is better to specify a directly.

The model description and parameters are summarized in Tabs. 13–15. Note that the default value of parameter m is equal to 1 for the integral model but for the gradient model it is equal to 2. Also note that the internal length parameter r has the meaning of the radius of interaction R for the integral version (and thus has the dimension of length) but for the gradient version it has the meaning of

Description	Gradient-enhanced Mises plasticity with isotropic damage
Record Format	**MisesMatGrad** $_{\rm (in)}$ # d$_{\rm (rn)}$ # E$_{\rm (rn)}$ # n$_{\rm (rn)}$ # sig0$_{\rm (rn)}$ # H$_{\rm (rn)}$ # omega_crit$_{\rm (rn)}$ #a$_{\rm (rn)}$ #r$_{\rm (rn)}$ #m$_{\rm (rn)}$ #
Parameters	- material number - d material density - E Young's modulus - n Poisson's ratio - *sig0* initial yield stress in uniaxial tension (compression) - H hardening modulus - *omega_crit* critical damage - a exponent in damage law - r internal length scale parameter l^2 from eq. (51) - m over-nonlocal parameter
Supported modes	1dMat, PlaneStrain, 3dMat

Table 12: Gradient-enhanced Mises plasticity – summary.

the coefficient l^2 multiplying the Laplacean in (51), and thus has the dimension of length squared.

For the gradient model it is possible to specify parameter *negligible_damage*, which sets the minimum value of damage that is considered as nonzero. The approximate solution of Helmholtz equation (51) can lead to very small but nonzero nonlocal kappa at some points that are actually elastic. If such small values are positive, they lead to a very small but nonzero damage. If this is interpreted as "loading", the tangent terms are activated, but damage will not actually grow at such points and the convergence rate is slowed down. It is better to consider such points as elastic. By default, *negligible_damage* is set to 0, but it is recommended to set it e.g. to 1.e-6.

1.4.6 Perfectly plastic material with Mises yield condition - Steel1

This is an older model, kept here for compatibility with previous versions. It uses Mises plasticity condition with no hardening and under small strain only. The model description and parameters are summarized in Tab. 16. All its features are included in the model described in Section 1.4.3.

1.4.7 Composite plasticity model for masonry - Masonry02

Masonry is a composite material made of bricks and mortar. Nonlinear behavior of both components should be considered to obtain a realistic model able to describe cracking, slip, and crushing of the material. The model is based on paper by Lourenco and Rots [17]. It is formulated on the basis of softening plasticity for tension, shear, and compression (see fig.(1)). Numerical implementation is based on modern algorithmic concepts such as implicit integration of the rate equations and consistent tangent stiffness matrices.

The approach used in this work is based on idea of concentrating all the damage in the relatively weak joints and, if necessary, in potential tension cracks in the bricks. The joint interface constitutive model should include all important damage mechanisms. Here, the concept of interface elements is used. An

Description	Rankine plasticity with isotropic hardening and damage
Record Format	**RankMat** (in) # d(rn) # E(rn) # n(rn) # plasthardtype(in) # sig0(rn) # H(rn) # delSigY(rn) # yieldtol(rn) # (gf(rn) # ‖ a(rn) #)
Parameters	- material number - *d* material density - *E* Young's modulus - *n* Poisson's ratio - *plasthardtype* type of plastic hardening (0=linear=default, 1=exponential) - *sig0* initial yield stress in uniaxial tension (compression) - *H* initial hardening modulus (default value 0.) - *delSigY* final increment of yield stress (default value 0., needed only if plasthardtype=1) - *yieldtol* relative tolerance in the yield condition - *gf* dissipation per unit volume - *a* exponent in damage law (45)
Supported modes	PlaneStress

Table 13: Rankine plasticity – summary.

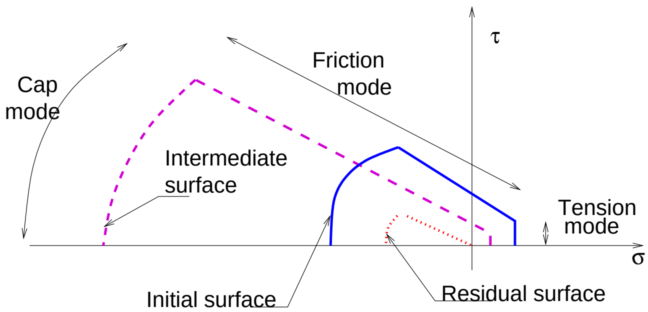

Figure 1: Composite yield surface model for masonry

interface element allows to incorporate discontinuities in the displacement field and its behavior is described in terms of a relation between the tractions and relative displacement across the interface. In the present work, these quantities will be denoted as $\boldsymbol{\sigma}$, generalized stress, and $\boldsymbol{\varepsilon}$, generalized strain. For 2D configuration, $\boldsymbol{\sigma} = \{\sigma, \tau\}^T$ and $\boldsymbol{\varepsilon} = \{u_n, u_s\}^T$, where σ and τ are the normal and shear components of the traction interface vector and n and s subscripts distinguish between normal and shear components of displacement vector. The elastic response is characterized in terms of elastic constitutive matrix $\boldsymbol{D}$ as

$$\boldsymbol{\sigma} = \boldsymbol{D}\boldsymbol{\varepsilon} \tag{55}$$

For a 2D configuration $\boldsymbol{D} = diag\{k_n, k_s\}$. The terms of the elastic stiffness matrix can be obtained from the properties of both masonry and joints as

$$k_n = \frac{E_b E_m}{t_m(E_b - E_m)};\; k_s = \frac{G_b G_m}{t_m(G_b - G_m)} \tag{56}$$

<table>
<tr><td>Description</td><td>Nonlocal Rankine plasticity with isotropic hardening and damage</td></tr>
<tr><td>Record Format

Parameters</td><td>RankMatNl (in) # d(rn) # E(rn) # n(rn) # plasthardtype(in) # sig0(rn) # H(rn) # delSigY(rn) # yieldtol(rn) # (gf(rn) # ‖ a(rn) #)r(rn) #m(rn) #[wft(in) #][scalingType(in) #]
- material number
- d material density
- E Young's modulus
- n Poisson's ratio
- plasthardtype type of plastic hardening (0=linear=default, 1=exponential)
- sig0 initial yield stress in uniaxial tension (compression)
- H initial hardening modulus (default value 0.)
- delSigY final increment of yield stress (default value 0.)
- yieldtol relative tolerance in the yield condition
- gf dissipation per unit volume
- a exponent in damage law (45)
- r internal length scale parameter l^2 from eq. (51)
- m over-nonlocal parameter (default value 1.)
- wft selects the type of nonlocal weight function (see Section 1.5.7):
1 - default, quartic spline (bell-shaped function with bounded support)
2 - Gaussian function
3 - exponential function (Green function in 1D)
4 - uniform averaging up to distance R
5 - uniform averaging over one finite element
6 - special function obtained by reducing the 2D exponential function to 1D (by numerical integration)

- scalingType selects the type of scaling of the weight function (e.g. near a boundary; see Section 1.5.7):
1 - default, standard scaling with integral of weight function in the denominator
2 - no scaling (the weight function normalized in an infinite body is used even near a boundary)
3 - Borino scaling (local complement)</td></tr>
<tr><td>Supported modes</td><td>PlaneStress</td></tr>
</table>

Table 14: Nonlocal integral Rankine plasticity – summary.

where E_b and E_m are Young's moduli, G_b and G_m shear moduli for brick and mortar, and t_m is the thickness of joint. One should note, that there is no contact algorithm assumed between bricks, this means that the overlap of neighboring units will be visible. On the other hand, the interface model includes a compressive cap, where the compressive inelastic behavior of masonry is lumped.

Description	Gradient-enhanced Rankine plasticity with isotropic hardening and damage
Record Format	**RankMatGrad** (in) # d(rn) # E(rn) # n(rn) # plasthardtype(in) # sig0(rn) # H(rn) # delSigY(rn) # yieldtol(rn) # (gf(rn) # ‖ a(rn) #)r(rn) #m(rn) #negligible_damage(rn) #
Parameters	- material number - *d* material density - *E* Young's modulus - *n* Poisson's ratio - *plasthardtype* type of plastic hardening (0=linear=default, 1=exponential) - *sig0* initial yield stress in uniaxial tension (compression) - *H* hardening modulus (default value 0.) - *delSigY* final increment of yield stress (default value 0.) - *yieldtol* relative tolerance in the yield condition - *gf* dissipation per unit volume - *a* exponent in damage law (45) - *r* internal length scale parameter *l* from eq. (51) - *m* over-nonlocal parameter (default value 2.) - *negligible_damage* optional parameter (default value 0.)
Supported modes	PlaneStress

Table 15: Gradient-enhanced Rankine plasticity – summary.

Description	Perfectly plastic material with Mises condition
Record Format	**Steel1** num(in) # d(rn) # E(rn) # n(rn) # tAlpha(rn) # Ry(rn) #
Parameters	- *num* material model number - *d* material density - *E* Young modulus - *n* Poisson ratio - *tAlpha* thermal dilatation coefficient - *Ry* uniaxial yield stress
Supported modes	3dMat, PlaneStress, PlaneStrain, 1dMat, 2dPlateLayer, 2dBeamLayer, 3dShellLayer 3dBeam, PlaneStressRot

Table 16: Perfectly plastic material with Mises condition – summary.

Tension mode In the tension mode, the exponential softening law is assumed (see fig.(3)). The yield function has the following form

$$f_1(\boldsymbol{\sigma}, \kappa_1) = \sigma - f_t(\kappa_1) \tag{57}$$

where the yield value f_t is defined as

$$f_t = f_{t0} \exp\left(-\frac{f_{t0}}{G_f^I}\kappa_1\right) \tag{58}$$

The f_{t0} represents tensile strength of joint or interface; and G_f^I is mode-I fracture energy. For the tension mode, the associated flow hypothesis is assumed.

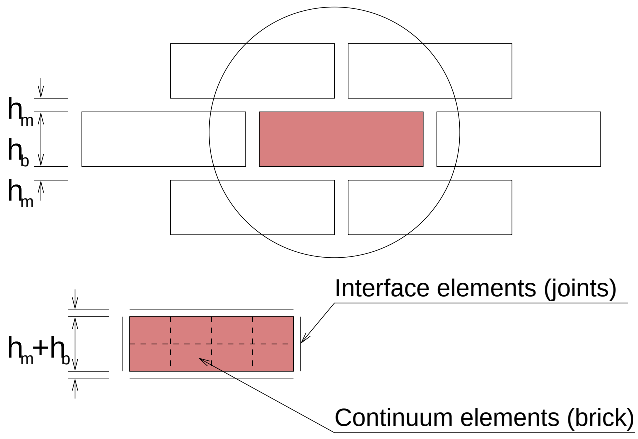

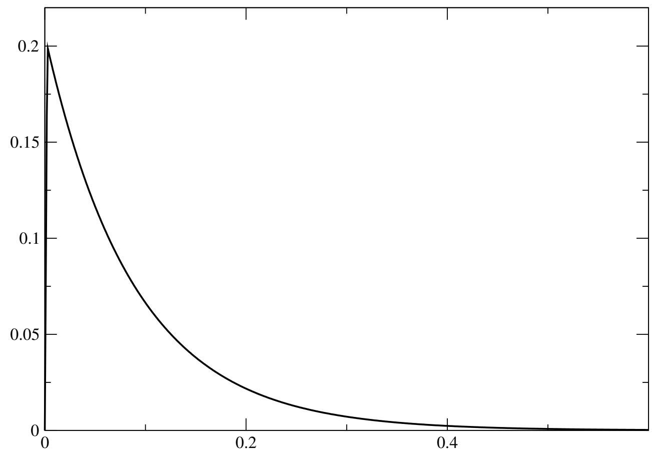

Figure 3: Tensile behavior of proposed model (f_t = 0.2 MPa, G_f^I = 0.018 N/mm)

Shear mode For the shear mode a Coulomb friction envelope is used. The yield function has the form

$$f_2(\boldsymbol{\sigma}, \kappa_2) = |\tau| + \sigma \tan\phi(\kappa_2) - c(\kappa_2) \tag{59}$$

According to [17] the variations of friction angle ϕ and cohesion c are assumed as

$$c = c_0 \exp\left(-\frac{c_0}{G_f^{II}}\kappa_2\right) \tag{60}$$

$$\tan\phi = \tan\phi_0 + (\tan\phi_r - \tan\phi_0)\left(\frac{c_0 - c}{c_0}\right) \tag{61}$$

where c_0 is initial cohesion of joint, ϕ_0 initial friction angle, ϕ_r residual friction angle, and G_f^{II} fracture energy in mode II failure. A non-associated plastic potential g_2 is considered as

$$g_2 = |\tau| + \sigma \tan \Phi - c \tag{62}$$

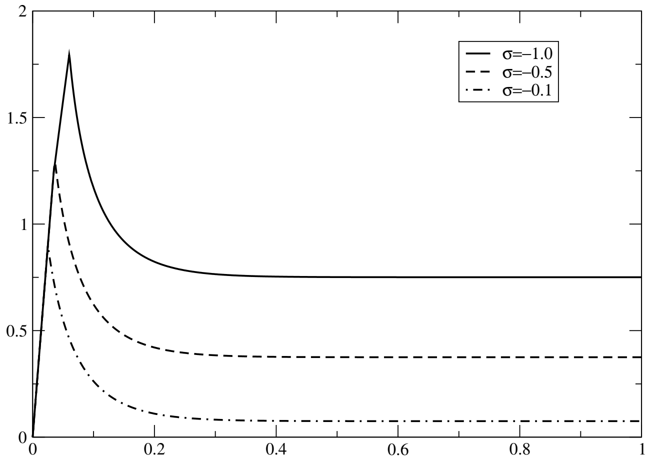

Figure 4: Shear behavior of proposed model for different confinement levels in MPa ($c_0 = 0.8$ MPa, $\tan\phi_0 = 1.0$, $\tan\phi_{\rm r} = 0.75,$ and $\mathrm{G_f^{II}} = 0.05$ N/mm)

Coupling of tension/shear modes The tension and Coulomb friction modes are coupled with isotropic softening. This means that the percentage of softening in the cohesion is assumed to be the same as on the tensile strength

$$\dot\kappa_1 = \lambda_1 + \frac{G_f^I}{G_f^{II}}\frac{c_0}{f_{t0}}\lambda_2; \quad \dot\kappa_2 = \frac{G_f^{II}}{G_f^I}\frac{f_{t0}}{c_0}\lambda_1 + \lambda_2 \tag{63}$$

This follows from (58) and (60). However, in the corner region, when both yield surfaces are activated, such approach will lead to a non-acceptable penalty. For this reason a quadratic combination is assumed

$$\dot\kappa_1 = \sqrt{(\lambda_1)^2 + \left(\frac{G_f^I}{G_f^{II}}\frac{c_0}{f_{t0}}\lambda_2\right)^2}; \quad \dot\kappa_2 = \sqrt{\left(\frac{G_f^{II}}{G_f^I}\frac{f_{t0}}{c_0}\lambda_1\right)^2 + (\lambda_2)^2} \tag{64}$$

Cap mode For the cap mode, an ellipsoid interface model is used. The yield condition is assumed as

$$f_3(\boldsymbol{\sigma}, \kappa_3) = C_{nn}\sigma^2 + C_{ss}\tau^2 + C_n\sigma - \bar\sigma^2(\kappa_3) \tag{65}$$

where C_{nn}, C_{ss}, and C_n are material model parameters and $\bar{\sigma}$ is yield value, originally assumed in the following form of hardening/softening law [17]

$$\begin{aligned}
\bar{\sigma}_1(\kappa_3) &= \bar{\sigma}_i + (\bar{\sigma}_p - \bar{\sigma}_i)\sqrt{\frac{2\kappa_3}{\kappa_p} - \frac{\kappa_3^2}{\kappa_p^2}}; \quad \kappa_3 \in (0, \kappa_p) \\
\bar{\sigma}_2(\kappa_3) &= \bar{\sigma}_p + (\bar{\sigma}_m - \bar{\sigma}_p)\left(\frac{\kappa_3 - \kappa_p}{\kappa_m - \kappa_p}\right)^2; \quad \kappa_3 \in (\kappa_p, \kappa_m) \qquad (66) \\
\bar{\sigma}_3(\kappa_3) &= \bar{\sigma}_r + (\bar{\sigma}_m - \bar{\sigma}_r)\exp\left(m\frac{\kappa_3 - \kappa_m}{\bar{\sigma}_m - \bar{\sigma}_r}\right); \quad \kappa_3 \in (\kappa_m, \infty)
\end{aligned}$$

with $m = 2(\bar{\sigma}_m - \bar{\sigma}_p)/(\kappa_m - \kappa_p)$. The hardening/softening law (66) is shown in fig.(5). Note that the curved diagram is a C^1 continuous $\sigma - \kappa_3$ relation. The energy under the load-displacement diagram can be related to a "compressive fracture energy". The original hardening law (66.1) exhibits indefinite slope for $\kappa_3 = 0$, which can cause the problems with numerical implementation. This has been overcomed by replacing this hardening law with parabolic equation given by

$$\bar{\sigma}_1(\kappa_3) = \bar{\sigma}_i - 2 * (\bar{\sigma}_i - \bar{\sigma}_p) * \frac{\kappa_3}{\kappa_p} + (\bar{\sigma}_i - \bar{\sigma}_p)\frac{\kappa_3}{\kappa_p} \qquad (67)$$

An associated flow and strain hardening hypothesis are being considered. This yields

$$\dot{\kappa}_3 = \lambda_3\sqrt{(2C_{nn}\sigma + C_n) * (2C_{nn}\sigma + C_n) + (2C_{ss}\tau) * (2C_{ss}\tau)} \qquad (68)$$

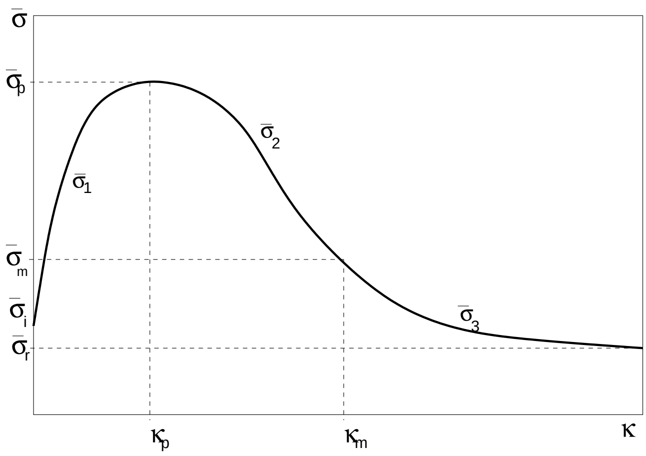

Figure 5: Hardening/softening law for cap mode

The model parameters are summarized in Tab. 17. There is one algorithmic issue, that follows from the model formulation. Since the cap mode hardening/softening is not coupled to hardening/softening of shear and tension modes the it may happen that when the cap and shear modes are activated, the return directions become parallel for both surfaces. This should be avoided by adjusting the input parameters accordingly (one can modify dilatancy angle, for example).

Description	Composite plasticity model for masonry
Record Format	**Masonry02** num(in) # d(rn) # E(rn) # n(rn) # ft0(rn) # gfi(rn) # gfii(rn) # kn(rn) # ks(rn) # c0(rn) # tanfi0(rn) # tanfir(rn) # tanpsi(rn) # si(rn) # sp(rn) # sm(rn) # sr(rn) # kp(rn) # km(rn) # kr(rn) # cnn(rn) # css(rn) # cn(rn) #
Parameters	- *num* material model number - *d* material density - *E* Young modulus - *n* Poisson ratio - *ft0* tensile strength - *gfi* fracture energy for mode I - *gfii* fracture energy for mode II - *kn* joint elastic property - *ks* joint elastic property - *c0* initial cohesion - *tanfi0* initial friction angle - *tanfir* residual friction angle - *tanpsi* dilatancy - {*si, sp, sm, sr*} cap parameters $\{\bar{\sigma}_i, \bar{\sigma}_p, \bar{\sigma}_m, \bar{\sigma}_r\}$ - {*kp, km,kr*} cap parameters $\{\kappa_p, \kappa_m, \kappa_r\}$ - *cnn,css,cn* cap mode parametrs
Supported modes	_2dInterface

Table 17: Composite model for masonry - summary.

1.4.8 Nonlinear elasto-plastic material model for concrete plates and shells - Concrete2

Nonlinear elasto-plastic material model with hardening. Takes into account uniaxial stress + transverse shear in concrete layers with transverse stirrups. Can be used only for 2d plates and shells with layered cross section and together with explicit integration method (stiffness matrix is not provided). The model description and parameters are summarized in Tab. 18.

1.5 Material models for tensile failure

1.5.1 Nonlinear elasto-plastic material model for concrete plates and shells - Concrete2

The description can be found is section 1.4.8.

1.5.2 Smeared rotating crack model - Concrete3

Implementation of smeared rotating crack model. Virgin material is modeled as isotropic linear elastic material (described by Young modulus and Poisson ratio). The onset of cracking begins, when principal stress reaches tensile strength. Further behavior is then determined by softening law, governed by principle of preserving of fracture energy G_f. For large elements, the tension strength can be artificially reduced to preserve fracture energy. Multiple cracks are allowed. The elastic unloading and reloading is assumed. In compression regime, this

Description	Nonlinear elasto-plastic material model for concrete plates and shells
Record Format	**Concrete2** num(in) # d(rn) # E(rn) # n(rn) # SCCC(rn) # SCCT(rn) # EPP(rn) # EPU(rn) # EOPU(rn) # EOPP(rn) # SHEARTOL(rn) # IS_PLASTIC_FLOW(in) # IFAD(in) # STIRR_E(rn) # STIRR_Ft(rn) # STIRR_A(rn) # STIRR_TOL(rn) # STIRR_EREF(rn) # STIRR_LAMBDA(rn) #
Parameters	- *num* material model number - *d* material density - *E* Young modulus - *n* Poisson ratio - *SCCC* pressure strength - *SCCT* tension strength - *EPP* threshold effective plastic strain for softening in compression - *EPU* ultimate eff. plastic strain - *EOPP* threshold volumetric plastic strain for softening in tension - *EOPU* ultimate volumetric plastic strain - *SHEARTOL* threshold value of the relative shear deformation (psi**2/eef) at which shear is considered in layers. For lower relative shear deformations the transverse shear remains elastic decoupled from bending. default value SHEARTOL = 0.01 - *IS_PLASTIC_FLOW* indicates that plastic flow (not deformation theory) is used in pressure - *IFAD* State variables will not be updated, otherwise update state variables - *STIRR_E* Young modulus of stirrups - *STIRR_R* stirrups uniaxial strength = elastic limit - *STIRR_A* stirrups area/unit length (beam) or /unit area (shell) - *STIRR_TOL* stirrups tolerance of equilibrium in the z direction (=0 no iteration) - *STIRR_EREF* stirrups reference strain rate for Peryzna's material - *STIRR_LAMBDA* coefficient for that material (stirrups) - *SHTIRR_H* isotropic hardening factor for stirrups
Supported modes	3dShellLayer, 2dPlateLayer

Table 18: Nonlinear elasto-plastic material model for concrete - summary.

model correspond to isotropic linear elastic material. The model description and parameters are summarized in Tab. 19.

Description	Rotating crack model for concrete
Record Format	**Concrete3** d(rn) # E(rn) # n(rn) # Gf(rn) # Ft(rn) # exp_soft(in) # tAlpha(rn) #
Parameters	- *num* material model number - *d* material density - *E* Young modulus - *n* Poisson ratio - *Gf* fracture energy - *Ft* tension strength - *exp_soft* determines the type of softening (0 = exponential, 1 = linear) - *tAlpha* thermal dilatation coefficient
Supported modes	3dMat, PlaneStress, PlaneStrain, 1dMat, 2dPlateLayer, 2dBeamLayer, 3dShellLayer

Table 19: Rotating crack model for concrete - summary.

1.5.3 Smeared rotating crack model with transition to scalar damage - linear softening - RCSD

Implementation of smeared rotating crack model with transition to scalar damage with linear softening law. Improves the classical rotating model (see section 1.5.2) by introducing the transition to scalar damage model in later stages of tension softening.

Traditional smeared-crack models for concrete fracture are known to suffer by stress locking (meaning here spurious stress transfer across widely opening cracks), mesh-induced directional bias, and possible instability at late stages of the loading process. The combined model keeps the anisotropic character of the rotating crack but it does not transfer spurious stresses across widely open cracks. The new model with transition to scalar damage (RC-SD) keeps the anisotropic character of the RCM but it does not transfer spurious stresses across widely open cracks.

Virgin material is modeled as isotropic linear elastic material (described by Young modulus and Poisson ratio). The onset of cracking begins, when principal stress reaches tensile strength. Further behavior is then determined by **linear** softening law, governed by principle of preserving of fracture energy G_f. For large elements, the tension strength can be artificially reduced to preserve fracture energy. The transition to scalar damage model takes place, when the softening stress reaches the specified limit. Multiple cracks are allowed. The elastic unloading and reloading is assumed. In compression regime, this model correspond to isotropic linear elastic material. The model description and parameters are summarized in Tab. 20.

1.5.4 Smeared rotating crack model with transition to scalar damage - exponential softening - RCSDE

Implementation of smeared rotating crack model with transition to scalar damage with exponential softening law. The description and model summary (Tab. 21) are the same as for the RC-SD model with linear softening law (see section 1.5.3).

Description	Smeared rotating crack model with transition to scalar damage - linear softening
Record Format	**RCSD** d(rn) # E(rn) # n(rn) # Gf(rn) # Ft(rn) # sdtransitioncoeff(rn) # tAlpha(rn) #
Parameters	- *num* material model number - *d* material density - *E* Young modulus - *n* Poisson ratio - *Gf* fracture energy - *Ft* tension strength - *sdtransitioncoeff* determines the transition from RC to SD model. Transition takes plase when ratio of current softening stress to tension strength is less than *sdtransitioncoeff* value - *tAlpha* thermal dilatation coefficient
Supported modes	3dMat, PlaneStress, PlaneStrain, 1dMat, 2dPlateLayer, 2dBeamLayer, 3dShellLayer

Table 20: RC-SD model for concrete - summary.

Description	Smeared rotating crack model with transition to scalar damage - exponential softening
Record Format	**RCSDE** d(rn) # E(rn) # n(rn) # Gf(rn) # Ft(rn) # sdtransitioncoeff(rn) # tAlpha(rn) #

Table 21: RC-SD model for concrete - summary.

1.5.5 Nonlocal smeared rotating crack model with transition to scalar damage - RCSDNL

Implementation of nonlocal version of smeared rotating crack model with transition to scalar damage. Improves the classical rotating model (see section 1.5.2) by introducing the transition to scalar damage model in later stages of tension softening. The improved RC-SD (see section 1.5.3) is further extended to a nonlocal formulation, which not only acts as a powerful localization limiter but also alleviates mesh-induced directional bias. A special type of material instability arising due to negative shear stiffness terms in the rotating crack model is resolved by switching to SD mode. A bell shaped nonlocal averaging function is used.

Virgin material is modeled as isotropic linear elastic material (described by Young modulus and Poisson ratio). The onset of cracking begins, when principal stress reaches tensile strength. Further behavior is then determined by **exponential** softening law.

The transition to scalar damage model takes place, when the softening stress reaches the specified limit or when the loss of material stability due to negative shear stiffness terms that may arise in the standard RCM formulation, which takes place when the ratio of minimal shear coefficient in stiffness to bulk material shear modulus reaches the limit.

Multiple cracks are allowed. The elastic unloading and reloading is assumed. In compression regime, this model correspond to isotropic linear elastic material. The model description and parameters are summarized in Tab. 22.

Description	Nonlocal smeared rotating crack model with transition to scalar damage for concrete
Record Format	**RCSDNL** d$_{(rn)}$ # E$_{(rn)}$ # n$_{(rn)}$ # Ft$_{(rn)}$ # sdtransitioncoeff$_{(rn)}$ # sdtransitioncoeff2$_{(rn)}$ # r$_{(rn)}$ # tAlpha$_{(rn)}$ #
Parameters	- *num* material model number - *d* material density - *E* Young modulus - *n* Poisson ratio - *ef* deformation corresponding to fully open crack - *Ft* tension strength - *sdtransitioncoeff* determines the transition from RC to SD model. Transition takes place when ratio of current softening stress to tension strength is less than *sdtransitioncoeff* value - *sdtransitioncoeff2* determines the transition from RC to SD model. Transition takes place when ratio of current minimal shear stiffness term to virgin shear modulus is less than *sdtransitioncoeff2* value - *r* parameter specifying the width of nonlocal averaging zone - *tAlpha* thermal dilatation coefficient - *regionMap* map indicating the regions (currently region is characterized by cross section number) to skip for nonlocal avaraging. The elements and corresponding IP are not taken into account in nonlocal averaging process if corresponding regionMap value is nonzero.
Supported modes	3dMat, PlaneStress, PlaneStrain, 1dMat, 2dPlateLayer, 2dBeamLayer, 3dShellLayer

Table 22: RC-SD-NL model for concrete - summary.

1.5.6 Isotropic damage model for tensile failure - Idm1

This isotropic damage model assumes that the stiffness degradation is isotropic, i.e., stiffness moduli corresponding to different directions decrease proportionally and independently of the loading direction. The damaged stiffness tensor is expressed as $\boldsymbol{D} = (1-\omega)\boldsymbol{D}_e$ where ω is a scalar damage variable and $\boldsymbol{D}_e$ is the elastic stiffness tensor. The damage evolution law is postulated in an explicit form, relating the damage variable ω to the largest previously reached equivalent strain level, κ.

The equivalent strain, $\tilde{\varepsilon}$, is a scalar measure derived from the strain tensor. The choice of the specific expression for the equivalent strain affects the shape of the elastic domain in the strain space and plays a similar role to the choice of a yield condition in plasticity. The following definitions of **equivalent strain** are currently supported:

- **Mazars** (1984) definition based on norm of positive part of strain:

$$\tilde{\varepsilon} = \sqrt{\sum_{I=1}^{3} \langle \varepsilon_I \rangle^2} \tag{69}$$

  where $\langle \varepsilon_I \rangle$ are positive parts of principal values of the strain tensor $\boldsymbol{\varepsilon}$.

- Definitions derived from the **Rankine** criterion of maximum principal stress:

$$\tilde{\varepsilon} = \frac{1}{E} \sqrt{\sum_{I=1}^{3} \langle \bar{\sigma}_I \rangle^2} \tag{70}$$

$$\tilde{\varepsilon} = \frac{1}{E} \max_{I=1}^{3} \bar{\sigma}_I \tag{71}$$

  where $\bar{\sigma}_I$, $I = 1, 2, 3$, are the principal values of the effective stress tensor $\bar{\boldsymbol{\sigma}} = \boldsymbol{D}_e : \boldsymbol{\varepsilon}$ and $\langle \bar{\sigma}_I \rangle$ are their positive parts.

- **Energy** norm scaled by Young's modulus to obtain a strain-like quantity:

$$\tilde{\varepsilon} = \frac{1}{E} \sqrt{\boldsymbol{\varepsilon} : \boldsymbol{D}_e : \boldsymbol{\varepsilon}} \tag{72}$$

- **Modified Mises** definition, proposed by de Vree [26]:

$$\tilde{\varepsilon} = \frac{(k-1) I_{1\varepsilon}}{2k(1-2\nu)} + \frac{1}{2k} \sqrt{\frac{(k-1)^2}{(1-2\nu)^2} I_{1\varepsilon}^2 + \frac{12 k J_{2\varepsilon}}{(1+\nu)^2}} \tag{73}$$

  where

$$I_{1\varepsilon} = \sum_{I=1}^{3} \varepsilon_I$$

  is the first strain invariant (trace of the strain tensor),

$$J_{2\varepsilon} = \frac{1}{2} \sum_{I=1}^{3} \varepsilon_I^2 - \frac{1}{6} I_{1\varepsilon}^2$$

  is the second deviatoric strain invariant, and k is a model parameter that corresponds to the ratio between the uniaxial compressive strength f_c and uniaxial tensile strength f_t.

- **Griffith** definition with a solution on inclined elipsoidal inclusion. This definition handles materials in pure tension and also in compression, where tensile stresses usually appear on specifically oriented elipsoidal inclusion. The derivation of Griffith's criterion is summarized in [14]. In impementation, first check if Rankine criterion applies

$$\tilde{\varepsilon} = \frac{1}{E} \max_{I=1}^{3} \bar{\sigma}_I \tag{74}$$

and if not, use Griffith's solution with ordered principal stresses $\sigma_1 > \sigma_3$. The optional parameter *griff_n* is by default 8 and represents the uniaxial compression/tensile strength ratio.

$$\tilde{\varepsilon} = \frac{1}{E} \cdot \frac{-(\sigma_1 - \sigma_3)^2}{griff\_n(\sigma_1 + \sigma_3)} \tag{75}$$

Note that all these definitions are based on the three-dimensional description of strain (and stress). If they are used in a reduced problem, the strain components that are not explicitly provided by the finite element approximation are computed from the underlying assumptions and used in the evaluation of equivalent strain. For instance, in a plane-stress analysis, the out-of-plane component of normal strain is calculated from the assumption of zero out-of-plane normal stress (using standard Hooke's law).

Since the growth of damage usually leads to softening and may induce localization of the dissipative process, attention should be paid to proper regularization. The most efficient approach is based on a nonlocal formulation; see Section 1.5.7. If the model is kept local, the damage law should be adjusted according to the element size, in the spirit of the crack-band approach. When done properly, this ensures a correct dissipation of energy in a localized band of cracking elements, corresponding to the fracture energy of the material. For various numerical studies, it may be useful to specify the parameters of the damage law directly, independently of the element size. One should be aware that in this case the model would exhibit pathological sensitivity to the size of finite elements if the mesh is changed.

The following **damage laws** are currently implemented:

- **Cohesive crack with exponential softening** postulates a relation between the normal stress σ transmitted by the crack and the crack opening w in the form
$$\sigma = f_t \exp\left(-\frac{w}{w_f}\right)$$
Here, f_t is the tensile strength and w_f is a parameter with the dimension of length (crack opening), which controls the ductility of the material. In fact, $w_f = G_f/f_t$ where G_f is the mode-I fracture energy. In the context of the crack-band approach, the crack opening w corresponds to the inelastic (cracking) strain ε_c multiplied by the effective thickness h of the crack band. The effective thickness h is estimated by projecting the finite element onto the direction of the maximum principal strain (and stress) at the onset of damage. The inelastic strain ε_c is the difference between the total strain ε and the elastic strain σ/E. For the damage model we obtain
$$\varepsilon_c = \varepsilon - \frac{\sigma}{E} = \varepsilon - (1-\omega)\varepsilon = \omega\varepsilon$$
and thus $w = h\varepsilon_c = h\omega\varepsilon$. Substituting this into the cohesive law and combining with the stress-strain law for the damage model, we get a nonlinear equation
$$(1-\omega)E\varepsilon = f_t \exp\left(-\frac{h\omega\varepsilon}{w_f}\right)$$

For a given strain ε, the corresponding damage variable ω can be solved from this equation by Newton iterations. It can be shown that the solution exists and is unique for every $\varepsilon \geq \varepsilon_0$ provided that the element size h does not exceed the limit size $h_{max} = w_f/\varepsilon_0$. For larger elements, a local snapback in the stress-strain diagram would occur, which is not admissible. In terms of the material properties, h_{max} can be expressed as EG_f/f_t^2, which is related to Irwin's characteristic length.

The derivation has been performed for monotonic loading and uniaxial tension. Under general conditions, ε is replaced by the internal variable κ, which represents the maximum previously reached level of equivalent strain.

In the list of input variables, the tensile strength f_t is not specified directly but through the corresponding strain at peak stress, $\varepsilon_0 = f_t/E$, denoted by keyword *e0*. Another input parameter is the characteristic crack opening w_f, denoted by keyword *wf*.

Derivative can be expressed explicitly

$$\frac{\partial \omega}{\partial \varepsilon} = -\frac{(\omega\varepsilon_f - \varepsilon_f)\exp\left(\frac{\omega\varepsilon}{\varepsilon_f}\right) - \omega\varepsilon_0}{\varepsilon_f\varepsilon\exp\left(\frac{\omega\varepsilon}{\varepsilon_f}\right) - \varepsilon_0\varepsilon}$$

- **Cohesive crack with linear softening** is based on the same correspondence between crack opening and inelastic strain, but the cohesive law is assumed to have a simpler linear form

$$\sigma = f_t\left(1 - \frac{w}{w_f}\right)$$

The relation between damage and strain can then be derived from the cohesive law and substituing $w = h\omega\varepsilon$

$$\sigma = (1-\omega)E\varepsilon = f_t\left(1 - \frac{h\omega\varepsilon}{w_f}\right),$$

which leads to explicit evaluation of the damage variable

$$\omega = \frac{1 - \dfrac{\varepsilon_0}{\varepsilon}}{1 - \dfrac{h\varepsilon_0}{w_f}}$$

and no iteration is needed. Parameter w_f, denoted again by keyword *wf*, has now the meaning of crack opening at complete failure (zero cohesive stress) and is related to fracture energy by a modified formula $w_f = 2G_f/f_t$. The expression for maximum element size, $h_{max} = w_f/\varepsilon_0$, remains the same as for cohesive law with exponential softening, but in terms of the material properties it is now translated as $h_{max} = 2EG_f/f_t^2$. The derivative with respect to ε yields

$$\frac{\partial \omega}{\partial \varepsilon} = \frac{\varepsilon_0}{\varepsilon^2\left(1 - \frac{h\varepsilon_0}{w_f}\right)}$$

- **Cohesive crack with bilinear softening** is implemented in an approximate fashion and gives for different mesh sizes the same total dissipation but different shapes of the softening diagram. Instead of properly transforming the crack opening into inelastic strain, the current implementation deals with a stress-strain diagram adjusted such that the areas marked in the right part of Fig. 6 are equal to the fracture energies G_f and G_{ft} divided by the element size. The third parameter defining the law is the strain $\boldsymbol{\varepsilon}_k$ at which the softening diagram changes slope. Since this strain is considered as fixed, the corresponding stress σ_k depends on the element size and for small elements gets close to the tensile strength (the diagram then gets close to linear softening with fracture energy G_{ft}).

- **Linear softening stress-strain law** works directly with strain and does not make any adjustment for the element size. The specified parameters ε_0 and ε_f, denoted by keywords *e0* and *ef*, have the meaning of (equivalent) strain at peak stress and at complete failure. The linear relation between stress and strain on the softening branch is obtained with the damage law

  $$\omega = \frac{\varepsilon_f}{\varepsilon_f - \varepsilon_0}\left(1 - \frac{\varepsilon_0}{\varepsilon}\right)$$

  Again, to cover general conditions, ε is replaced by κ.

  $$\frac{\partial\omega}{\partial\varepsilon} = \frac{\varepsilon_0\varepsilon_f}{\varepsilon^2(\varepsilon_f - \varepsilon_0)}$$

- **Exponential softening stress-strain law** also uses two parameters ε_0 and ε_f, denoted by keywords *e0* and *ef*, but leads to a modified dependence of damage on strain:

  $$\omega = 1 - \frac{\varepsilon_0}{\varepsilon}\exp\left(-\frac{\varepsilon - \varepsilon_0}{\varepsilon_f - \varepsilon_0}\right)$$

  $$\frac{\partial\omega}{\partial\varepsilon} = \left[\frac{1}{\varepsilon(\varepsilon_f - \varepsilon_0)} + \frac{1}{\varepsilon^2}\right]\varepsilon_0\exp\left(\frac{\varepsilon_0 - \varepsilon}{\varepsilon_f - \varepsilon_0}\right)$$

- **Mazars stress-strain law** uses three parameters, ε_0, A_t and B_t, denoted by keywords *e0*, *At* and *Bt*, and the dependence of damage on strain is given by

  $$\omega = 1 - \frac{(1 - A_t)\varepsilon_0}{\varepsilon} - A_t\exp\left(B_t(\varepsilon - \varepsilon_0)\right)$$

- **Smooth exponential stress-strain law** uses two parameters, ε_0 and M_d, denoted by keywords *e0* and *md*, and the dependence of damage on strain is given by

  $$\omega = 1 - \exp\left(-\left(\frac{\varepsilon}{\varepsilon_0}\right)^{M_d}\right)$$

  This leads to a stress-strain curve that immediately deviates from linearity (has no elastic part) and smoothly changes from hardening to softening, with tensile strength

  $$f_t = E\varepsilon_0\left(\mathrm{e}M_d\right)^{-1/M_d}$$

- **Extended smooth stress-strain law** is a special formulation used by Grassl and Jirásek [10]. The damage law has a rather complicated form:

$$\omega = \begin{cases} 1 - \exp\left(-\dfrac{1}{m}\left(\dfrac{\varepsilon}{\varepsilon_\mathrm{p}}\right)^m\right) & \text{if } \varepsilon \le \varepsilon_1 \\ 1 - \dfrac{\varepsilon_3}{\varepsilon}\exp\left(-\dfrac{\varepsilon - \varepsilon_1}{\varepsilon_\mathrm{f}\left[1 + \left(\frac{\varepsilon - \varepsilon_1}{\varepsilon_2}\right)^n\right]}\right) & \text{if } \varepsilon > \varepsilon_1 \end{cases} \tag{76}$$

  The primary model parameters are the uniaxial tensile strength f_t, the strain at peak stress (under uniaxial tension) ε_p, and additional parameters ε_1, ε_2 and n, which control the post-peak part of the stress-strain law. In the input record, they are denoted by keywords *ft, ep, e1, e2, nd*. Other parameters that appear in (76) can be derived from the condition of zero slope of the stress-strain curve at $\kappa = \varepsilon_\mathrm{p}$ and from the conditions of stress and stiffness continuity at $\kappa = \varepsilon_1$:

$$m = \frac{1}{\ln(E\varepsilon_\mathrm{p}/f_\mathrm{t})} \tag{77}$$

$$\varepsilon_\mathrm{f} = \frac{\varepsilon_1}{(\varepsilon_1/\varepsilon_\mathrm{p})^m - 1} \tag{78}$$

$$\varepsilon_3 = \varepsilon_1 \exp\left(-\frac{1}{m}\left(\frac{\varepsilon_1}{\varepsilon_p}\right)^m\right) \tag{79}$$

Note that parameter *damlaw* determines which type of damage law should be used, but the adjustment for element size is done only if parameter *wf* is specified for *damlaw*=0 or *damlaw*=1. For other values of *damlaw*, or if parameter *ef* is specified instead of *wf*, the stress-strain curve does not depend on element size and the model would exhibit pathological sensitivity to the mesh size. These cases are intended to be used in combination with a nonlocal formulation. An alternative formulation uses fracture energy to determine fracturing strain.

The model parameters are summarized in Tab. 23. Figure 6 shows three modes of a softening law with corresponding variables.

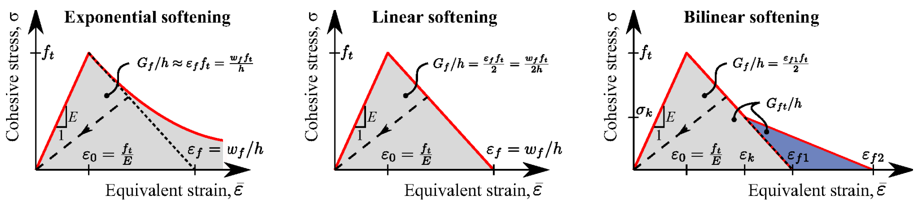

Figure 6: Implemented stress-strain diagrams for isotropic damage material. Fracturing strain ε_f and crack opening at zero stress w_f are interrelated through effective thickness h of the crack band. Note that exponential softening approach based on an exponential cohesive law is not exactly equivalent to the approach based on an exponential softening branch of the stress-strain diagram; see the detailed discussion of the damage laws.

Description	Isotropic damage model for concrete in tension

Record Format	**Idm1** $_{\text{(in)}}$ # d$_{\text{(rn)}}$ # E$_{\text{(rn)}}$ # n$_{\text{(rn)}}$ # [tAlpha$_{\text{(rn)}}$ #] [equivstraintype$_{\text{(in)}}$ #] [k$_{\text{(rn)}}$ #] [damlaw$_{\text{(in)}}$ #] e0$_{\text{(rn)}}$ # [wf$_{\text{(rn)}}$ #] [ef$_{\text{(rn)}}$ #] [ek$_{\text{(rn)}}$ #] [wk$_{\text{(rn)}}$ #] [sk$_{\text{(rn)}}$ #] [wkwf$_{\text{(rn)}}$ #] [skft$_{\text{(rn)}}$ #] [gf$_{\text{(rn)}}$ #] [gft$_{\text{(rn)}}$ #] [At$_{\text{(rn)}}$ #] [Bt$_{\text{(rn)}}$ #] [md$_{\text{(rn)}}$ #] [ft$_{\text{(rn)}}$ #] [ep$_{\text{(rn)}}$ #] [e1$_{\text{(rn)}}$ #] [e2$_{\text{(rn)}}$ #] [nd$_{\text{(rn)}}$ #] [maxOmega$_{\text{(rn)}}$ #] [checkSnapBack$_{\text{(rn)}}$ #]
Parameters	- material number - *d* material density - *E* Young's modulus - *n* Poisson's ratio - *tAlpha* thermal expansion coefficient - *equivstraintype* allows to choose from different definitions of equivalent strain: 0 - default = Mazars, eq. (69) 1 - smooth Rankine, eq. (70) 2 - scaled energy norm, eq. (72) 3 - modified Mises, eq. (73) 4 - standard Rankine, eq. (71) 5 - elastic energy based on positive stress 6 - elastic energy based on positive strain 7 - Griffith criterion eq. (75) - *k* ratio between uniaxial compressive and tensile strength, needed only if equivstraintype=3, default value 1 - *damlaw* allows to choose from different damage laws: 0 - exponential softening (default) with parameters e0 and wf | ef | gf 1 - linear softening with parameters e0 and wf | ef | gf 2 - bilinear softening with (e0, gf, gft, ek) | (e0, wk, sk, wf) | (e0, wkwf, skft, wf) | (e0, gf, gft, wk) 3 - Hordijk softening (not implemented yet) 4 - Mazars damage law with parameters At and Bt 5 - smooth stress-strain curve with parameters e0 and md 6 - disable damage (dummy linear elastic material) 7 - extended smooth damage law (76) with parameters ft, ep, e1, e2, nd - *e0* strain at peak stress (for damage laws 0,1,2,3), limit elastic strain (for damage law 4), characteristic strain (for damage law 5) - *wf* parameter controling ductility, has the meaning of crack opening (for damage laws 0 and 1) - *ef* parameter controling ductility, has the meaning of strain (for damage laws 0 and 1) - *ek* strain at knee point in bilinear softening type (for damage law 2)

	- *wk* crack opening at knee point in bilinear softening type (for damage law 2)
	- *sk* stress at knee point in bilinear softening type (for damage law 2)
	- *wkwf* ratio of wk/wf $< 0, 1 >$ in bilinear softening type (for damage law 2)
	- *skft* ratio of sk/ft $< 0, 1 >$ in bilinear softening type (for damage law 2)
	- *gf* fracture energy (for damage laws 0–2)
	- *gft* total fracture energy (for damage law 2)
	- *At* parameter of Mazars damage law, used only by law 4
	- *Bt* parameter of Mazars damage law, used only by law 4
	- *md* exponent used only by damage law 5, default value 1
	- *ft* tensile strength, used only by damage law 7
	- *ep* strain at peak stress, used only by damage law 7
	- *e1* parameter used only by damage law 7
	- *e2* parameter used only by damage law 7
	- *nd* exponent used only by damage law 7
	- *griff_n* uniaxial compression/tensile ratio for Griffith's criterion
	- *maxOmega* maximum damage, used for convergence improvement (its value is between 0 and 0.999999 (default), and it affects only the secant stiffness but not the stress)
	- *checkSnapBack* parameter for snap back checking, 0 no check, 1 check (default)
Supported modes	3dMat, PlaneStress, PlaneStrain, 1dMat
Features	Adaptivity support

Table 23: Isotropic damage model for tensile failure – summary.

1.5.7 Nonlocal isotropic damage model for tensile failure - Idmnl1

Nonlocal version of isotropic damage model from Section 1.5.6. The nonlocal averaging acts as a powerful localization limiter. In the standard version of the model, damage is driven by the nonlocal equivalent strain $\bar{\varepsilon}$, defined as a weighted average of the local equivalent strain:

$$\bar{\varepsilon}(\boldsymbol{x}) = \int_V \alpha(\boldsymbol{x}, \boldsymbol{\xi})\tilde{\varepsilon}(\boldsymbol{\xi})\ \mathrm{d}\boldsymbol{\xi}$$

In the "undernonlocal" formulation, the damage-driving variable is a combination of local and nonlocal equivalent strain, $m\bar{\varepsilon} + (1-m)\tilde{\varepsilon}$, where m is a parameter between 0 and 1. (If $m > 1$, the formulation is called "overnonlocal"; this case is useful for nonlocal plasticity but not for nonlocal damage.)

Instead of averaging the equivalent strain, one can average the compliance variable γ, directly related to damage according to the formula $\gamma = \omega/(1-\omega)$.

The weight function α contains a certain parameter with the dimension of length, which is in general called the characteristic length. Its specific meaning depends on the type of weight function. The following functions are currently supported:

- Truncated quartic spline, also called the bell-shaped function,

$$\alpha_0(s) = \left\langle 1 - \frac{s^2}{R^2} \right\rangle^2$$

where R is the interaction radius (characteristic length) and s is the distance between the interacting points. This function is exactly zero for $s \geq R$, i.e., it has a bounded support.

- Gaussian function

$$\alpha_0(s) = \exp\left(-\frac{s^2}{R^2}\right)$$

which is theoretically nonzero for an arbitrary large s and thus has an unbounded support. However, in the numerical implementation the value of α_0 is considered as zero for $s > 2.5R$.

- Exponential function

$$\alpha_0(s) = \exp\left(-\frac{s}{R}\right)$$

which also has an unbounded support, but is considered as zero for $s > 6R$. This function is sometimes called the Green function, because in 1D it corresponds to the Green function of the Helmholtz-like equation used by implicit gradient approaches.

- Piecewise constant function

$$\alpha_0(s) = \begin{cases} 1 & \text{if } s \leq R \\ 0 & \text{if } s > R \end{cases}$$

which corresponds to uniform averaging over a segment, disc or ball of radius R.

- Function that is constant over the finite element in which point $\boldsymbol{x}$ is located, and is zero everywhere else. Of course, this is not a physically objective definition of nonlocal averaging, since it depends on the discretization. However, this kind of averaging was proposed in a boundary layer by Prof. Bažant and was implemented into OOFEM for testing purposes.

- Special function

$$\alpha_0(s) = \int_{-\infty}^{\infty} \exp\left(-\frac{\sqrt{s^2+t^2}}{R}\right) \mathrm{d}t$$

obtained by reduction of the exponential function from 2D to 1D. The integral cannot be evaluated in closed form and is computed by OOFEM numerically. This function can be used in one-dimensional simulations of a two-dimensional specimen under uniaxial tension; for more details see [11].

The above functions depend only on the distance s between the interacting points and are not normalized. If the normalizing condition

$$\int_{V_\infty} \alpha(\boldsymbol{x}, \boldsymbol{\xi})\, \mathrm{d}\boldsymbol{\xi} = 1$$

is imposed in an infinite body V_∞, it is sufficient to scale α_0 by a constant and set

$$\alpha(\boldsymbol{x},\boldsymbol{\xi}) = \frac{\alpha_0(\|\boldsymbol{x}-\boldsymbol{\xi}\|)}{V_{r\infty}}$$

where

$$V_{r\infty} = \int_{V_\infty} \alpha_0(\|\boldsymbol{\xi}\|)\,\mathrm{d}\boldsymbol{\xi}$$

Constant $V_{r\infty}$ can be computed analytically depending on the specific type of weight function and the number of spatial dimensions in which the analysis is performed. Since the factor $1/V_{r\infty}$ can be incorporated directly in the definition of α_0, this case is referred to as "no scaling".

If the body of interest is finite (or even semi-infinite), the averaging integral can be performed only over the domain filled by the body, and the volume contributing to the nonlocal average at a point $\boldsymbol{x}$ near the boundary is reduced as compared to points $\boldsymbol{x}$ far from the boundary or in an infinite body. To make sure that the normalizing condition

$$\int_V \alpha(\boldsymbol{x},\boldsymbol{\xi})\,\mathrm{d}\boldsymbol{\xi} = 1$$

holds for the specific domain V, different approaches can be used. The standard approach defines the nonlocal weight function as

$$\alpha(\boldsymbol{x},\boldsymbol{\xi}) = \frac{\alpha_0(\|\boldsymbol{x}-\boldsymbol{\xi}\|)}{V_r(\boldsymbol{x})}$$

where

$$V_r(\boldsymbol{x}) = \int_V \alpha_0(\|\boldsymbol{x}-\boldsymbol{\xi}\|)\,\mathrm{d}\boldsymbol{\xi}$$

According to the approach suggested by Borino, the weight function is defined as

$$\alpha(\boldsymbol{x},\boldsymbol{\xi}) = \frac{\alpha_0(\|\boldsymbol{x}-\boldsymbol{\xi}\|)}{V_{r\infty}} + \left(1 - \frac{V_r(\boldsymbol{x})}{V_{r\infty}}\right)\delta(\boldsymbol{x}-\boldsymbol{\xi})$$

where δ is the Dirac distribution. One can also say that the nonlocal variable is evaluated as

$$\bar{\varepsilon}(\boldsymbol{x}) = \frac{1}{V_{r\infty}}\int_V \alpha_0(\|\boldsymbol{x}-\boldsymbol{\xi}\|)\tilde{\epsilon}(\boldsymbol{\xi})\,\mathrm{d}\boldsymbol{\xi} + \left(1 - \frac{V_r(\boldsymbol{x})}{V_{r\infty}}\right)\tilde{\varepsilon}(\boldsymbol{x})$$

The term on the right-hand side after the integral is a multiple of the local variable, and so it can be referred to as the local complement.

In a recent paper [11], special techniques that modify the averaging procedure based on the distance from a physical boundary of the domain or on the stress state have been considered. The details are explained in [11]. These techniques can be invoked by setting the optional parameter *nlVariation* to 1, 2 or 3 and specifying additional parameters β and ζ for distance-based averaging, or β for stress-based averaging.

The model parameters are summarized in Tabs. 24 and 25.

Description	Nonlocal isotropic damage model for concrete in tension
Record Format	**Idmnl1** (in) # d(rn) # E(rn) # n(rn) # [tAlpha(rn) #] [equivstraintype(in) #] [k(rn) #] [damlaw(in) #] e0(rn) # [ef(rn) #] [At(rn) #] [Bt(rn) #] [md(rn) #] r(rn) # [regionMap(ia) #] [wft(in) #] [averagingType(in) #] [m(rn) #] [scalingType(in) #] [averagedQuantity(in) #] [nlVariation(in) #] [beta(rn) #] [zeta(rn) #] [maxOmega(rn) #]
Parameters	- material number - *d* material density - *E* Young's modulus - *n* Poisson's ratio - *tAlpha* thermal expansion coefficient - *equivstraintype* allows to choose from different definitions of equivalent strain, same as for the local model; see Tab. 23 - *k* ratio between uniaxial compressive and tensile strength, needed only if equivstraintype=3, default value 1 - *damlaw* allows to choose from different damage laws, same as for the local model; see Tab. 23 (note that parameter *wf* cannot be used for the nonlocal model) - *e0* strain at peak stress (for damage laws 0,1,2,3), limit elastic strain (for damage law 4), characteristic strain (for damage law 5) - *ef* strain parameter controling ductility, has the meaning of strain (for damage laws 0 and 1), the tangent modulus just after the peak is $E_t = -f_t/(\varepsilon_f - \varepsilon_0)$ - *At* parameter of Mazars damage law, used only by law 4 - *Bt* parameter of Mazars damage law, used only by law 4 - *md* exponent, used only by damage law 5, default value 1 - *r* nonlocal characteristic length R; its meaning depends on the type of weight function (e.g., interaction radius for the quartic spline) - *regionMap* map indicating the regions (currently region is characterized by cross section number) to skip for nonlocal avaraging. The elements and corresponding IP are not taken into account in nonlocal averaging process if corresponding regionMap value is nonzero. - *wft* selects the type of nonlocal weight function: 1 - default, quartic spline (bell-shaped function with bounded support) 2 - Gaussian function 3 - exponential function (Green function in 1D) 4 - uniform averaging up to distance R 5 - uniform averaging over one finite element 6 - special function obtained by reducing the 2D exponential function to 1D (by numerical integration) — *continued in Tab. 25* —

Table 24: Nonlocal isotropic damage model for tensile failure – summary.

Description	Nonlocal isotropic damage model for concrete in tension
	- *averagingType* activates a special averaging procedure, default value 0 does not change anything, value 1 means averaging over one finite element (equivalent to *wft*=5, but kept here for compatibility with previous version) - *m* multiplier for overnonlocal or undernonlocal formulation, which use *m*-times the local variable plus $(1-m)$-times the nonlocal variable, default value 1 - *scalingType* selects the type of scaling of the weight function (e.g. near a boundary): 1 - default, standard scaling with integral of weight function in the denominator 2 - no scaling (the weight function normalized in an infinite body is used even near a boundary) 3 - Borino scaling (local complement) - *averagedQuantity* selects the variable to be averaged, default value 1 corresponds to equivalent strain, value 2 activates averaging of compliance variable - *nlVariation* activates a special averaging procedure, default value 0 does not change anything, value 1 means distance-based averaging (the characteristic length is linearly reduced near a physical boundary), value 2 means stress-based averaging (the averaging is anisotropic and the characteristic length is affected by the stress), value 3 means distance-based averaging (the characteristic length is exponentially reduced near a physical boundary) - *beta* parameter β, required only for distance-based and stress-based averaging (i.e., for *nlVariation*=1, 2 or 3) - *zeta* parameter ζ, required only for distance-based averaging (i.e., for *nlVariation*=1 or 3) - *maxOmega* maximum damage, used for convergence improvement (its value is between 0 and 0.999999 (default), and it affects only the secant stiffness but not the stress)
Supported modes	3dMat, PlaneStress, PlaneStrain, 1dMat
Features	Adaptivity support

Table 25: Nonlocal isotropic damage model for tensile failure – continued.

1.5.8 Anisotropic damage model - Mdm

Local formulation The concept of isotropic damage is appropriate for materials weakened by voids, but if the physical source of damage is the initiation and propagation of microcracks, isotropic stiffness degradation can be considered only as a first rough approximation. More refined damage models take into account the highly oriented nature of cracking, which is reflected by the anisotropic character of the damaged stiffness or compliance matrices.

A number of anisotropic damage formulations have been proposed in the literature. Here we use a model outlined by Jirásek [16], which is based on the principle of energy equivalence and on the construction of the inverse integrity tensor by integration of a scalar over all spatial directions. Since the model uses certain concepts from the microplane theory, it is called the microplane-based damage model (MDM).

The general structure of the MDM model is schematically shown in Fig. 7 and the basic equations are summarized in Tab. 26. Here, $\boldsymbol{\varepsilon}$ and $\boldsymbol{\sigma}$ are the (nominal) second-order strain and stress tensors with components ε_{ij} and σ_{ij}; $\boldsymbol{e}$ and $\boldsymbol{s}$ are first-order strain and stress tensors with components e_i and s_i, which characterize the strain and stress on "microplanes" of different orientations given by a unit vector $\boldsymbol{n}$ with components n_i; ψ is a dimensionless compliance parameter that is a scalar but can have different values for different directions $\boldsymbol{n}$; the symbol δ denotes a virtual quantity; and a sumperimposed tilde denotes an effective quantity, which is supposed to characterize the state of the intact material between defects such as microcracks or voids.

Table 26: Basic equations of microplane-based anisotropic damage model

$\tilde{\boldsymbol{e}} = \tilde{\boldsymbol{\varepsilon}} \cdot \boldsymbol{n}$	$\boldsymbol{s}^T = \psi \boldsymbol{s}$	$\boldsymbol{s} = \boldsymbol{\sigma} \cdot \boldsymbol{n}$
$\tilde{\boldsymbol{\sigma}} : \delta\tilde{\boldsymbol{\varepsilon}} = \dfrac{3}{2\pi} \displaystyle\int_\Omega \boldsymbol{s}^T \cdot \delta\tilde{\boldsymbol{e}}\, \mathrm{d}\Omega$	$\delta\boldsymbol{s} \cdot \boldsymbol{e} = d\boldsymbol{s}^T \cdot \tilde{\boldsymbol{e}}$	$\delta\boldsymbol{\sigma} : \boldsymbol{\varepsilon} = \dfrac{3}{2\pi} \displaystyle\int_\Omega \delta\boldsymbol{s} \cdot \boldsymbol{e}\, \mathrm{d}\Omega$
$\tilde{\boldsymbol{\sigma}} = \dfrac{3}{2\pi} \displaystyle\int_\Omega (\boldsymbol{s}^T \otimes \boldsymbol{n})_{\mathrm{sym}}\, \mathrm{d}\Omega$	$\boldsymbol{e} = \psi \tilde{\boldsymbol{e}}$	$\boldsymbol{\varepsilon} = \dfrac{3}{2\pi} \displaystyle\int_\Omega (\boldsymbol{e} \otimes \boldsymbol{n})_{\mathrm{sym}}\, \mathrm{d}\Omega$

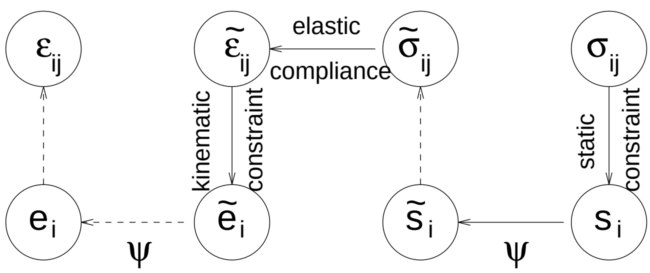

Figure 7: Structure of microplane-based anisotropic damage model

Combining the basic equations, it is possible to show that the components of the damaged material compliance tensor are given by

$$C_{ijkl} = M_{pqij} M_{rskl} C^e_{pqrs} \tag{80}$$

where C^e_{pqrs} are the components of the elastic material compliance tensor,

$$M_{ijkl} = \tfrac{1}{4}\left(\psi_{ik}\delta_{jl} + \psi_{il}\delta_{jk} + \psi_{jk}\delta_{il} + \psi_{jl}\delta_{ik}\right) \tag{81}$$

are the components of the so-called damage effect tensor, and

$$\psi_{ij} = \frac{3}{2\pi}\int_\Omega \psi\, n_i n_j \,\mathrm{d}\Omega \tag{82}$$

are the components of the second-order inverse integrity tensor. The integration domain Ω is the unit hemisphere. In practice, the integral over the unit hemisphere is evaluated by summing the contribution from a finite number of directions, according to one of the numerical integration schemes that are used by microplane models.

The scalar variable ψ characterizes the relative compliance in the direction given by the vector $\boldsymbol{n}$. If ψ is the same in all directions, the inverse integrity tensor evaluated from (82) is equal to the unit second-order tensor (Kronecker delta) multiplied by ψ, the damage effect tensor evaluated from (81) is equal to the symmetric fourth-order unit tensor multiplied by ψ, and the damaged material compliance tensor evaluated from (80) is the elastic compliance tensor multiplied by ψ^2. The factor multiplying the elastic compliance tensor in the isotropic damage model is $1/(1-\omega)$, and so ψ corresponds to $1/\sqrt{1-\omega}$. In the initial undamaged state, $\psi = 1$ in all directions. The evolution of ψ is governed by the history of the projected strain components. In the simplest case, ψ is driven by the normal strain $e_N = \boldsymbol{\varepsilon}_{ij} n_i n_j$. Analogy with the isotropic damage model leads to the damage law

$$\psi = f(\kappa) \tag{83}$$

and loading-unloading conditions

$$g(e_N, \kappa) \equiv e_N - \kappa \le 0, \qquad \dot\kappa \ge 0, \qquad \dot\kappa g(e_N, \kappa) = 0 \tag{84}$$

in which κ is a history variable that represents the maximum level of normal strain in the given direction ever reached in the previous history of the material. An appropriate modification of the exponential softening law leads to the damage law

$$f(\kappa) = \begin{cases} 1 & \text{if } \kappa \le e_0 \\ \sqrt{\frac{\kappa}{e_0}\exp\left(\frac{\kappa - e_0}{e_f - e_0}\right)} & \text{if } \kappa > e_0 \end{cases} \tag{85}$$

where e_0 is a parameter controlling the elastic limit, and $e_f > e_0$ is another parameter controlling ductility. Note that softening in a limited number of directions does not necessarily lead to softening on the macroscopic level, because the response in the other directions remains elastic. Therefore, e_0 corresponds to the elastic limit but not to the state at peak stress.

If the MDM model is used in its basic form described above, the compressive strength turns out to depend on the Poisson ratio and, in applications to concrete, its value is too low compared to the tensile strength. The model is designed primarily for tensile-dominated failure, so the low compressive strength is not considered as a major drawback. Still, it is desirable to introduce a modification that would prevent spurious compressive failure in problems where moderate compressive stresses appear. The desired effect is achieved by redefining the projected strain e_N as

$$e_N = \frac{\boldsymbol{\varepsilon}_{ij} n_i n_j}{1 - \dfrac{m}{Ee_0}\sigma_{kk}} \tag{86}$$

where m is a nonnegative parameter that controls the sensitivity to the mean stress, σ_{kk} is the trace of the stress tensor, and the normalizing factor Ee_0 is introduced in order to render the parameter m dimensionless. Under compressive stress states (characterized by $\sigma_{kk} < 0$), the denominator in (86) is larger than 1, and the projected strain is reduced, which also leads to a reduction of damage. A typical recommended value of parameter m is 0.05.

Nonlocal formulation Nonlocal formulation of the MDM model is based on the averaging of the inverse integrity tensor. This roughly corresponds to the nonlocal isotropic damage model with averaging of the compliance variable $\gamma = \omega/(1-\omega)$, which does not cause any spurious locking effects. In equation (81) for the evaluation of the damage effect tensor, the inverse integrity tensor is replaced by its weighted average with components

$$\bar{\psi}_{ij}(\boldsymbol{x}) = \int_V \alpha(\boldsymbol{x}, \boldsymbol{\xi}) \psi_{ij}(\boldsymbol{\xi}) \mathrm{d}\boldsymbol{\xi} \tag{87}$$

By fitting a wide range of numerical results, it has been found that the parameters of the nonlocal MDM model can be estimated from the measurable material properties using the formulas

$$\lambda_f = \frac{EG_f}{Rf_t^2} \tag{88}$$

$$\lambda = \frac{\lambda_f}{1.47 - 0.0014\lambda_f} \tag{89}$$

$$e_0 = \frac{f_t}{(1-m)E(1.56 + 0.006\lambda)} \tag{90}$$

$$e_f = e_0[1 + (1-m)\lambda] \tag{91}$$

where E is Young's modulus, G_f is the fracture energy, f_t is the uniaxial tensile strength, m is the compressive correction factor, typically chosen as $m = 0.05$, and R is the radius of nonlocal interaction reflecting the internal length of the material.

Input Record The model description and parameters are summarized in Tab. 27.

Description	MDM Anisotropic damage model
Record Format Parameters	Common parameters **Mdm** d$_{(rn)}$ # nmp$_{(ins)}$ # talpha$_{(rn)}$ # parmd$_{(rn)}$ # nonloc$_{(in)}$ # formulation$_{(in)}$ # mode$_{(in)}$ # -*num* material model number - D material density - *nmp* number of microplanes used for hemisphere integration, supported values are 21,28, and 61 - *talpha* thermal dillatation coeff - *parmd* - *nonloc* - *formulation* - *mode*
Nonlocal variant I Additional params	 r$_{(rn)}$ # efp$_{(rn)}$ # ep$_{(rn)}$ # -r nonlocal interaction radius -*efp* $\varepsilon_f p$ is a model parameter that controls the post-peak slope $\varepsilon_f p = \varepsilon_f - \varepsilon_0$, where ε_f is strain at zero stress level. -*ep* max effective strain at peak ε_0
Nonlocal variant II Additional params	 r$_{(rn)}$ # gf$_{(rn)}$ # ft$_{(rn)}$ # -r nonlocal intraction radius -*gf* fracture energy -*ft* tensile strength
Local variant I Additional params	 efp$_{(rn)}$ # ep$_{(rn)}$ # -*efp* $\varepsilon_f p$ is a model parameter that controls the post-peak slope $\varepsilon_f p = \varepsilon_f - \varepsilon_0$, where ε_f is strain at zero stress level. -*ep* max effective strain at peak ε_0
Local variant II Additional params	 gf$_{(rn)}$ # ep$_{(rn)}$ # -*gf* fracture energy -*ep* max effective strain at peak ε_0
Supported modes Features	3dMat, PlaneStress Adaptivity support

Table 27: MDM model - summary.

1.5.9 Isotropic damage model for interfaces

The model provides an interface law which can be used to describe a damageable interface between two materials (e.g. between steel reinforcement and concrete). The law is formulated in terms of the traction vector and the displacement jump vector. The basic response is elastic, with stiffness kn in the normal direction and ks in the tangential direction. Similar to other isotropic damage models, this model assumes that the stiffness degradation is isotropic, i.e., both stiffness moduli decrease proportionally and independently of the loading direction. The damaged stiffnesses are $kn \times (1-\omega)$ and $ks \times (1-\omega)$ where ω is a scalar damage variable. The damage evolution law is postulated in an explicit form, relating the damage variable ω to the largest previously reached equivalent "strain" level, κ.

The equivalent "strain", $\tilde{\varepsilon}$, is a scalar measure of the displacement jump vector. The choice of the specific expression for the equivalent strain affects the shape of the elastic domain in the strain space and plays a similar role to the choice of a yield condition in plasticity. Currently, in the present implementation, the equivalent strain is given by

$$\tilde{\varepsilon} = \sqrt{\langle w_n \rangle^2 + \beta w_s^2}$$

where $\langle w_n \rangle$ is the positive part of the normal displacement jump (opening of the interface) and w_s is the norm of the tangential part of displacement jump (sliding of the interface). Parameter β is optional and its default value is 0, in which case damage depends on the opening only (not on the sliding). The dependence of damage ω on maximum equivalent strain κ is described by the following damage law which corresponds to exponential softening:

$$\omega = \begin{cases} 0 & \text{for } \kappa \leq \varepsilon_0 \\ 1 - \dfrac{\varepsilon_0}{\kappa} \exp\left(-\dfrac{f_t(\kappa - \varepsilon_0)}{G_f}\right) & \text{for } \kappa > \varepsilon_0 \end{cases}$$

Here, $\varepsilon_0 = f_t/k_n$ is the value of equivalent strain at the onset of damage. Note that if the interface is subjected to shear traction only (with zero or negative normal traction), the propagation of damage starts when the magnitude of the sliding displacement is $|w_s| = \varepsilon_0/\sqrt{\beta}$, i.e., when the magnitude of the shear traction is equal to

$$f_s = \frac{k_s \varepsilon_0}{\sqrt{\beta}} = f_t \frac{k_s}{k_n \sqrt{\beta}}$$

So the ratio between the shear strength and tensile strength of the interface, f_s/f_t, is equal to $k_s/k_n\sqrt{\beta}$.

The model parameters are summarized in Tab. 28.

1.5.10 Isotropic damage model for interfaces using tabulated data for damage

The model provides an interface law which can be used to describe a damageable interface between two materials (e.g. between steel reinforcement and concrete). The law is formulated in terms of the traction vector and the displacement jump vector. The basic response is elastic, with stiffness kn in the normal direction and ks in the tangential direction. Similar to other isotropic damage models,

Description	Isotropic damage model for concrete in tension
Record Format Parameters	**isointrfdm01** kn(rn) # ks(rn) # ft(rn) # gf(rn) # [maxomega(rn) #] talpha(rn) # d(rn) # - *d* material density - *tAlpha* thermal dilatation coefficient - *kn* elastic stifness in normal direction - *ks* elastic stifness in tangential direction - *ft* tensile strength - *gf* fracture energy - [*maxomega*] maximum damage, used for convergence improvement (its value is between 0 and 0.999999 (default), and it affects only the secant stiffness but not the stress) - [*beta*] parameter controlling the effect of sliding part of displacement jump on equivalent strain, default value 0
Supported modes	2dInterface, 3dInterface
Features	

Table 28: Isotropic damage model for interface elements – summary.

this model assumes that the stiffness degradation is isotropic, i.e., both stiffness moduli decrease proportionally and independently of the loading direction. The damaged stiffnesses are $kn \times (1-\omega)$ and $ks \times (1-\omega)$ where ω is a scalar damage variable.

The equivalent "strain", $\tilde{\varepsilon}$, is a scalar measure derived from the displacement jump vector. The choice of the specific expression for the equivalent strain affects the shape of the elastic domain in the strain space and plays a similar role to the choice of a yield condition in plasticity. Currently, in the present implementation, $\tilde{\varepsilon}$ is equal to the positive part of the normal displacement jump (opening of the interface).

The damage evolution law is postulated in a separate file that should have the following format. Each line should contain one strain, damage pair separated by a whitespace character. The exception to this is the first line which should contain a single integer stating how many strain, damage pairs that the file will contain. The strains given in the file is defined as the equivalent strain minus the limit of elastic deformation. To find the damage for arbitrary strains linear interpolation between the tabulated values is used. If a strain larger than one in the given table is achieved the respective damage for the largest tabulated strain will be used. Both the strains and damages must be given in a strictly increasing order.

The model parameters are summarized in Tab. 29.

1.6 Material models specific to concrete

1.6.1 Mazars damage model for concrete - MazarsModel

This isotropic damage model assumes that the stiffness degradation is isotropic, i.e., stiffness moduli corresponding to different directions decrease proportionally and independently of direction of loading. It introduces two damage parameters ω_t and ω_c that are computed from the same equivalent strain using two different damage functions g_t and g_c. The g_t is identified from the uniaxial tension tests, while g_c from compressive test. The damage parameter for general stress states

Description	Isotropic damage model for concrete in tension
Record Format	**isointrfdm02** kn(rn) # ks(rn) # ft(rn) # tablename(rn) # [maxomega(rn) #] talpha(rn) # d(rn) #
Parameters	- *d* material density - *tAlpha* thermal dilatation coefficient - *kn* elastic stifness in normal direction - *ks* elastic stifness in tangential direction - *ft* tensile strength - *tablename* file name of the table with the strain damage pairs - *maxomega* maximum damage, used for convergence improvement (its value is between 0 and 0.999999 (default), and it affects only the secant stiffness but not the stress)
Supported modes	2dInterface, 3dInterface
Features	

Table 29: Isotropic damage model for interface elements using tabulated data for damage – summary.

ω is obtained as a linear combination of ω_t and ω_c: $\omega = \alpha_t g_t + \alpha_c g_c$, where the coefficients α_t and α_c take into account the character of the stress state. The damaged stiffness tensor is expressed as $\boldsymbol{D} = (1-\omega)\boldsymbol{D}^e$. Damage evolution law is postulated in an explicit form, relating damage parameter and scalar measure of largest reached strain level in material, taking into account the principle of preserving of fracture energy G_f. The equivalent strain, i.e., a scalar measure of the strain level is defined as norm from positive principal strains. The model description and parameters are summarized in Tab. 30.

1.6.2 Nonlocal Mazars damage model for concrete - MazarsModelnl

The nonlocal variant of Mazars damage model for concrete. Model based on nonlocal averaging of equivalent strain. The nonlocal averaging acts as a powerful localization limiter. The bell-shaped nonlocal averaging function is used. The model description and parameters are summarized in Tab. 31.

1.6.3 CebFip78 model for concrete creep with aging - CebFip78

Implementation of aging viscoelastic model for concrete creep according to the CEB-FIP Model Code. The model parameters are summarized in Tab. 32.

1.6.4 Double-power law model for concrete creep with aging - DoublePowerLaw

Implementation of aging viscoelastic model for concrete creep with compliance function given by the double-power law. The model parameters are summarized in Tab. 33.

1.6.5 Eurocode 2 model for concrete creep and shrinkage - EC2CreepMat

Implementation of aging viscoelastic model for concrete creep according to Eurocode 2 for concrete structures The model parameters are summarized in Tab. 34.

Description	Mazars damage model for concrete
Record Format	**MazarsModel** d$_{(rn)}$ # E$_{(rn)}$ # n$_{(rn)}$ # e0$_{(rn)}$ # ac$_{(rn)}$ # [bc$_{(rn)}$ #] [beta$_{(rn)}$ #] at$_{(rn)}$ # [bt$_{(rn)}$ #] [hreft$_{(rn)}$ #] [hrefc$_{(rn)}$ #] [version$_{(in)}$ #] [tAlpha$_{(rn)}$ #] [equivstrain-type$_{(in)}$ #] [maxOmega$_{(rn)}$ #]
Parameters	- *num* material model number - *d* material density - *E* Young modulus - *n* Poisson ratio - *e0* max effective strain at peak - *ac*,*bc* material parameters related to the shape of uniaxial compression curve (A sample set used by Saouridis is $A_c = 1.34, B_c = 2537$ - *beta* coefficient reducing the effect of damage under response under shear. Default value set to 1.06 - *at*, [*bt*] material parameters related to the shape of uniaxial tension curve. Meaning dependent on *version* parameter. - *hreft*, *hrefc* reference characteristic lengths for tension and compression. The material parameters are specified for element with these characteristic lengths. The current element then will have the same COD (Crack Opening Displacement) as reference one. - *version* Model variant. if 0 specified, the original form $g_t = 1.0 - (1.0 - A_t) * \varepsilon_0/\kappa - A_t * \exp(-B_t * (\kappa - \varepsilon_0))$; of tension damage evolution law is used, if equal 1, the modified law used which asymptotically tends to zero $g_t = 1.0 - (\varepsilon_0/\kappa) * \exp((\varepsilon_0 - \kappa)/\varepsilon_f)$ - *tAlpha* thermal dilatation coefficient - *equivstraintype* see Tab. 23 - *maxOmega* limit maximum damage, use for convergency improvement
Supported modes	3dMat, PlaneStress, PlaneStrain, 1dMat

Table 30: Mazars damage model – summary.

According to EC2, the compliance function is defined using the creep coefficient φ as

$$J(t,t') = \frac{1}{E(t')} + \frac{\varphi(t,t')}{1.05E_{cm}} \tag{92}$$

where E_{cm} is the mean elastic modulus at the age of 28 days and $E(t')$ is the elastic modulus at the age of loading, t'.

Current implementation supports only linear creep which is valid only for stresses below 0.45 of the characteristic compressive strength at the time of loading.

The elastic modulus at age t (in days) is defined as

$$E(t) = \left[\exp\left(s\left(1 - \sqrt{28/t}\right)\right)\right]^{0.3} E_{cm} \tag{93}$$

Description	Nonlocal Mazars damage model for concrete
Record Format	**MazarsModelnl** r(rn) # E(rn) # n(rn) # e0(rn) # ac(rn) # bc(rn) # beta(rn) # version(in) # at(rn) # [bt(rn) #] r(rn) # tAlpha(rn) #
Parameters	- *num* material model number - *d* material density - *E* Young modulus - *n* Poisson ratio - *maxOmega* limit maximum damage, use for convergency improvement - *tAlpha* thermal dilatation coefficient - *version* Model variant. if 0 specified, the original form $g_t = 1.0 - (1.0 - A_t) * \varepsilon_0/\kappa - A_t * \exp(-B_t * (\kappa - \varepsilon_0))$; of tension damage evolution law is used, if equal 1, the modified law used which asymptotically tends to zero $g_t = 1.0 - (\varepsilon_0/\kappa) * \exp((\varepsilon_0 - \kappa)/A_t)$ - *ac*,*bc* material parameters related to the shape of uniaxial compression curve (A sample set used by Saouridis is $A_c = 1.34, B_c = 2537$ - *at*, [*bt*] material parameters related to the shape of uniaxial tension curve. Meaning dependent on *version* parameter. - *beta* coefficient reducing the effect of damage under response under shear. Default value set to 1.06 - *r* parameter specifying the width of nonlocal averaging zone
Supported modes	3dMat, PlaneStress, PlaneStrain, 1dMat

Table 31: Nonlocal Mazars damage model – summary.

Description	CebFip78 model for concrete creep with aging
Record Format	**CebFip78** n(rn) # relMatAge(rn) # E28(rn) # fibf(rn) # kap_a(rn) # kap_c(rn) # kap_tt(rn) # u(rn) #
Parameters	- *num* material model number - *E28* Young modulus at age of 28 days [MPa] - *n* Poisson ratio - *fibf* basic creep coefficient - *kap_a* coefficient of hydrometric conditions - *kap_c* coefficient of type of cement - *kap_tt* coeficient of temperature effects - *u* surface imposed to environment [mm^2]; temporary here; should be in crosssection level - *relmatage* relative material age
Supported modes	3dMat, PlaneStress, PlaneStrain, 1dMat, 2dPlateLayer,2dBeamLayer, 3dShellLayer

Table 32: CebFip78 material model – summary.

where s is a cement-type dependent constant (0.2 for class R, 0.25 for class N

Description	Double-power law model for concrete creep with aging
Record Format	**DoublePowerLaw** n(rn) # relMatAge(rn) # E28(rn) # fi1(rn) # m(rn) # n(rn) # alpha(rn) #
Parameters	- *num* material model number - *E28* Young modulus at age of 28 days [MPa] - *n* Poisson ratio - *fibf* basic creep coefficient - *m* coefficient - *n* coefficient - *alpha* coeficient - *relmatage* relative material age
Supported modes	3dMat, PlaneStress, PlaneStrain, 1dMat, 2dPlateLayer,2dBeamLayer, 3dShellLayer

Table 33: Double-power law model – summary.

and finally 0.38 for type S), and the mean secant elastic modulus at 28 days can be estimated from the mean compressive strength

$$E_{cm} = 22\ (0.1 f_{cm,28})^{0.3} \tag{94}$$

where $f_{cm,28}$ is in MPa and the resulting modulus is in GPa.

The creep coefficient is given by the expression from Annex B of the standard.

$$\varphi(t,t') = \varphi_{RH} \times \frac{16.8}{f_{cm}} \times \frac{1}{0.1 + t'^{0.2}} \left(\frac{t - t'}{\beta_H + t - t'_T} \right)^{0.3} \tag{95}$$

with

$$\varphi_{RH} = \left(1 + \alpha_1 \frac{1 - h_{env}}{0.1\ (h_0)^{1/3}} \right) \times \alpha_2 \tag{96}$$

$$\beta_H = 1.5 \left(1 + (1.2 h_{env})^{18} \right) h_0 + 250\, \alpha_3 \le 1500\, \alpha_3 \tag{97}$$

and

$$\alpha_1 = \alpha_2 = \alpha_3 = 1 \quad \text{for } f_{cm} \le 35\,\text{MPa} \tag{98}$$

else

$$\alpha_1 = \left(\frac{35}{f_{cm}} \right)^{0.7} \tag{99}$$

$$\alpha_2 = \left(\frac{35}{f_{cm}} \right)^{0.2} \tag{100}$$

$$\alpha_3 = \left(\frac{35}{f_{cm}} \right)^{0.5} \tag{101}$$

and t'_T is the temperature-adusted age according to B.9 in the code. It is computed automatically if string *temperatureDependent* appears in the input record.

The shrinkage deformation is additively split into two parts: drying shrinkage $\varepsilon_{sh,d}$ and autogenous shrinkage $\varepsilon_{sh,a}$. Drying shrinkage strain at time t is computed from

$$\varepsilon_{sh,d} = \frac{t - t_0}{t - t_0 + 0.04\, h^{3/2}}\, k_h\, \varepsilon_{sh,d,0} \tag{102}$$

where t_0 is the duration of curing, k_h is a thickness-dependent parameter and

$$\varepsilon_{sh,d,0} = 1.3175 \times 10^{-6} \left[(220 + 110\alpha_{ds1}) \exp\left(-0.1\alpha_{ds2}\, f_{cm}\right)\right] \left(1 - h_{env}^3\right) \tag{103}$$

with $\alpha_{ds1} = 3$ for cement class S, 4 for class N, and 6 for class R, and $\alpha_{ds2} = 0.13$ for cement class S, 0.12 for class N, and 0.11 for class R.

Autogenous shrinkage strain can be comptued as

$$\varepsilon_{sh,a} = 2.5\,(f_{cm} - 18) \left[1 - \exp\left(-0.2\sqrt{t}\right)\right] \times 10^{-6} \tag{104}$$

1.6.6 B3 and MPS models for concrete creep with aging

Model B3 is an aging viscoelastic model for concrete creep and shrinkage, developed by Prof. Bažant and coworkers. In OOFEM it is implemented in three different ways.

The first version, "B3mat", is kept in OOFEM for compatibility. It is based on an aging Maxwell chain. The moduli of individual units in the chain are evaluated in each step using the least-squares method.

The second, more recent version, is referred to as "B3solidmat". Depending on the specified input it exploits either a non-aging Kelvin chain combined with the solidification theory, or an aging Kelvin chain. It is extended to the so-called Microprestress-Solidification theory (MPS), which in this implementation takes into account only the effects of variable humidity on creep; the effects of temperature on creep are not considered. The underlying rheological chain consists of four serially coupled components. The solidifying Kelvin chain represents short-term creep; it is serially coupled with a non-aging elastic spring that reflects instantaneous deformation. Long-term creep is captured by an aging dashpot with viscosity dependent on the microprestress, the evolution of which is affected by changes of humidity. The last unit describes volumetric deformations (shrinkage and thermal strains). Drying creep is incorporated either by the "averaged cross-sectional approach", or by the "point approach".

The latest version is denoted as "MPS" and is based on the microprestress-solidification theory [28] [29] [30]. The rheological model consists of the same four components as in "B3solidmat", but now the implemented exponential algorithm is designed especially for the solidifying Kelvin chain, which is a special case of an aging Kelvin chain. This model takes into account both humidity and temperature effects on creep. Drying creep is incorporated exclusively by the so-called "point approach". The model can operate in four modes, controlled by the keyword $CoupledAnalysisType$. The first mode ($CoupledAnalysisType = 0$) solves only the basic creep and runs as a single problem, while the remaining three modes need to be run as a staggered problem with humidity and/or temperature analysis preceding the mechanical problem; both humidity and temperature fields are read when $CoupledAnalysisType = 1$, only the field of relative humidity is taken into account when $CoupledAnalysisType = 2$ and finally, only temperature when $CoupledAnalysisType = 3$.

The basic creep is in the microprestress-solidification theory influenced by the same four parameters q_1 - q_4 as in the model B3. Values of these parameters can be estimated from the composition of concrete mixture and its compressive strength using the following empirical formulae:

$$q_1 = 126.77 \bar{f}_c^{-0.5} \quad [10^{-6}/\text{MPa}] \tag{105}$$

$$q_2 = 185.4 c^{0.5} \bar{f}_c^{-0.9} \quad [10^{-6}/\text{MPa}] \tag{106}$$

$$q_3 = 0.29\,(w/c)^4\, q_2 \quad [10^{-6}/\text{MPa}] \tag{107}$$

$$q_4 = 20.3\,(a/c)^{-0.7} \quad [10^{-6}/\text{MPa}] \tag{108}$$

Here, $\bar{f}_c$ is the average compressive cylinder strength at age of 28 days [MPa], a, w and c is the weight of aggregates, water and cement per unit volume of concrete [kg/m^3].

The non-aging spring stiffness represents the asymptotic modulus of the material; it is equal to $1/q_1$. The solidifying Kelvin chain is composed of M Kelvin units with fixed retardation times τ_μ, $\mu = 1, 2, \ldots, M$, which form a geometric progression with quotient 10. The lowest retardation time τ_1 is equal to 0.3 $begoftimeofinterest$, the highest retardation time τ_M is bigger than 0.5 $endoftimeofinterest$. The chain also contains a spring with stiffness E_0^∞ (a special case of Kelvin unit with zero retardation time). Moduli E_μ^∞ of individual Kelvin units are determined such that the chain provides a good approximation of the non-aging micro-compliance function of the solidifying constituent, $\Phi(t - t') = q_2 \ln\left(1 + \left((t-t')/\lambda_0\right)^n\right)$, where $\lambda_0 = 1$ day and $n = 0.1$. The technique based on the continuous retardation spectrum leads to the following formulae:

$$\frac{1}{E_0^\infty} = q_2 \ln(1 + \tilde{\tau}_0) - \frac{q_2 \tilde{\tau}_0}{10\,(1 + \tilde{\tau}_0)} \qquad \text{where} \quad \tilde{\tau}_0 = \left(\frac{2\tau_1}{\sqrt{10}}\right)^{0.1} \tag{109}$$

$$\frac{1}{E_\mu^\infty} = (\ln 10) \frac{q_2 \tilde{\tau}_\mu\,(0.9 + \tilde{\tau}_\mu)}{10\,(1 + \tilde{\tau}_\mu)^2} \qquad \text{where} \quad \tilde{\tau}_\mu = (2\tau_\mu)^{0.1}, \qquad \mu = 1, 2, \ldots \tag{110}$$

Viscosities η_μ^∞ of individual Kelvin units are obtained from simple relation $\eta_\mu^\infty = \tau_\mu / E_\mu^\infty$. A higher accuracy is reached if all retardation times are in the end multiplied by the factor 1.35 and the last modulus E_M is divided by 1.2.

The actual viscosities η_μ and stiffnesses E_μ of the solidifying chain change in time according to $\eta_\mu(t) = v(t)\eta_\mu^\infty$ and $E_\mu(t) = v(t) E_\mu^\infty$, where

$$v(t) = \frac{1}{\frac{q_3}{q_2} + \left(\frac{\lambda_0}{t}\right)^m} \tag{111}$$

is the volume growth function, and exponent $m = 0.5$. In the case of variable temperature or humidity, the actual age of concrete t is replaced by the equivalent time t_e, which is obtained by integrating (114).

Evolution of viscosity of the aging dashpot is governed by the differential equation

$$\dot{\eta} + \frac{1}{\mu_S T_0} \left| T \frac{\dot{h}}{h} - \kappa_T k_T \dot{T} \right| (\mu_S \eta)^{p/(p-1)} = \frac{\psi_S}{q_4} \tag{112}$$

where h is the relative pore humidity, T is the absolute temperature [K], $T_0 = 298$ K is the room temperature, and parameter $p = 2$. Parameter k_T is different for monotonically increasing and for cyclic temperature, and is defined as

$$\kappa_T = \begin{cases} k_{Tm} & \text{if } T = T_{max} \text{ and } \dot{T} > 0 \\ k_{Tc} & \text{if } T < T_{max} \text{ or } \dot{T} \leq 0 \end{cases} \tag{113}$$

in which k_{Tm} [-] and k_{Tc} [-] are new parameters and $T_{\max}$ is the maximum temperature attained in the previous history of the material point.

Equation (112) differs from the one presented in the original work; it replaces the differential equation for microprestress, which is not used here. The evolution of viscosity can be captured directly, without the need for microprestress. What matters is only the relative humidity and temperature and their rates. Parameters c_0 and k_1 of the original MPS theory are replaced by $\mu_S = c_0 T_0^{p-1} k_1^{p-1} q_4 (p-1)^p$. The initial value of viscosity is defined as $\eta(t_0) = t_0/q_4$, where t_0 is age of concrete at the onset drying or when the temperature starts changing, in the present implementation it is set $relMatAge$ which corresponds to the material age when the material is cast.

As mentioned above, under variable humidity and temperature conditions the physical time t in function $v(t)$ describing evolution of the solidified volume is replaced by the equivalent time t_e. In a similar spirit, t is replaced by the solidification time t_s in the equation describing creep of the solidifying constituent, and by the reduced time t_r in equation $\mathrm{d}\varepsilon_f/\mathrm{d}t_r = \sigma/\eta(t)$ relating the flow strain rate to the stress. Factors transforming the physical time t into t_e, t_r and t_s are defined as follows:

$$\frac{dt_e}{dt} = \psi_e(t) = \beta_{eT}(T(t))\,\beta_{eh}(h(t)) \tag{114}$$

$$\frac{dt_r}{dt} = \psi_r(t) = \beta_{rT}(T(t))\,\beta_{rh}(h(t)) \tag{115}$$

$$\frac{dt_s}{dt} = \psi_s(t) = \beta_{sT}(T(t))\,\beta_{sh}(h(t)) \tag{116}$$

Functions describing the influence of temperature have the form

$$\beta_{eT}(T) = \exp\left[\frac{Q_e}{R}\left(\frac{1}{T_0} - \frac{1}{T}\right)\right] \tag{117}$$

$$\beta_{rT}(T) = \exp\left[\frac{Q_r}{R}\left(\frac{1}{T_0} - \frac{1}{T}\right)\right] \tag{118}$$

$$\beta_{sT}(T) = \exp\left[\frac{Q_s}{R}\left(\frac{1}{T_0} - \frac{1}{T}\right)\right] \tag{119}$$

motivated by the rate process theory. R is the universal gas constant and Q_e, Q_r, Q_s are activation energies for hydration, viscous processes and microprestress relaxation, respectively. Only the ratios Q_e/R, Q_r/R and Q_s/R have to be specified. Functions describing the influence of humidity have the form

$$\beta_{eh}(h) = \frac{1}{1 + [\alpha_e (1-h)]^4} \tag{120}$$

$$\beta_{rh}(h) = \alpha_r + (1-\alpha_r)\,h^2 \tag{121}$$

$$\beta_{sh}(h) = \alpha_s + (1-\alpha_s)\,h^2 \tag{122}$$

where α_e, α_r and α_s are parameters.

At sealed conditions (or $CoupledAnalysisType = 2$) the auxiliary coefficients $\beta_{eT} = \beta_{rT} = \beta_{sT} = 1$ while at room temperature (or with $CoupledAnalysisType = 3$) factors $\beta_{e,h} = \beta_{r,h} = \beta_{s,h} = 1$.

It turned out that both the size effect on drying creep as well as its delay behind drying shrinkage can be addressed through parameter p in the governing equation (112). In the experiments, the average (cross-sectional) drying creep is decreasing with specimen size. Unfortunately, for the standard value $p = 2$, the MPS model exhibits the opposite trend. For $p = \infty$ the size effect disappears, and for $p < 0$ it corresponds to the experiments. It should be noted that for negative or infinite values of p the underlying theory loses its original physical background. If the experimental data of drying creep measured on different sizes are missing, the exponent $p = \infty$ can be taken as a realistic estimate.

When parameter p is changed from its recommended value $p = 2$ it is advantageous to rewrite the governing differential equation to the following form

$$\dot{\eta}_f + \frac{k_3}{T_0} \left| T \frac{\dot{h}}{h} - \kappa_T \dot{T} \right| \eta_f^{\tilde{p}} = \frac{\psi_S}{q_4} \tag{123}$$

with newly introduced parameters

$$\tilde{p} = p/(p-1) \tag{124}$$

$$k_3 = \mu_S^{\frac{1}{p-1}} \tag{125}$$

With the "standard value" $p = 2$ (reverted size effect) the new parameter $\tilde{p}$ is also 2, for $p < 0$ (correct size effect) $\tilde{p} < 1$ and finally with $p = \infty$ the first parameter $\tilde{p} = 1$ and the second parameter k_3 becomes dimensionless. The other advantage of $\tilde{p} = 1$ is that the governing differential equation becomes linear and can be solved directly.

The rate of thermal strain is expressed as $\dot{\varepsilon}_T = \alpha_T \dot{T}$ and the rate of drying shrinkage strain as $\dot{\varepsilon}_{sh} = k_{sh} \dot{h}$, where both α_T and k_{sh} are assumed to be constant in time and independent of temperature and humidity.

There are two options to simulate the autogenous shrinkage in the MPS material model. The first one is according to the B4 model

$$\varepsilon_{sh,au,B4}(t_e) = \varepsilon_{sh,au,B4}^{\infty} \left[1 + \left(\frac{\tau_{au}}{t_e} \right)^{w/c/0.38} \right]^{-4.5} \tag{126}$$

and the second one is proposed in the Model Code 2010

$$\varepsilon_{sh,au,fib}(t_e) = \varepsilon_{sh,au,fib}^{\infty} \left(1 - \exp\left(-0.2 \sqrt{t_e} \right) \right) \tag{127}$$

For the normally hardening cement, the ultimate value of the autogenous shrinkage can be estimated from the composition using the empirical formula of the B4 model

$$\varepsilon_{sh,au,B4}^{\infty} = -210 \times 10^{-6} \left(\frac{a/c}{6} \right)^{-0.75} \left(\frac{w/c}{0.38} \right)^{-3.5} \tag{128}$$

Similarly, in the Model Code, the ultimate shrinkage strain can be estimated from the mean concrete strength at the age of 28 days and from the cement grade

$$\varepsilon^{\infty}_{sh,au,fib} = -\alpha_{as}\left(\frac{0.1 f_{cm}}{6 + 0.1 f_{cm}}\right)^{2.5} \times 10^{-6} \tag{129}$$

where α_{as} is 600 for cement grades 42.5 R and 52.5 R and N, 700 for 32.5 R and 42.5 N and 800 for 32.5 N.

The model description and parameters are summarized in Tab. 35 for "B3mat", in Tab. 36 for "B3solidmat", and in Tab. 37 for "MPS". Since some model parameters are determined from the composition and strength using empirical formulae, it is necessary to use the specified units (e.g. compressive strength always in MPa, irrespectively of the units used in the simulation for stress). For "B3mat" and "B3solidmat" it is strictly required to use the specified units in the material input record (stress always in MPa, time in days etc.). The "MPS" model is almost unit-independent, except for $\bar{f}_c$ in MPa and c in kg/m^3, which are used in empirical formulae.

For illustration, sample input records for the material considered in Example 3.1 of the creep book by Bažant and Jirásek is presented. The concrete mix is composed of 170 kg/m^3 of water, 450 kg/m^3 of type-I cement and 1800 kg/m^3 of aggregates, which corresponds to ratios $w/c = 0.3778$ and $a/c = 4$. The compressive strength is $\bar{f}_c = 45.4$ MPa. The concrete slab of thickness 200 mm is cured in air with initial protection against drying until the age of 7 days. Subsequently, the slab is exposed to an environment with relative humidity of 70%. The following input record can be used for the first version of the model (B3mat):

```
B3mat 1 n 0.2 d 0.  talpha 1.2e-5 relMatAge 28.  fc 45.4 cc 450.
w/c 0.3778 a/c 4.  t0 7.  timefactor 1.  alpha1 1.  alpha2 1.2 ks 1.
hum 0.7 vs 0.1 shmode 1
```

Parameter $\alpha_1 = 1$ corresponds to type-I cement, parameter $\alpha_2 = 1.2$ to curing in air, parameter $k_s = 1$ to an infinite slab. The volume-to-surface ratio is in this case equal to one half of the slab thickness and must be specified in meters, independently of the length units that are used in the finite element analysis (e.g., for nodal coordinates). The value of relMatAge must be specified in days. Parameter `relMatAge 28.` means that time 0 of the analysis corresponds to concrete age 28 days. If material B3mat is used, the finite element analysis must use days as the units of time (not only for relMatAge, but in general, e.g. for the time increments).

If only the basic creep (without shrinkage) should be computed, then the material input record reduces to following: `B3mat 1 n 0.2 d 0.  talpha 1.2e-5 relMatAge 28.  fc 45.4 cc 450.  w/c 0.3778 a/c 4.  t0 7.  timefactor 1.  shmode 0`

Now consider the same conditions for "B3solidmat". In all the examples below, the input record with the material description can start by

```
B3solidmat 1 d 2420.  n 0.2 talpha 12.e-6 begtimeofinterest 1.e-2
endtimeofinterest 3.e4 timefactor 86400.  relMatAge 28.
```

Parameters `begoftimeofinterest 1.e-2` and `endoftimeofinterest 3.e4` mean that the computed response (e.g., deflection) should be accurate in the range from 0.01 day to 30,000 days after load application. Parameter `timefactor 86400.` means that the time unit used in the finite element analysis is 1 second (because 1 day = 86,400 seconds). Note that the values of begtimeofinterest, endtimeofinterest and relMatAge are always specified in days, independently of the actual time units in the analysis. Parameter `EmoduliMode` is not specified, which means that the moduli of the Kelvin chain will be determined using the default method, based on the continuous retardation spectrum.

Additional parameters depend on the specific type of analysis:

1. Computing basic creep only, shrinkage not considered, parameters q_i estimated from composition.
   ```
   mode 0 fc 45.4 cc 450.  w/c 0.3778 a/c 4.
   t0 7.  microprestress 0 shmode 0
   ```

2. Computing basic creep only, shrinkage not considered, parameters q_i specified by the user.
   ```
   mode 1 q1 18.81 q2 126.9 q3 0.7494 q4 7.692
   microprestress 0 shmode 0
   ```

3. Computing basic creep only, shrinkage handled using the sectional approach, parameters estimated from composition.
   ```
   mode 0 fc 45.4 cc 450.  w/c 0.3778 a/c 4.  t0 7.
   microprestress 0 shmode 1 ks 1.  alpha1 1.  alpha2 1.2 hum 0.7
   vs 0.1
   ```

4. Computing basic creep only, shrinkage handled using the sectional approach, parameters specified by the user.
   ```
   mode 1 q1 18.81 q2 126.9 q3 0.7494 q4 7.692
   microprestress 0 shmode 1 ks 1.  q5 326.7 kt 28025 EpsSinf 702.4
   t0 7.  hum 0.7 vs 0.1
   ```

5. Computing basic creep only, shrinkage handled using the point approach (B3), parameters specified by the user.
   ```
   mode 1 q1 18.81 q2 126.9 q3 0.7494 q4 7.692
   microprestress 0 shmode 2 es0 ...  r ...  rprime ...  at ...
   ```

6. Computing drying creep, shrinkage handled using the point approach (MPS), parameters q_i estimated from composition.
   ```
   mode 0 fc 45.4 w/c 0.3778 a/c 4.  t0 7.  microprestress 1
   shmode 3 c0 1.  c1 0.2 tS0 7.  w_h 0.0476 ncoeff 0.182 a 4.867
   kSh 1.27258e-003
   ```

Finally consider the same conditions for "MPS material". In all the examples below, the input record with the material description can start by

```
mps 1 d 2420.  n 0.2 talpha 12.e-6 referencetemperature 296.
```

Additional parameters depend on the specific type of analysis:

1. Computing basic creep only, shrinkage not considered, parameters q_i estimated from composition and simulation time in days and stiffnesses in MPa.
   ```
   mode 0 fc 45.4 cc 450.  w/c 0.3778 a/c 4.  stiffnessFactor 1.e6
   timefactor 1.  lambda0 1.  begoftimeofinterest 1.e-2
   endoftimeofinterest 3.e4 relMatAge 28.  CoupledAnalysisType 0.
   ```

2. Computing basic creep only, shrinkage not considered, parameters q_i specified by user, simulation time in seconds and stiffnesses in Pa.
`mode 1 q1 18.81e-12 q2 126.9e-12 q3 0.7494e-12 q4 7.6926e-12 timefactor 1. lambda0 86400. begoftimeofinterest 864. endoftimeofinterest 2.592e9 relMatAge 2419200. CoupledAnalysisType 0.`

3. Computing both basic and drying creep, parameters q_i specified by user, simulation time in seconds and stiffnesses in MPa.
`mode 1 q1 18.81e-6 q2 126.9e-6 q3 0.7494e-6 q4 7.6926e-6 timefactor 1. lambda0 86400. begoftimeofinterest 864. endoftimeofinterest 2.592e9 relMatAge 2419200. CoupledAnalysisType 1.`
`ksh 0.0004921875. t0 2419200. kappaT 0.005051 mus 4.0509259e-8`

Final recommendations:

- to simulate basic creep without shrinkage it is possible to use all three models
  - B3mat with $shmode = 0$
  - B3Solidmat with $shmode = 0$ and $microprestress = 0$
  - MPS with $CoupledAnalysisType = 0$
- to simulate drying creep with shrinkage using "sectional approach", only the first material model (B3mat) is suitable can be used (with $shmode = 1$)
- to simulate drying creep without shrinkage using "sectional approach", only the first material model (B3mat) is suitable (with $shmode = 1$, $mode = 1$ and $EpsSinf = 0.0$)
- to simulate drying creep with shrinkage using "point approach" according to B3 model there are two options:
  - B3mat (with $shmode = 2$)
  - B3Solidmat (with $shmode = 2$)

  In order to suppress shrinkage set $es0 = 0.0$
- to simulate drying creep with shrinkage using "point approach" according to MPS model there are two options:
  - B3Solidmat (with $shmode = 3$)
  - MPS with $CoupledAnalysisType = 1$

  In order to suppress shrinkage set $kSh = 0.0$

1.6.7 MPS damage model

This model extends the model based on the Microprestress-Solidification theory, described in previous section and summarized in Tab. 37 for "MPS", by tensile cracking.

This extension uses the isotropic damage model with Rankine definition of the equivalent deformation defined as the biggest principal effective stress divided by the elastic modulus. The softening law cannot deal directly with the strain because due to creep strain increases and this would lead to further softening without additional loading.

Two different approaches are implemented. The first one, default, (#1) reduces the stiffness only in the directions of tension (in case the tensile strength is exceeded). A full stiffness is restored in compression and after unloading from tension.

The other approach (#2) is the standard isotropic damage model which reduces the stiffness equally in all directions independently of loading. This approach leads to faster convergence because the secant stiffness can be used instead of the incremental viscoelastic stiffness which must be used in the first approach. The second approach becomes useful when the loading is monotonic or when the benefit of the accelerated computation prevails over the consequences of the reduced/underestimated stiffness in compression.

Proper energy dissipation is guaranteed by the crack-band approach.

The following algorithm is used to compute the stress vector (in each time step and until the iteration criteria are met):

1. Compute effective stress

$$\sigma_{\text{eff},k+1} = \sigma_{\text{eff},k} + \bar{E}_k \boldsymbol{D}_\nu (\Delta\varepsilon_k - \Delta\varepsilon''_k - \Delta\varepsilon_{sh,k} - \Delta\varepsilon_{T,k}) \tag{130}$$

   where $\sigma_{\text{eff},k}$ is the effective stress vector in the preceding step, $\bar{E}_k$ is the incremental stiffness, $\boldsymbol{D}_\nu$ is a unit stiffness matrix and $\Delta\varepsilon_k$, $\Delta\varepsilon''_k$, $\Delta\varepsilon_{sh,k}$, $\Delta\varepsilon_{T,k}$ are the increments of the total strain, strain due to creep, shrinkage strain (sum of drying and autogenous shrinkage) and thermal strain, respectively.

2. Compute principal effective stresses $\sigma_{\text{eff},1}$, $\sigma_{\text{eff},2}$, $\sigma_{\text{eff},3}$

3. Evaluate equivalent deformation

$$\tilde{\varepsilon} = \max(\sigma_{\text{eff},1}, \sigma_{\text{eff},2}, \sigma_{\text{eff},3})/E \tag{131}$$

4. If the stress exceeds the material strength, initialize and fix the fracture parameters f_t and G_F (exponential softening assumed).

$$\varepsilon_{c,f} = \frac{G_f}{f_t\, h} \tag{132}$$

   where h is the characteristic length of the finite element in the direction of the biggest principal stress.

5. Evaluate corresponding damage if $\tilde{\varepsilon} > \varepsilon_0$

$$\omega = 1 - \frac{\varepsilon_0}{\tilde{\varepsilon}} \exp\left(-\frac{\tilde{\varepsilon} - \varepsilon_0}{\varepsilon_{c,f} - \varepsilon_0} \right) \tag{133}$$

6. Compute principal nominal stresses

   - approach #1:
     for $i = 1, 2, 3$
     if $\sigma_{\text{eff},i} > 0$, $\sigma_i = (1 - \omega)\sigma_{\text{eff},i}$
     else $\sigma_i = \sigma_{\text{eff},i}$
   - approach #2:
     for $i = 1, 2, 3$
     $\sigma_i = (1 - \omega)\sigma_{\text{eff},i}$

7. Construct the stress vector in the original configuration

$$\boldsymbol{\sigma} = \boldsymbol{T}\boldsymbol{\sigma}_{princ} \tag{134}$$

   where $\boldsymbol{T}$ is the stress transformation matrix.

The tensile strength and fracture energy can be defined either as fixed, time-independent values (parameters ft, gf) or as variable, depending on the equivalent hydration time t_e. The latter case is activated by keyword $timeDepFracturing$; tensile strength and fracture energy are then linked to the current value of the mean compressive strength using (slightly modified) formulae from the *fib* Model Code 2010.

For $0\,\text{MPa} \leq f_{cm}(t) \leq 20$ MPa the tensile strength is computed from a linear function

$$f_{tm}(t) = 0.015 \cdot 12^{2/3} \cdot f_{cm}(t) = 0.07862 f_{cm}(t) \tag{135}$$

which starts at the origin and at $f_{cm}(t) = 20$ MPa connects to expression

$$f_{tm}(t) = 0.3(f_{cm}(t) - 8\,\text{MPa})^{2/3} \tag{136}$$

which is valid for $20\,\text{MPa} \leq f_{cm}(t) \leq 58$ MPa. Finally, for $f_{cm}(t) > 58$ MPa

$$f_{tm}(t) = 2.12\,\ln(1 + 0.1 f_{cm}(t)) \tag{137}$$

Following the guidelines from the Model Code 2010 (section 5.1.5.2), the fracture energy G_f can be estimated from the mean compressive strength at 28 days using an empirical formula

$$G_{f,28} = 73 \times (f_{cm,28})^{0.18} \tag{138}$$

In this function, the mean compressive strength must be provided in MPa and the resulting fracture energy is in N/m.

The growth in fracture energy is approximately proportional to the tensile strength. The current value of fracture energy is very simply computed as

$$G_f(t) = G_{f,28} \times f_{tm}(t)/f_{tm,28}(28) \tag{139}$$

The development of the mean compressive strength in time is adopted entirely from the Model Code 2010 (see section 5.1.9.1)

$$f_{cm}(t) = f_{cm,28} \exp\left(fib\_s\, \left(1 - \sqrt{28/t_e}\right)\right) \tag{140}$$

where fib_s is a cement-type dependent coefficient (0.38 for cement 32.5 N; 0.25 for 32.5 R and 42.5 N; 0.2 for 42.5 R and 52.5 N and R), t_e is the equivalent age and $f_{cm,28}$ is the mean compressive strength at the age of 28 days.

For some concretes the prediction formulae do not provide accurate predictions, therefore it is possible to scale the evolution of tensile strength and fracture energy by providing their 28-day values *ft28* and *gf28*.

The model description and parameters are summarized in Tab. 38.

Description	EC2CreepMat model for concrete creep and shrinkage
Record Format	**EC2CreepMat** n$_{(rn)}$ # [begOfTimeOfInterest$_{(rn)}$ #] [endOfTimeOfInterest$_{(rn)}$ #] relMatAge$_{(rn)}$ # [timeFactor$_{(rn)}$ #] stiffnessFactor$_{(rn)}$ # [tAlpha$_{(rn)}$ #] fcm28$_{(rn)}$ # t0$_{(rn)}$ # cemType$_{(in)}$ # [henv$_{(rn)}$ #] h0$_{(rn)}$ # shType$_{(in)}$ # [spectrum] [temperatureDependent]
Parameters	- *num* material model number - *n* Poisson's ratio - *begOfTimeOfInterest* determines the shortest time which is reasonably well captured by the approximated compliance function (default value is 0.1); the units are the time units of the analysis - *endOfTimeOfInterest* determines the longest time which is reasonably well captured by the approximated compliance function (if not provided it is read from the engineering model); the units are the time units of the analysis - *relMatAge* time shift used to specify the age of material on the begging of the analysis, the meaning is the material age at time t = 0; - *timeFactor* scaling factor transforming the actual time into appropriate units needed by the formulae of the eurocode. For analysis in days timeFactor = 1, for analysis in seconds timeFactor = 86,400. - *stiffnessFactor* scaling factor transforming predicted stiffness into appropriate units of the analysis, for analysis in MPa stiffnessFactor = 1.e6 (default), for Pa stiffnessFactor = 1 - *fcm28* mean compressive strength measured on cylinders at the age of 28 days in MPa - *t0* duration of curing [day] (this is relevant only for drying shrinkage, not for creep) - *cemType* type of cement, 1 = class *R*, 2 = class *N*, 3 = class *S* - *henv* ambient relative humidity expressed as decimal - *h0* effective member thickness in [mm] calculated according to EC2 as 2×A/u where A is the cross-section are and u is the cross-section perimeter exposed to drying - *shType* shrinkage type; 0 = no shrinkage, 1 = both drying and autogenous shrinkage, 2 = drying shrinkage only, 3 = autogenous shrinkage only - *spectrum* this string switches on evaluation of the moduli of the aging Kelvin chain using the retardation spectrum of the compliance function, otherwise (default option) the least-squares method is used - *temperatureDependent* turns on the influence of temperature on concrete maturity (equivalent age concept) by default this option is not activated.
Supported modes	3dMat, PlaneStress, PlaneStrain, 1dMat, 2dPlateLayer,2dBeamLayer, 3dShellLayer

Table 34: EC2Creep material model – summary.

Description	B3 material model for concrete aging
Record Format	**B3mat** d$_{(rn)}$ # n$_{(rn)}$ # talpha$_{(rn)}$ # [begoftimeofinterest$_{(rn)}$ #] [endoftimeofinterest$_{(rn)}$ #] timefactor$_{(rn)}$ # relMatAge$_{(rn)}$ # [mode$_{(in)}$ #] fc$_{(rn)}$ # cc$_{(rn)}$ # w/c$_{(rn)}$ # a/c$_{(rn)}$ # t0$_{(rn)}$ # q1$_{(rn)}$ # q2$_{(rn)}$ # q3$_{(rn)}$ # q4$_{(rn)}$ # shmode$_{(in)}$ # ks$_{(rn)}$ # vs$_{(rn)}$ # hum$_{(rn)}$ # [alpha1$_{(rn)}$ #] [alpha2$_{(rn)}$ #] kt$_{(rn)}$ # EpsSinf$_{(rn)}$ # q5$_{(rn)}$ # es0$_{(rn)}$ # r$_{(rn)}$ # rprime$_{(rn)}$ # at$_{(rn)}$ # w_h$_{(rn)}$ # ncoeff$_{(rn)}$ # a$_{(rn)}$ #
Parameters	- *num* material model number - *d* material density - *n* Poisson ratio - *talpha* coefficient of thermal expansion - *begoftimeofinterest* optional parameter; lower boundary of time interval with good approximation of the compliance function [day]; default 0.1 day - *endoftimeofinterest* optional parameter; upper boundary of time interval with good approximation of the compliance function [day] - *timefactor* scaling factor transforming the simulation time units into days - *relMatAge* relative material age [day] - *mode* if *mode* = 0 (default value) creep and shrinkage parameters are predicted from composition; for *mode* = 1 parameters must be user-specified. - *fc* 28-day mean cylinder compression strength [MPa] - *cc* cement content of concrete [kg/m^3] - *w/c* ratio (by weight) of water to cementitious material - *a/c* ratio (by weight) of aggregate to cement - *t0* age when drying begins [day] - *q1*-*q4* parameters of B3 model for basic creep [1/TPa] - *shmode* shrinkage mode; 0 = no shrinkage; 1 = average shrinkage (the following parameters must be specified: *ks*, *vs*, *hum* and additionally *alpha1 alpha2* for *mode* = 0 and *kt EpsSinf q5 t0* for *mode* = 1; 2 = point shrinkage (needed: *es0*, *r*, *rprime*, *at*, *w_h*, *ncoeff*, *a*) - *ks* cross-section shape factor [-] - *vs* volume to surface ratio [m] - *hum* relative humidity of the environment [-] - *alpha1* shrinkage parameter – influence of cement type [-] - *alpha2* shrinkage parameter – influence of curing type [-] - *kt* shrinkage parameter [day/m^2] - *EpsSinf* shrinkage parameter [10^{-6}] - *q5* drying creep parameter [1/TPa] - *es0* final shrinkage at material point - *r*, *rprime* coefficients - *at* oefficient relating stress-induced thermal strain and shrinkage - *w_h*, *ncoeff*, *a* sorption isotherm parameters obtained from experiments [Pedersen, 1990]
Supported modes	3dMat, PlaneStress, PlaneStrain, 1dMat, 2dPlateLayer,2dBeamLayer, 3dShellLayer

Table 35: B3 creep and shrinkage model – summary.

Description	B3solid material model for concrete creep
Record Format	**B3solidmat** d$_{(rn)}$ # n$_{(rn)}$ # talpha$_{(rn)}$ # mode$_{(in)}$ # [EmoduliMode$_{(in)}$ #] Microprestress$_{(in)}$ # shm$_{(in)}$ # [begoftimeofinterest$_{(rn)}$ #] [endoftimeofinterest$_{(rn)}$ #] timefactor$_{(rn)}$ # relMatAge$_{(rn)}$ # fc$_{(rn)}$ # cc$_{(rn)}$ # w/c$_{(rn)}$ # a/c$_{(rn)}$ # t0$_{(rn)}$ # q1$_{(rn)}$ # q2$_{(rn)}$ # q3$_{(rn)}$ # q4$_{(rn)}$ # c0$_{(rn)}$ # c1$_{(rn)}$ # tS0$_{(rn)}$ # w_h$_{(rn)}$ # ncoeff$_{(rn)}$ # a$_{(rn)}$ # ks$_{(rn)}$ # [alpha1$_{(rn)}$ #] [alpha2$_{(rn)}$ #] hum$_{(rn)}$ # vs$_{(rn)}$ # q5$_{(rn)}$ # kt$_{(rn)}$ # EpsSinf$_{(rn)}$ # es0$_{(rn)}$ # r$_{(rn)}$ # rprime$_{(rn)}$ # at$_{(rn)}$ # kSh$_{(rn)}$ # inithum$_{(rn)}$ # finalhum$_{(rn)}$ #
Parameters	- *num* material model number - *d* material density - *n* Poisson ratio - *talpha* coefficient of thermal expansion - *mode* optional parameter; if *mode* = 0 (default), parameters $q1-q4$ are predicted from composition of the concrete mixture (parameters fc, cc, w/c, a/c and t0 need to be specified). Otherwise values of parameters $q1-q4$ are expected. - *EmoduliMode* optional parameter; analysis of retardation spectrum (= 0, default value) or least-squares method (= 1) is used for evaluation of Kelvin units moduli - *Microprestress* 0 = basic creep; 1 = drying creep (must be run as a staggered problem with preceding analysis of humidity diffusion. Parameter *shm* must be equal to 3. The following parameters must be specified: *c0*, *c1*, *tS0*, *w_h*, *ncoeff*, *a*) - *shmode* shrinkage mode; 0 = no shrinkage; 1 = average shrinkage (the following parameters must be specified: *ks*, *vs*, *hum* and additionally *alpha1 alpha2* for *mode* = 0 and *kt EpsSinf q5* for *mode* = 1; 2 = point shrinkage (needed: *es0*, *r*, *rprime*, *at*), *w_h ncoeff a*; 3 = point shrinkage based on MPS theory (needed: parameter *kSh* or value of *kSh* can be approximately determined if following parameters are given: *inithum*, *finalhum*, *alpha1* and *alpha2*) - *begoftimeofinterest* optional parameter; lower boundary of time interval with good approximation of the compliance function [day]; default 0.1 day - *endoftimeofinterest* optional parameter; upper boundary of time interval with good approximation of the compliance function [day] - *timefactor* scaling factor transforming the simulation time units into days - *relMatAge* relative material age [day]

	- *fc* 28-day mean cylinder compression strength [MPa] - *cc* cement content of concrete mixture [kg/m^3] - *w/c* water to cement ratio (by weight) - *a/c* aggregate to cement ratio (by weight) - *t0* age of concrete when drying begins [day] - *q1*, *q2*, *q3*, *q4* parameters (compliances) of B3 model for basic creep [1/TPa] - *c0* MPS theory parameter [MPa^{-1} day^{-1}] - *c1* MPS theory parameter [MPa] - *tS0* MPS theory parameter - time when drying begins [day] - *w_h*, *ncoeff*, *a* sorption isotherm parameters obtained from experiments [Pedersen, 1990] - *ks* cross section shape factor [-] - *alpha1* optional shrinkage parameter - influence of cement type (optional parameter, default value is 1.0) - *alpha2* optional shrinkage parameter - influence of curing type (optional parameter, default value is 1.0) - *hum* relative humidity of the environment [-] - *vs* volume to surface ratio [m] - *q5* drying creep parameter [1/TPa] - *kt* shrinkage parameter [day/m^2] - *EpsSinf* shrinkage parameter [10^{-6}] - *es0* final shrinkage at material point - *at* coefficient relating stress-induced thermal strain and shrinkage - *rprime*, *r* coefficients - *kSh* influences magnitude of shrinkage in MPS theory [-] - *inithum* [-], *finalhum* [-] if provided, approximate value of *kSh* can be computed
Supported modes	3dMat, PlaneStress, PlaneStrain, 1dMat, 2dPlateLayer, 2dBeamLayer, 3dShellLayer

Table 36: B3solid creep and shrinkage model – summary.

Description	Microprestress-solidification theory material model for concrete creep
Record Format	**mps** d(rn) # n(rn) # talpha(rn) # referencetemperature(rn) # mode(in) # [CoupledAnalysisType(in) #] [begoftimeofinterest(rn) #] [endoftimeofinterest(rn) #] timefactor(rn) # relMatAge(rn) # lambda0(rn) # fc(rn) # cc(rn) # w/c(rn) # a/c(rn) # stiffnessfactor(rn) # q1(rn) # q2(rn) # q3(rn) # q4(rn) # ksh(rn) # [mus(rn) #] k3(rn) # [alphaE(rn) #] [alphaR(rn) #] [alphaS(rn) #] [QEtoR(rn) #] [QRtoR(rn) #] [QStoR(rn) #] kTm(rn) # [kTc(rn) #] [p(rn) #] [p_tilde(rn) #] [alpha_as(rn) #] [eps_cas0(rn) #] [b4_eps_au_infty(rn) #] [b4_tau_au(rn) #] [b4_alpha(rn) #] [b4_r_t(rn) #] [b4_cem_type(rn) #] [temperInCelsius]
Parameters	- *num* material model number - *d* material density - *n* Poisson ratio - *talpha* coefficient of thermal expansion - *referencetemperature* reference temperature only to thermal expansion of material - *mode* optional parameter; if *mode* = 0 (default), parameters $q1 - q4$ are predicted from composition of the concrete mixture (parameters fc, cc, w/c, a/c and stiffnessfactor need to be specified). Otherwise values of parameters $q1 - q4$ are expected. - *CoupledAnalysisType* 0 = basic creep; 1 = (default) drying creep, shrinkage, temperature transient creep and creep at elevated temperature; 2 = drying creep, shrinkage; 3 = temperature transient creep and creep at elevated temperature; for choice # 1, 2, 3 the problem must be run as a staggered problem with preceding analysis of humidity and/or temperature distribution; Following parameters must be specified: *mus* or *k3* (according to exponent *p*), *kTm* (compulsory for choice #3 otherwise optional) - *lambda0* scaling factor equal to 1.0 day in time units of analysis (e.g. 86400 if the analysis runs in seconds) - *begoftimeofinterest* lower boundary of time interval with good approximation of the compliance function; default value = 0.01 $lambda0$ - *endoftimeofinterest* upper boundary of time interval with good approximation of the compliance function; default value = 10000. $lambda0$ - *timefactor* scaling factor, for mps material must be equal to 1.0 - *relMatAge* relative material age = age at time when the material is cast in the structure

	- *fc* 28-day standard cylinder compression strength [MPa] - *cc* cement content of concrete mixture [kg m^{-3}] - *w/c* water to cement weight ratio - *a/c* aggregate to cement weight ratio - *stiffnessfactor* scaling factor converting "predicted" parameters q_1 - q_4 into proper units (e.g. 1.0 if stiffness is measured in Pa, 1.e6 for MPa) - *q1*, *q2*, *q3*, *q4* parameters of B3 model for basic creep - *p* and *p_tilde* replaceable parameters in the governing equation for viscosity, default value is $p = 2$ - *mus* parameter governing to the evolution of viscosity; for exponent $p = 2$, $\mu_S = c_0 c_1 q_4$ [Pa^{-1} s^{-1}] - *k3* dimensionless parameter governing to the evolution of viscosity replacing *mus* in the special case when $p > 100$ (then p is automatically set to ∞ which is equivalent to $p\_tilde = 1$) - *ksh* parameter relating rate of shrinkage to rate of humidity [-], default value is 0.0, i.e. no shrinkage - *alphaE* constant, default value 10. - *alphaR* constant, default value 0.1 - *alphaS* constant, default value 0.1 - *QEtoR* activation energy ratio, default value 2700. K - *QRtoR* activation energy ratio, default value 5000. K - *QStoR* activation energy ratio, default value 3000. K - *kTm* replaces $\ln h$ in the governing equation for viscosity - *kTc* controls creep at cyclic temperature - *alpha_as* and *eps_cas0* control the ultimate value of autogenous shrinkage according to *fib* Model Code 2010; this ultimate value can be provided either directly via *eps_cas0* (negative value for contraction) or using *alpha_as*, see equation (129) - *b4_eps_au_infty*, *b4_tau_au*, *b4_alpha*, *b4_r_t*, *b4_cem_type* control the evolution and the ultimate value of autogenous shrinkage according to model B4; all parameters are predicted from composition if the *b4_cem_type* is provided; however, this prediction can be manually overridden - *temperInCelsius* this string enables to run the supplementary transport problem with temperature in Celsius instead of Kelvin
Supported modes	3dMat, PlaneStress, PlaneStrain, 1dMat, 2dPlateLayer, 2dBeamLayer, 3dShellLayer

Table 37: MPS theory—summary.

Description	MPS damage model for concrete creep with cracking **(additionaly all parameters from Table 37)**
Record Format	**MPSDamMat** [ft$_{(rn)}$ #] [gf$_{(rn)}$ #] [timeDepFracturing] [fib_s$_{(rn)}$ #] [ft28$_{(rn)}$ #] [gf28$_{(rn)}$ #] [damlaw$_{(in)}$ #] [isotropic] [checksnapback$_{(in)}$ #]
Parameters	- *ft* tensile strength (constant in time) - *gf* fracture energy (constant in time) - *timeDepFracturing* string activating *fib* MC 2010 prediction for tensile strength and fracture energy + their time evolution - *ft28* manual override for the *fib* MC 2010 prediction of hydration-dependent tensile strength - *gf28* manual override for the *fib* MC 2010 prediction of hydration-dependent fracture energy - *fib_s* cement-type dependent coefficient (compulsory with *timeDepFracturing*) - *damageLaw* traction-separation law: 0 = exponential softening (default), 1 = linear softening, 6 = damage disabled - *isotropic* string activating same reduction of stiffness after the onset of cracking both in in compression and tension (enables to use secant stiffness matrix for faster convergence) - *checkSnapBack* switch for snap-back checking; 1 = activated (default), 0 = deactiavated
Supported modes	3dMat, PlaneStress, PlaneStrain

Table 38: MPS damage–summary.

1.6.8 Microplane model M4 - Microplane_M4

Model M4 covers inelastic behavior of concrete under complex triaxial stress states. It is based on the microplane concept and can describe softening. However, objectivity with respect to element size is not ensured – the parameters need to be manually adjusted to the element size. Since the tangent stiffness matrix is not available, elastic stiffness is used. This can lead to a very slow convergence when used within an implicit approach. The model parameters are summarized in Tab. 39.

Description	M4 material model
Record Format	**Microplane_M4** nmp(in) # c3(rn) # c20(rn) # k1(rn) # k2(rn) # k3(rn) # k4(rn) # E(rn) # n(rn) #
Parameters	- *nmp* number of microplanes, supported values are 21, 28 and 61 - *n* Poisson ratio - *E* Young modulus - *c3*,*c20*, *k1*, *k2*, *k3*, *k4* model parameters
Supported modes	3dMat

Table 39: Microplane model M4 – summary.

1.6.9 Damage-plastic model for concrete - ConcreteDPM

This model, developed by Grassl and Jirásek for failure of concrete under general triaxial stress, is described in detail in [8]. It belongs to the class of damage-plastic models with yield condition formulated in terms of the effective stress $\bar{\boldsymbol{\sigma}} = \boldsymbol{D}_e : (\boldsymbol{\varepsilon} - \boldsymbol{\varepsilon}_p)$. The stress-strain law is postulated in the form

$$\boldsymbol{\sigma} = (1-\omega)\bar{\boldsymbol{\sigma}} = (1-\omega)\boldsymbol{D}_e : (\boldsymbol{\varepsilon} - \boldsymbol{\varepsilon}_p) \tag{141}$$

where $\boldsymbol{D}_e$ is the elastic stiffness tensor and ω is a scalar damage parameter. The plastic part of the model consists of a three-invariant yield condition, nonassociated flow rule and pressure-dependent hardening law. For simplicity, damage is assumed to be isotropic. In contrast to pure damage models with damage driven by the total strain, here the damage is linked to the evolution of plastic strain.

The **yield surface** is described in terms of the cylindrical coordinates in the principal effective stress space (Haigh-Westergaard coordinates), which are the volumetric effective stress $\bar{\sigma}_{\mathrm{V}} = I_1(\bar{\boldsymbol{\sigma}})/3$, the norm of the deviatoric effective stress $\bar{\rho} = \sqrt{2J_2(\bar{\boldsymbol{\sigma}})}$, and the Lode angle θ defined by the relation

$$\cos 3\theta = \frac{3\sqrt{3}}{2}\frac{J_3}{J_2^{3/2}} \tag{142}$$

where J_2 and J_3 are the second and third deviatoric invariants. The yield function

$$f_{\mathrm{p}}(\bar{\sigma}_{\mathrm{V}}, \bar{\rho}, \bar{\theta}; \kappa_{\mathrm{p}}) = \left([1 - q_{\mathrm{h}}(\kappa_{\mathrm{p}})] \left(\frac{\bar{\rho}}{\sqrt{6}\bar{f}_c} + \frac{\bar{\sigma}_{\mathrm{V}}}{\bar{f}_c} \right)^2 + \sqrt{\frac{3}{2}} \frac{\bar{\rho}}{\bar{f}_c} \right)^2 + $$
$$+ m_0 q_{\mathrm{h}}^2(\kappa_{\mathrm{p}}) \left(\frac{\bar{\rho} r(\bar{\theta})}{\sqrt{6}\bar{f}_c} + \frac{\bar{\sigma}_{\mathrm{V}}}{\bar{f}_c} \right) - q_{\mathrm{h}}^2(\kappa_{\mathrm{p}}) \tag{143}$$

depends on the effective stress (which enters in the form of cylindrical coordinates) and on the hardening variable κ_{p} (which enters through a dimensionless variable q_{h}). Parameter $\bar{f}_c$ is the uniaxial compressive strength. Note that, under uniaxial compression characterized by axial stress $\bar{\sigma} < 0$, we have $\bar{\sigma}_{\mathrm{V}} = \bar{\sigma}/3$, $\bar{\rho} = -\sqrt{2/3}\,\bar{\sigma}$ and $\bar{\theta} = 60^o$. The yield function then reduces to $f_{\mathrm{p}} = (\bar{\sigma}/\bar{f}_c)^2 - q_{\mathrm{h}}^2$. This means that function q_{h} describes the evolution of the uniaxial compressive yield stress normalized by its maximum value, $\bar{f}_c$.

The evolution of the yield surface during hardening is presented in Fig. 8. The parabolic shape of the meridians (Fig. 8a) is controlled by the hardening variable q_{h} and the friction parameter m_0. The initial yield surface is closed, which allows modeling of compaction under highly confined compression. The initial and intermediate yield surfaces have two vertices on the hydrostatic axis but the ultimate yield surface has only one vertex on the tensile part of the hydrostatic axis and opens up along the compressive part of the hydrostatic axis. The deviatoric sections evolve as shown in Fig. 8b, and their final shape at full hardening is a rounded triangle at low confinement and almost circular at high confinement. The shape of the deviatoric section is controlled by the Willam-Warnke function

$$r(\theta) = \frac{4(1-e^2)\cos^2\theta + (2e-1)^2}{2(1-e^2)\cos\theta + (2e-1)\sqrt{4(1-e^2)\cos^2\theta + 5e^2 - 4e}} \tag{144}$$

The eccentricity parameter e that appears in this function, as well as the friction parameter m_0, are calibrated from the values of uniaxial and equibiaxial compressive strengths and uniaxial tensile strength.

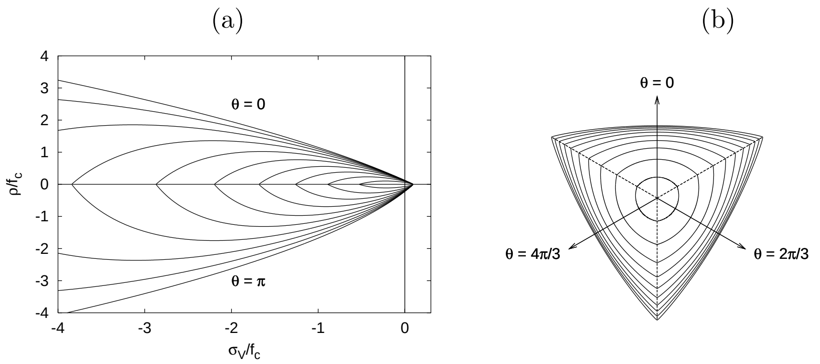

Figure 8: Evolution of the yield surface during hardening: a) meridional section, b) deviatoric section for a constant volumetric effective stress of $\bar{\sigma}_{\mathrm{V}} = -\bar{f}_c/3$

The maximum size of the elastic domain is attained when the variable q_{h} is equal to one (which is its maximum value, as follows from the hardening law, to be specified in (149)). The yield surface is then described by the equation

$$f_\mathrm{p}\left(\bar{\sigma}_\mathrm{V},\bar{\rho},\bar{\theta};1\right) \equiv \frac{3}{2}\frac{\bar{\rho}^2}{\bar{f}_c^2} + m_0\left(\frac{\bar{\rho}}{\sqrt{6}\bar{f}_c}r(\bar{\theta}) + \frac{\bar{\sigma}_\mathrm{V}}{\bar{f}_c}\right) - 1 = 0 \tag{145}$$

The **flow rule**

$$\dot{\boldsymbol{\varepsilon}}_\mathrm{p} = \dot{\lambda}\frac{\partial g_\mathrm{p}}{\partial \bar{\sigma}} \tag{146}$$

is non-associated, which means that the yield function f_p and the plastic potential

$$\begin{aligned} g_\mathrm{p}(\bar{\sigma}_\mathrm{V},\bar{\rho};\kappa_\mathrm{p}) \quad = \quad & \left([1-q_\mathrm{h}(\kappa_\mathrm{p})]\left(\frac{\bar{\rho}}{\sqrt{6}\bar{f}_c} + \frac{\bar{\sigma}_\mathrm{V}}{\bar{f}_c}\right)^2 + \sqrt{\frac{3}{2}}\frac{\bar{\rho}}{\bar{f}_c}\right)^2 + \\ & + q_\mathrm{h}^2(\kappa_\mathrm{p})\left(\frac{m_0\bar{\rho}}{\sqrt{6}\bar{f}_c} + \frac{m_\mathrm{g}(\bar{\sigma}_\mathrm{V})}{\bar{f}_c}\right) \end{aligned} \tag{147}$$

do not coincide and, therefore, the direction of the plastic flow $\partial g_\mathrm{p}/\partial\bar{\boldsymbol{\sigma}}$ is not normal to the yield surface. The ratio of the volumetric and the deviatoric parts of the flow direction is controled by function m_g, which depends on the volumetric stress and is defined as

$$m_\mathrm{g}(\bar{\sigma}_\mathrm{V}) = A_\mathrm{g}B_\mathrm{g}\bar{f}_c \exp\frac{\bar{\sigma}_\mathrm{V} - \bar{f}_t/3}{B_\mathrm{g}\bar{f}_c} \tag{148}$$

where A_g and B_g are model parameters that are determined from certain assumptions on the plastic flow in uniaxial tension and compression.

The dimensionless variable q_h that appears in the yield function (143) is a function of the hardening variable κ_p. It controls the size and shape of the yield surface and, thereby, of the elastic domain. The **hardening law** is given by

$$q_\mathrm{h}(\kappa_\mathrm{p}) = \begin{cases} q_{\mathrm{h}0} + (1-q_{\mathrm{h}0})\kappa_\mathrm{p}({\kappa_\mathrm{p}}^2 - 3\kappa_\mathrm{p} + 3) & \text{if } \kappa_\mathrm{p} < 1 \\ 1 & \text{if } \kappa_\mathrm{p} \geq 1 \end{cases} \tag{149}$$

The initial inclination of the hardening curve (at $\kappa_\mathrm{p} = 0$) is positive and finite, and the inclination at peak (i.e., at $\kappa_\mathrm{p} = 1$) is zero.

The evolution law for the hardening variable,[2]

$$\dot{\kappa}_\mathrm{p} = \frac{\|\dot{\boldsymbol{\varepsilon}}_\mathrm{p}\|}{x_\mathrm{h}\left(\bar{\sigma}_\mathrm{V}\right)}(2\cos\bar{\theta})^2 \tag{150}$$

sets the rate of the hardening variable equal to the norm of the plastic strain rate scaled by a hardening ductility measure

$$x_\mathrm{h}\left(\bar{\sigma}_\mathrm{V}\right) = \begin{cases} A_\mathrm{h} - (A_\mathrm{h} - B_\mathrm{h})\exp\left(-R_\mathrm{h}(\bar{\sigma}_\mathrm{V})/C_\mathrm{h}\right) & \text{if } R_\mathrm{h}(\bar{\sigma}_\mathrm{V}) \geq 0 \\ \\ E_\mathrm{h}\exp(R_\mathrm{h}(\bar{\sigma}_\mathrm{V})/F_\mathrm{h}) + D_\mathrm{h} & \text{if } R_\mathrm{h}(\bar{\sigma}_\mathrm{V}) < 0 \end{cases} \tag{151}$$

The dependence of the scaling factor x_h on the volumetric effective stress $\bar{\sigma}_\mathrm{V}$ is constructed such that the model response is more ductile under compression. The variable

$$R_\mathrm{h}(\bar{\sigma}_\mathrm{V}) = -\frac{\bar{\sigma}_\mathrm{V}}{\bar{f}_c} - \frac{1}{3} \tag{152}$$

[2] In the original paper [8], equation (150) was written with $\cos^2\bar{\theta}$ instead of $(2\cos\bar{\theta})^2$, but all the results presented in that paper were computed with OOFEM using an implementation based on (150).

is a linear function of the volumetric effective stress. Model parameters $A_{\mathrm{h}}, B_{\mathrm{h}}, C_{\mathrm{h}}$ and D_{h} are calibrated from the values of strain at peak stress under uniaxial tension, uniaxial compression and triaxial compression, whereas the parameters

$$E_{\mathrm{h}} = B_{\mathrm{h}} - D_{\mathrm{h}} \tag{153}$$

$$F_{\mathrm{h}} = \frac{(B_{\mathrm{h}} - D_{\mathrm{h}})\, C_{\mathrm{h}}}{B_{\mathrm{h}} - A_{\mathrm{h}}} \tag{154}$$

are determined from the conditions of a smooth transition between the two parts of equation (151) at $R_{\mathrm{h}} = 0$.

For the present model, the **evolution of damage** starts after full saturation of plastic hardening, i.e., at $\kappa_{\mathrm{p}} = 1$. This greatly facilitates calibration of model parameters, because the strength envelope is fully controled by the plastic part of the model and damage affects only the softening behavior. In contrast to pure damage models, damage is assumed to be driven by the plastic strain, more specifically by its volumetric part, which is closely related to cracking. To slow down the evolution of damage under compressive stress states, the damage-driving variable κ_{d} is not set equal to the volumetric plastic strain, but it is defined incrementally by the rate equation

$$\dot{\kappa}_{\mathrm{d}} = \begin{cases} 0 & \text{if } \kappa_{\mathrm{p}} < 1 \\ \mathrm{Tr}(\dot{\boldsymbol{\varepsilon}}_{\mathrm{p}})/x_{\mathrm{s}}\,(\bar{\sigma}_{\mathrm{V}}) & \text{if } \kappa_{\mathrm{p}} \geq 1 \end{cases} \tag{155}$$

where

$$x_{\mathrm{s}}(\bar{\sigma}_{\mathrm{V}}) = \begin{cases} 1 + A_{\mathrm{s}} R_{\mathrm{s}}^2(\bar{\sigma}_{\mathrm{V}}) & \text{if } R_{\mathrm{s}}(\bar{\sigma}_{\mathrm{V}}) < 1 \\ \\ 1 - 3A_{\mathrm{s}} + 4A_{\mathrm{s}}\sqrt{R_{\mathrm{s}}(\bar{\sigma}_{\mathrm{V}})} & \text{if } R_{\mathrm{s}}(\bar{\sigma}_{\mathrm{V}}) \geq 1 \end{cases} \tag{156}$$

is a softening ductility measure. Parameter A_{s} is determined from the softening response in uniaxial compression. The dimensionless variable $R_{\mathrm{s}} = \dot{\varepsilon}_{\mathrm{pV}}^{-}/\dot{\varepsilon}_{\mathrm{pV}}$ is defined as the ratio between the "negative" volumetric plastic strain rate

$$\dot{\varepsilon}_{\mathrm{pV}}^{-} = \sum_{I=1}^{3} \langle -\dot{\varepsilon}_{\mathrm{pI}} \rangle \tag{157}$$

and the total volumetric plastic strain rate $\dot{\varepsilon}_{\mathrm{pV}}$. This ratio depends only on the flow direction $\partial g_{\mathrm{p}}/\partial\bar{\boldsymbol{\sigma}}$, and thus R_{s} can be shown to be a unique function of the volumetric effective stress. In (157), $\dot{\varepsilon}_{\mathrm{pI}}$ are the principal components of the rate of plastic strains and $\langle\cdot\rangle$ denotes the McAuley brackets (positive-part operator). For uniaxial tension, for instance, all three principal plastic strain rates are nonnegative, and so $\dot{\varepsilon}_{\mathrm{pV}}^{-} = 0$, $R_{\mathrm{s}} = 0$ and $x_{\mathrm{s}} = 1$. This means that under uniaxial tensile loading we have $\kappa_{\mathrm{d}} = \kappa_{\mathrm{p}} - 1$. On the other hand, under compressive stress states the negative principal plastic strain rates lead to a ductility measure x_{s} greater than one and the evolution of damage is slowed down. It should be emphasized that the flow rule for this specific model is constructed such that the volumetric part of plastic strain rate at the ultimate yield surface cannot be negative.

The relation between the damage variable ω and the internal variable κ_{d} (maximum level of equivalent strain) is assumed to have the exponential form

$$\omega = 1 - \exp\left(-\kappa_{\mathrm{d}}/\varepsilon_f\right) \tag{158}$$

Description	Damage-plastic model for concrete
Record Format	**ConcreteDPM** d(rn) # E(rn) # n(rn) # tAlpha(rn) # ft(rn) # fc(rn) # wf(rn) # Gf(rn) # ecc(rn) # kinit(rn) # Ahard(rn) # Bhard(rn) # Chard(rn) # Dhard(rn) # Asoft(rn) # helem(rn) # href(rn) # dilation(rn) # yieldtol(rn) # newtoniter(in) #
Parameters	- *d* material density - *E* Young modulus - *n* Poisson ratio - *tAlpha* thermal dilatation coefficient - *ft* uniaxial tensile strength f_t - *fc* uniaxial compressive strength - *wf* parameter w_f that controls the slope of the softening branch (serves for the evaluation of $\varepsilon_f = w_f/h$ to be used in (158)) - *Gf* fracture energy, can be specified instead of wf, it is converted to $w_f = G_f/f_t$ - *ecc* eccentricity parameter e from (144), optional, default value 0.525 - *kinit* parameter $q_{\mathrm{h}0}$ from (149), optional, default value 0.1 - *Ahard* parameter A_{h} from (151), optional, default value 0.08 - *Bhard* parameter B_{h} from (151), optional, default value 0.003 - *Chard* parameter C_{h} from (151), optional, default value 2 - *Dhard* parameter D_{h} from (151), optional, default value 10^{-6} - *Asoft* parameter A_{s} from (156), optional, default value 15 - *helem* element size h, optional (if not specified, the actual element size is used) - *href* reference element size h_{ref}, optional (if not specified, the standard adjustment of the damage law is used) - *dilation* dilation factor (ratio between lateral and axial plastic strain rates in the softening regime under uniaxial compression), optional, default value -0.85 - *yieldtol* tolerance for the implicit stress return algorithm, optional, default value 10^{-10} - *newtoniter* maximum number of iterations in the implicit stress return algorithm, optional, default value 100
Supported modes	3dMat

Table 40: Damage-plastic model for concrete – summary.

where ε_f is a parameter that controls the slope of the softening curve. In fact, equation (158) is used by the nonlocal version of the damage-plastic model, with κ_{d} replaced by its weighted spatial average (not yet available in the public version of OOFEM). For the local model, it is necessary to adjust softening according to the element size, otherwise the results would suffer by pathological mesh sensitivity. It is assumed that localization takes place at the peak of the stress-strain diagram, i.e., at the onset of damage. After that, the strain is decomposed into the distributed part, which corresponds to unloading from peak, and the localized part, which is added if the material is softening. The localized part of strain is transformed into an equivalent crack opening, w, which is under uniaxial tension linked to the stress by the exponential law

$$\sigma = (1-\omega)f_t = f_t \exp\left(-w/w_f\right) \tag{159}$$

Here, f_t is the uniaxial tensile strength and w_f is the characteristic crack opening, playing a similar role to ε_f. Under uniaxial tension, the localized strain can be expressed as the sum of the post-peak plastic strain (equal to variable $\kappa_{\rm d}$) and the unloaded part of elastic strain (equal to $\omega f_t/E$). Denoting the effective element size as h, we can write

$$w = h(\kappa_{\rm d} + \omega f_t/E) \tag{160}$$

and substituting this into (159), we obtain a nonlinear equation

$$1-\omega = \exp\left(-\frac{h}{w_f}\left(\kappa_{\rm d} + \omega f_t/E\right)\right) \tag{161}$$

from which the damage variable ω corresponding to the given internal variable $\kappa_{\rm d}$ can be computed by Newton iteration. The effective element size h is obtained by projecting the element onto the direction of the maximum principal strain at the onset of cracking, and afterwards it is held fixed. The evaluation of ω from $\kappa_{\rm d}$ is no longer explicit, but the resulting load-displacement curve of a bar under uniaxial tension is totally independent of the mesh size. A simpler approach would be to use (158) with $\varepsilon_f = w_f/h$, but then the scaling would not be perfect and the shape of the load-displacement curve (and also the dissipated energy) would slightly depend on the mesh size. With the present approach, the energy per unit sectional area dissipated under uniaxial tension is exactly $G_f = w_f f_t$. The input parameter controling the damage law can be either the characteristic crack opening w_f, or the fracture energy G_f. If both are specified, w_f is used and G_f is ignored. If only G_f is specified, w_f is set to G_f/f_t.

The onset of damage corresponds to the peak of the stress-strain diagram under proportional loading, when the ratios of the stress components are fixed. This is the case e.g. for uniaxial tension, uniaxial compression, or shear under free expansion of the material (with zero normal stresses). However, for shear under confinement the shear stress can rise even after the onset of damage, due to increasing hydrostatic pressure, which increases the mobilized friction. It has been observed that the standard approach leads to strong sensitivity of the peak shear stress to the element size. To reduce this pathological effect, a modified approach has been implemented. The second-order work (product of stress increment and strain increment) is checked after each step and the element-size dependent adjustment of the damage law is applied only after the second-order work becomes negative. Up to this stage, the damage law corresponds to a fixed reference element size, which is independent of the actual size of the element. This size is set by the optional parameter *href*. If this parameter is not specified, the standard approach is used. For testing purposes, one can also specify the actual element size, *helem*, as a "material property". If this parameter is not specified, the element size is computed for each element separately and represents its actual size.

The damage-plastic model contains 15 parameters, but only 6 of them need to be actually calibrated for different concrete types, namely Young's modulus E, Poisson's ratio ν, tensile strength f_{t}, compressive strength f_{c}, parameter w_f (or fracture energy G_f), and parameter A_{s} in the ductility measure (156) of the damage model. The remaining parameters can be set to their default values specified in [8].

The model parameters are summarized in Tab. 40. Note that it is possible to specify the "size" of finite element, h, which (if specified) replaces the actual element size in (161). The usual approach is to consider h as the actual element size (evaluated automatically by OOFEM), in which case the optional parameter h is missing (or is set to 0., which has the same effect in the code). However, for various studies of mesh sensitivity it is useful to have the option of specifying h as an input "material" value.

If the element is too large, it may become too brittle and local snap-back occurs in the stress-strain diagram, which is not acceptable. In such a case, an error message is issued and the program execution is terminated. The maximum admissible element size

$$h_{\max} = \frac{EG_f}{f_t^2} = \frac{Ew_f}{f_t} \tag{162}$$

happens to be equal to Hillerborg's characteristic material length. For typical concretes it is in the order of a few hundred mm. If the condition $h < h_{\max}$ is violated, the mesh needs to be refined. Note that the effective element size h is obtained by projecting the element. For instance, if the element is a cube of edge length 100 mm, its effective size in the direction of the body diagonal can be 173 mm.

1.6.10 CDPM2

This model is an extension of the ConcreteDPM presented in 1.6.9. CDPM2 has been developed by Grassl, Xenos, Nyström, Rempling and Gylltoft for modelling the failure of concrete for both static and dynamic loading. It is is described in detail in [9]. The main differences between CDPM2 and ConcreteDPM are that in CDPM2 the plasticity part exhibits hardening once damage is active. Furthermore, two independent damage parameters describing tensile and compressive damage are introduced. The parameters of CDPM2 are summarised in Tab. 41

The stress for the anisotropic damage plasticity model (ISOFLAG=0) is defined as

$$\boldsymbol{\sigma} = (1-\omega_{\mathrm{t}})\,\bar{\boldsymbol{\sigma}}_{\mathrm{t}} + (1-\omega_{\mathrm{c}})\,\bar{\boldsymbol{\sigma}}_{\mathrm{c}} \tag{163}$$

where $\bar{\boldsymbol{\sigma}}_{\mathrm{t}}$ and $\bar{\boldsymbol{\sigma}}_{\mathrm{c}}$ are the positive and negative parts of the effective stress tensor $\bar{\boldsymbol{\sigma}}$, respectively, and ω_{t} and ω_{c} are two scalar damage variables, ranging from 0 (undamaged) to 1 (fully damaged).

The stress for the isotropic damage plasticity model (ISOFLAG=1) is defined as

$$\boldsymbol{\sigma} = (1-\omega_{\mathrm{t}})\,\bar{\boldsymbol{\sigma}} \tag{164}$$

The effective stress $\bar{\boldsymbol{\sigma}}$ is defined according to the damage mechanics convention as

$$\bar{\boldsymbol{\sigma}} = \mathbf{D}_{\mathrm{e}} : (\boldsymbol{\varepsilon} - \boldsymbol{\varepsilon}_{\mathrm{p}}) \tag{165}$$

Plasticity:

The yield surface is described by the Haigh-Westergaard coordinates: the volumetric effective stress σ_{V}, the norm of the deviatoric effective stress ρ and the Lode angle θ. The yield surface is

$$f_{\mathrm{p}}(\bar{\sigma}_{\mathrm{V}}, \bar{\rho}, \bar{\theta}; \kappa_{\mathrm{p}}) = \left\{ [1 - q_{\mathrm{h1}}(\kappa_{\mathrm{p}})] \left(\frac{\bar{\rho}}{\sqrt{6} f_{\mathrm{c}}} + \frac{\bar{\sigma}_{\mathrm{V}}}{f_{\mathrm{c}}} \right)^2 + \sqrt{\frac{3}{2}} \frac{\bar{\rho}}{f_{\mathrm{c}}} \right\}^2 + m_0 q_{\mathrm{h1}}^2(\kappa_{\mathrm{p}}) q_{\mathrm{h2}}(\kappa_{\mathrm{p}}) \left[\frac{\bar{\rho}}{\sqrt{6} f_{\mathrm{c}}} r(\cos\bar{\theta}) + \frac{\bar{\sigma}_{\mathrm{V}}}{f_{\mathrm{c}}} \right] - q_{\mathrm{h1}}^2(\kappa_{\mathrm{p}}) q_{\mathrm{h2}}^2(\kappa_{\mathrm{p}}) \tag{166}$$

It depends also on the hardening variable κ_{p} (which enters through the dimensionless variables q_{h1} and q_{h2}). Parameter f_{c} is the uniaxial compressive strength. For $q_{\mathrm{h2}} = 1$, the yield function is identical to the one of CDPM. The shape of the deviatoric section is controlled by the Willam-Warnke function

$$r(\cos\bar{\theta}) = \frac{4(1-e^2)\cos^2\bar{\theta} + (2e-1)^2}{2(1-e^2)\cos\bar{\theta} + (2e-1)\sqrt{4(1-e^2)\cos^2\bar{\theta} + 5e^2 - 4e}} \tag{167}$$

Here, e is the eccentricity parameter. The friction parameter m_0 is given by

$$m_0 = \frac{3\left(f_{\mathrm{c}}^2 - f_{\mathrm{t}}^2\right)}{f_{\mathrm{c}} f_{\mathrm{t}}} \frac{e}{e+1} \tag{168}$$

where f_{t} is the tensile strength.

The flow rule (26) is split into a volumetric and a deviatoric part, i.e., the gradient of the plastic potential is decomposed as

$$\mathbf{m} = \frac{\partial g}{\partial \bar{\boldsymbol{\sigma}}} = \frac{\partial g}{\partial \bar{\sigma}_{\mathrm{V}}} \frac{\partial \bar{\sigma}_{\mathrm{V}}}{\partial \bar{\boldsymbol{\sigma}}} + \frac{\partial g}{\partial \bar{\rho}} \frac{\partial \bar{\rho}}{\partial \bar{\boldsymbol{\sigma}}} \tag{169}$$

Taking into account that $\partial\bar{\sigma}_{\mathrm{V}}/\partial\bar{\boldsymbol{\sigma}} = \boldsymbol{\delta}/3$ and $\partial\bar{\rho}/\partial\bar{\boldsymbol{\sigma}} = \bar{\boldsymbol{s}}/\bar{\rho}$, restricting attention to the post-peak regime (in which $q_{\mathrm{h1}} = 1$) and differentiating the plastic potential (147), we rewrite equation (169) as

$$\boldsymbol{m} = \frac{\partial g}{\partial \bar{\boldsymbol{\sigma}}} = \frac{\partial m_{\mathrm{g}}}{\partial \bar{\sigma}_{\mathrm{V}}} \frac{\boldsymbol{\delta}}{3 f_{\mathrm{c}}} + \left(\frac{3}{f_{\mathrm{c}}} + \frac{m_0}{\sqrt{6}\bar{\rho}} \right) \frac{\bar{\boldsymbol{s}}}{f_{\mathrm{c}}} \tag{170}$$

The flow rule is non-associative which means that the direction of the plastic flow is not normal to the yield surface. This is important for concrete since an associative flow rule would give an overestimated maximum stress for passive confinement.

The dimensionless variables q_{h1} and q_{h2} that appear in (143), (147) and (148) are functions of the hardening variable κ_{p}. They control the evolution of the size and shape of the yield surface and plastic potential. The first hardening law q_{h1} is

$$q_{\mathrm{h1}}(\kappa_{\mathrm{p}}) = \begin{cases} q_{\mathrm{h0}} + (1 - q_{\mathrm{h0}})\left(\kappa_{\mathrm{p}}^3 - 3\kappa_{\mathrm{p}}^2 + 3\kappa_{\mathrm{p}}\right) - H_{\mathrm{p}}\left(\kappa_{\mathrm{p}}^3 - 3\kappa_{\mathrm{p}}^2 + 2\kappa_{\mathrm{p}}\right) & \text{if } \kappa_{\mathrm{p}} < 1 \\ 1 & \text{if } \kappa_{\mathrm{p}} \geq 1 \end{cases} \tag{171}$$

The second hardening law q_{h2} is given by

$$q_{\mathrm{h2}}(\kappa_{\mathrm{p}}) = \begin{cases} 1 & \text{if } \kappa_{\mathrm{p}} < 1 \\ 1 + H_{\mathrm{p}}(\kappa_{\mathrm{p}} - 1) & \text{if } \kappa_{\mathrm{p}} \geq 1 \end{cases} \tag{172}$$

The evolution law for the hardening variable,

$$\dot{\kappa}_{\mathrm{p}} = \frac{\|\dot{\boldsymbol{\varepsilon}_{\mathrm{p}}}\|}{x_{\mathrm{h}}\left(\bar{\sigma}_{\mathrm{V}}\right)}\left(2\cos\bar{\theta}\right)^2 = \frac{\dot{\lambda}\|\boldsymbol{m}\|}{x_{\mathrm{h}}\left(\bar{\sigma}_{\mathrm{V}}\right)}\left(2\cos\bar{\theta}\right)^2 \tag{173}$$

sets the rate of the hardening variable equal to the norm of the plastic strain rate scaled by a hardening ductility measure, which is identical to the one used for the CDPM.

Damage:

Damage is initiated when the maximum equivalent strain in the history of the material reaches the threshold $\varepsilon_0 = f_{\mathrm{t}}/E$. This expression is determined from the yield surface ($f_{\mathrm{p}} = 0$) by setting $q_{\mathrm{h1}} = 1$ and $q_{\mathrm{h2}} = \tilde{\varepsilon}/\varepsilon_0$. From this quadratic equation for $\tilde{\varepsilon}$, the equivalent strain is determined as

$$\tilde{\varepsilon} = \frac{\varepsilon_0 m_0}{2}\left(\frac{\bar{\rho}}{\sqrt{6}f_{\mathrm{c}}}r\left(\cos\theta\right) + \frac{\bar{\sigma}_{\mathrm{V}}}{f_c}\right) + \sqrt{\frac{\varepsilon_0^2 m_0^2}{4}\left(\frac{\bar{\rho}}{\sqrt{6}f_{\mathrm{c}}}r\left(\cos\theta\right) + \frac{\bar{\sigma}_{\mathrm{V}}}{f_{\mathrm{c}}}\right)^2 + \frac{3\varepsilon_0^2\bar{\rho}^2}{2f_{\mathrm{c}}^2}} \tag{174}$$

Tensile damage is described by a stress-inelastic displacement law. For linear and exponential damage type the stress value f_{t} and the displacement value w_{f} must be defined. For the bi-linear type two additional parameters f_{t1} and w_{f1} are required.

For the compressive damage variable, an evolution based on an exponential stress-inelastic strain law is used. The stress versus inelastic strain in the softening regime in compression is

$$\sigma = f_{\mathrm{t}}\exp\left(-\frac{\varepsilon_{\mathrm{i}}}{\varepsilon_{\mathrm{fc}}}\right) \quad \text{if } 0 < \varepsilon_{\mathrm{i}} \tag{175}$$

where $\varepsilon_{\mathrm{fc}}$ is an inelastic strain threshold which controls the initial inclination of the softening curve. The use of different damage evolution for tension and compression is one important improvement over CDPM.

The history variables κ_{dt1}, κ_{dt2}, κ_{dc1} and κ_{dc2} depend on a ductility measure x_{s}, which takes into account the influence of multiaxial stress states on the damage evolution. This ductility measure is given by

$$x_{\mathrm{s}} = 1 + \left(A_{\mathrm{s}} - 1\right)R_{\mathrm{s}} \tag{176}$$

where R_{s} is

$$R_{\mathrm{s}} = \begin{cases} -\dfrac{\sqrt{6}\bar{\sigma}_{\mathrm{V}}}{\bar{\rho}} & \text{if } \bar{\sigma}_{\mathrm{V}} \leq 0 \\ 0 & \text{if } \bar{\sigma}_{\mathrm{V}} > 0 \end{cases} \tag{177}$$

and A_{s} is a model parameter.

Strain rate:

Concrete is strongly rate dependent. If the loading rate is increased, the tensile and compressive strength increase and are more prominent in tension then in compression. The dependency is taken into account by an additional variable $alpha_{\mathrm{r}}$. The rate dependency is included by scaling both the equivalent strain rate and the inelastic strain. The rate parameter is defined by

$$\alpha_{\mathrm{r}} = (1 - X)\alpha_{\mathrm{rt}} + X\alpha_{\mathrm{rc}} \tag{178}$$

where X is the continuous compression measure (= 1 means only compression, = 0 means only tension).

The functions α_{rt} and α_{rc} depend on the input parameter f_{c0}. A recommended value for f_{c0} is 10 MPa.

1.6.11 Fixed crack model for concrete - ConcreteFCM

Implementation of a fixed crack model. Uncracked material is modeled as isotropic linear elastic characterized by Young's modulus and Poisson's ratio. Cracking is initiated when principal stress reaches tensile strength. Further loading is governed by a softening law. Proper amount energy dissipation is guaranteed by the crack-band approach. Multiple cracking is allowed; the maximum number of allowed cracks is controlled by *ncracks* parameter. Only mutually perpendicular cracks are supported. If cracking occurs in more directions, the behavior on the crack planes is considered to be independent. The secant stiffness is used for unloading and reloading. In a compression regime, this model correspond to an isotropic linear elastic material. The model supports 3 different options for stiffness reduction in shear after cracking, 2 options for the limit of the maximum shear stress on a crack plane and 6 different laws for postpeak behavior. The model parameters are summarized in Tab. 42.

Sample syntax for a fixed crack model with volume density 24 kN/m^3, thermal dilation coefficient 12×10^{-6} K^{-1}, Young's modulus 20 GPa, Poisson's ratio 0.2, fracture energy 100 N/m, tensile strength 2 MPa, linear softening, constant shear retention factor $\beta = 0.05$, Collins' shear strength (with compressive strength 30 MPa, aggregate size 0.01 m) and all cracks contribute to the shear stiffness; the analysis uses [m], [MPa] and [MN]:

```
ConcreteFCM 1 d 24.e-3 talpha 12.e-6 E 20000. n 0.2 Gf 100e-6 ft 2.0
softType 2 shearType 1 beta 0.05 shearStrengthType 2 fc 30 ag 0.01
lengthscale 1. multipleCrackShear
```

Description	Fixed crack model for concrete
Record Format	**ConcreteFCM** $_{\mathrm{(in)}}$ # d$_{\mathrm{(rn)}}$ # tAlpha$_{\mathrm{(rn)}}$ # E$_{\mathrm{(rn)}}$ # n$_{\mathrm{(rn)}}$ # [ncracks$_{\mathrm{(in)}}$ #] [multipleCrackShear] [crackSpacing$_{\mathrm{(rn)}}$ #] [softType$_{\mathrm{(in)}}$ #] [shearType$_{\mathrm{(in)}}$ #] [shearStrengthType$_{\mathrm{(in)}}$ #] [ecsm$_{\mathrm{(rn)}}$ #] [Gf$_{\mathrm{(rn)}}$ #] [ft$_{\mathrm{(rn)}}$ #] [beta$_{\mathrm{(rn)}}$ #] [sf$_{\mathrm{(rn)}}$ #] [fc$_{\mathrm{(rn)}}$ #] [ag$_{\mathrm{(rn)}}$ #] [lengthscale$_{\mathrm{(rn)}}$ #] [soft_w$_{\mathrm{(ra)}}$ #] [soft(w)$_{\mathrm{(ra)}}$ #] [soft_eps$_{\mathrm{(ra)}}$ #] [soft(eps)$_{\mathrm{(ra)}}$ #] [beta_w$_{\mathrm{(ra)}}$ #] [beta(w)$_{\mathrm{(ra)}}$ #] [H$_{\mathrm{(rn)}}$ #] [eps_f$_{\mathrm{(rn)}}$ #]
Parameters	- material model number - *d* material density - *tAlpha* thermal dilatation coefficient - *E* Young's modulus - *n* Poisson's ratio - *ncracks* maximum allowed number of cracks - *crackSpacing* specified distance between parallel cracks - *multipleCrackShear* if not given, shear stiffness computed from the dominant crack, otherwise all cracks contribute

- *softType* allows to select suitable softening law:

0 - no softening (default)
1 - exponential softening with parameters *Gf* and *ft*
2 - linear softening with parameters *Gf* and *ft*
3 - Hordijk softening with parameters *Gf* and *ft*
4 - user-defined wrt crack opening with parameters *ft*, *soft_w*, and *soft(w)*
5 - linear hardening wrt strain with parameters *ft*, *H*, and optionally *eps_f*
6 - user-defined wrt strain with parameters *ft*, *soft_eps*, and *soft(eps)*

- *shearType* offers to choose from different approaches for shear stiffness reduction of a cracked element

0 - no shear reduction (default)
1 - constant shear retention factor with parameter *beta*
2 - constant shear factor coefficient with parameter *sf*
3 - user-defined shear retention factor with parameters *beta_w* and *beta(w)*

- *shearStrengthType* allows to select a shear stress limit on a crack plane

0 - no stress limit (default)
1 - constant strength = f_t
2 - Collins interlock with parameters *fc*, *ag*, and *length-scale*

- *ecsm* method used for evaluation of characteristic element size L: 1 = square root of area, 2 = projection centered, 3 = Oliver, 4 = Oliver modified, 0 (default) = projection
- *Gf* fracture energy
- *ft* tensile strength
- *beta* shear retention factor
- *sf* shear factor coefficient
- *fc* compressive strength in MPa
- *ag* aggregate size
- *lengthscale* factor to convert crack opening and aggregate size in case of Collins aggregate interlock; 1 = analysis in meters, 1000 = in millimeters, etc.
- *soft_w* specified values of crack opening and
- *soft(w)* corresponding values of traction normalized to *ft*
- *soft_eps* specified values of cracking strain and
- *soft(eps)* corresponding values of traction normalized to *ft*
- *beta_w* specified values of crack opening and
- *beta(w)* corresponding values of shear retention factor
- *H* hardening modulus (expressed wrt cracking strain)

	- *eps_f* threshold for cracking strain after which traction is zero (applicable for linear hardening only)
Supported modes	3dMat, PlaneStress, PlaneStrain

Table 42: Fixed crack model for concrete – summary.

1.6.12 Fixed crack model for fiber reinforced composites - FRCFCM

This material model is an extension of the ConcreteFCM described in Section 1.6.11.

It is possible to choose from three different "classes" of fibers. This choice is controlled by keyword *fiberType*: 0 = continuous aligned fibers (CAF), 1 = short aligned fibers (SAF) and 2 = short random fibers (SRF). Currently, it is not possible to combine more classes of fibers in one material model.

All of the above-mentioned fiber types are further defined by the material properties and geometry. Fiber quantity is captured by the dimensionless volume fraction *Vf* (as decimal). All fibers are assumed to have a circular cross-section (shape factor for shear *kfib* with default value 0.9) and to possess the same geometry characterized by the diameter *Df* and length *Lf*.

The overall elastic stiffness of the fiber-reinforced composite is calculated as a weighted average of the moduli of matrix E_m and fibers E_f and the Poisson's ratio is considered to be equal to the Poisson's ratio of the matrix. Similarly to `ConcreteFCM`, cracking is initiated once the tensile stress σ in matrix reaches the tensile strength f_t.

The nominal bridging stress for continuous aligned fibers which are not perpendicular to the crack plane $\sigma_{b,f,\theta}$ can be very easily obtained by multiplying the nominal bridging stress for perpendicular fibers $\sigma_{b,f}$ by two terms: the first one reflecting lower volume of inclined fibers passing through the crack plane and the second one capturing the snubbing effect:

$$\sigma_{b,f,\theta} = \sigma_{b,f} \cos(\theta) \exp(\theta f) \tag{179}$$

where f is a snubbing coefficient.

For the **CAF** perpendicular to the crack, the nominal bridging stress can be derived as

$$\sigma_{b,f} = 2V_f \sqrt{\frac{E_f(1+\eta)\tau_0}{D_f}\,\bar{w}} \tag{180}$$

where $\eta = (E_f V_f)/[E_m(1-V_f)]$.

For **SRF** the nominal bridging stress is

$$\sigma_{b,f}(w) = 2V_f \sqrt{\frac{E_f(1+\eta)\tau_0\bar{w}}{D_f}} - \frac{V_f E_f(1+\eta)\bar{w}}{L_f} \quad \text{for } \bar{w} < w^* \tag{181}$$

$$\sigma_{b,f}(w) = \frac{V_f L_f \tau_s(w)}{D_f}\left(1 - \frac{2\bar{w}}{L_f}\right)^2 \quad \text{for } w^* \leq \bar{w} < L_f/2 \tag{182}$$

$$\sigma_{b,f}(w) = 0 \quad \text{for } \bar{w} > L_f/2 \tag{183}$$

where $w^* = \left(L_f^2\tau_0\right)/[(1+\eta)E_f D_f]$; τ_0 is the bond shear strength between the fiber and matrix for small crack openings, $w < w^*$.

Larger pull-out displacements can lead to significant physical changes in the fiber surface which can result into changes in the bond shear stress. This phenomenon is captured by function $\tau_s(w)$ relating the frictional bond to the crack opening and is implemented in three alternative formulations. (In order to keep $\tau_s(w) = \tau_0$ use *fssType* $= 0$.) In conventional FRC with ordinary concrete matrix, the frictional bond usually decreases with increasing slip. To capture this type of behavior we adopt the function proposed by Sajdlová (activated with *fssType* $= 1$) reads

$$\tau_s(w) = \tau_0 \left[1 + \mathrm{sign}(b_0)\left(1 - \exp\left(-\frac{|b_0|w}{D_f}\right)\right)\right] \tag{184}$$

where b_0 is a micromechanical parameter. In composites with high-strength matrix and coated high-strength steel fibers (HSFRC, UHPFRC) as well as in SHCC materials with polymeric fibers, the frictional bond-slip relation often exhibits hardening; this phenomenon can be well approximated by a cubic function (activated with *fssType* $= 2$) proposed by Kabele

$$\tau_s(w) = \tau_0 \left[1 + b_1 \frac{w}{D_f} + b_2 \left(\frac{w}{D_f}\right)^2 + b_3 \left(\frac{w}{D_f}\right)^3\right] \tag{185}$$

or an alternative formulation which results in smooth changes in the bridging stress (activated with *fssType* $= 3$)

$$\tau_s(w) = \tilde{\tau}_0 + \tau_0 \left[b_1 \frac{\tilde{w}}{D_f} + b_2 \left(\frac{\tilde{w}}{D_f}\right)^2 + b_3 \left(\frac{\tilde{w}}{D_f}\right)^3\right] \tag{186}$$

In the last two equations b_1, b_2 and b_3 are micromechanical parameters and additionally in the last equation $\tilde{w} = w - w^*$, $\tilde{\tau}_0 = \tau_0(1. - w^*/L_f)^{-2}$ for SRF and $\tilde{\tau}_0 = \tau_0 E_f(1+\eta)D_f/[E_f(1+\eta)D_f - 2L_f\tau_0]$ for SAF.

The bridging stress for **SRF** is defined as

$$\sigma_{b,f}(w) = \frac{gV_f L_f \tau_0}{2D_f}\left(2\sqrt{\frac{\bar{w}}{w^*}} - \frac{\bar{w}}{w^*}\right) \quad \text{for } \bar{w} < w^* \tag{187}$$

$$\sigma_{b,f}(w) = \frac{gV_f L_f \tau_s(w)}{2D_f}\left(1 - \frac{2w}{L_f}\right)^2 \quad \text{for } w^* \leq \bar{w} < L_f/2 \tag{188}$$

$$\sigma_{b,f}(w) = 0 \quad \text{for } \bar{w} > L_f/2 \tag{189}$$

where g is the snubbing factor is defined as

$$g = 2\frac{1 + \exp(\pi f/2)}{4 + f^2} \tag{190}$$

It is possible to delay the activation of the stress in fibers using prameteter *fibreActivationOpening* which can be imagined as a “lag” of the fiber-related crack opening behind the matrix-related crack opening.

During unloading the stress in fibers does not decrease linearly to origin. Current implementation uses a power function

$$\sigma_{b,f}(w) = \sigma_{b,f}(w_{max})\left(\frac{\bar{w}}{\bar{w}_{max}}\right)^M \tag{191}$$

where $w_{\max}$ is the maximum crack width reached in the entire previous history and M is a positive constant, its default value is $M = 4$.

The influence of crack opening and sliding on the bridging shear stress only due to fibers is expressed as

$$\tau_{b,f} = \bar{V}_f k G_f \frac{u}{w_{max}} = \frac{\bar{V}_f k G_f}{\varepsilon_{cr,max}} \gamma_{cr} \tag{192}$$

where $\bar{V}_f$ is the effective volume of fibers crossing a crack plane ($V_f/2$ for SRF and $V_f \cos(\theta)$ for CAF and SAF), and G_f is the fiber shear modulus. This expression is motivated by assumption that the fibers bridging the crack planes behave as the Timoshenko beams subjected to shear. Note that the shear stiffness of fibers is not recovered upon unloading.

It has been found that in some high performance fiber reinforced cement composites, fibers rupture when cracks are exposed to shearing. This phenomenon is modeled by damage parameter ω, which accounts for the ratio of ruptured fibers and varies between the values of 0 and 1. It is assumed that ω depends on the maximum shear strain sustained by the protruding portions of bridging fibers throughout the loading history. This crack shear strain can be expressed as:

$$\gamma_{f,max} = \max\left(\frac{|u_i(t)|}{\max\left(w_i(t)\right)}\right) \quad \ldots w(t) > \Delta w \tag{193}$$

where u_i is the crack sliding displacement (CSD) and and w_i is the maximum value of the crack opening displacement of the i-th crack. This means that the damage does not grow if the crack closes (crack opening decreases). If more cracks exist, the maximum contribution is considered.

Two different one-parameter damage evolution laws are currently implemented. For *fDamType* = 0 the damage is deactivated, with *fDamType* = 1 damage is described by

$$\omega(\gamma_f) = \min\left(\frac{\gamma_f}{\gamma_{fc}}, 1\right) \tag{194}$$

and finally with *fDamType* = 2

$$\omega(\gamma_f) = 1 - \exp\left(-\frac{\gamma_f}{\gamma_{fc}}\right) \tag{195}$$

where γ_{fc} (*gammaCrack* in the input record) is a parameter.

Since damage reduces the number of crack-bridging fibers, which is proportional to the fiber volume fraction, its effect can be suitably implemented by introducing the effective volume fraction

$$V_f^* = V_f(1 - \omega) \tag{196}$$

The material parameters are summarized in Tables 42 (matrix) and 43 (fiber extension).

Sample syntax for a fixed crack model reinforced with fibers with volume density 24 kN/m^3, thermal dilation coefficient 12×10^{-6} K^{-1}, Young's modulus of the matrix 20 GPa, Poisson's ratio of matrix 0.2, fracture energy of matrix 100 N/m, tensile strength of matrix 2 MPa, linear tension softening, constant shear retention factor $\beta = 0.05$, unlimited shear strength (`shearStrengthType = 0`), continuous aligned fibers, fiber volume 2%, fiber diameter 0.04 mm, Young's modulus of fibers 20 GPa, shear modulus of fibers 1 GPa, fiber-matrix bond strength 1 MPa, snubbing coefficient 0.7, shear correction coefficient 0.9, deactivated fiber damage, fiber act if COD exceeds 10 μm (with smoothing from $w = 8to11$ μm), fiber orientation at 45 degrees in x-y plane, automatic evaluation of crack spacing from composition; the analysis uses [m], [MPa] and [MN]:

```
FRCFCM 1 d 24.e-3 talpha 12.e-6 E 20000. n 0.2 Gf 100e-6 ft 2.0
softType 2 shearType 1 beta 0.05 FiberType 0 Vf 0.02 Df 0.04e-3
Ef 20000. Gfib 1000. tau_0 1. FSStype 0 f 0.7 kfib 0.9 fDamType 0
fibreactivationopening 10.e-6 dw0 2.e-6 dw1 1.e-6 orientationVector
3 1. 1. 0. computeCrackSpacing
```

Description	Fixed crack model for FRC
Record Format	**FRCFCM** input record of ConcreteFCM Vf(rn) # Lf(rn) # Df(rn) # Ef(rn) # [nuf(rn) #] [Gfib(rn) #] [kfib(rn) #] tau_0(rn) # b0(rn) # b1(rn) # b2(rn) # b3(rn) # f(rn) # [M(in) #] [fibreOrientationVector(ra) #] [fssType(in) #] [fDamType(in) #] [fiberType(in) #] [gammaCrack(rn) #] [computeCrackSpacing] [fibreActivationOpening(rn) #] [dw0(rn) #] [dw1(rn) #]
Parameters	- *Vf* fiber content expressed as decimal - *Lf* fiber length - *Df* fiber diameter - *Ef* fiber Young's modulus - *nuf* fiber Poisson's ratio - *Gfib* fiber shear modulus (read when *nuf* is not provided) - *kfib* fiber cross-sectional shape correction factor - *tau_0* bond shear strength at zero slip - *b0* micromechanical parameter for fiber shear according to Sajdlov - *b1*, *b2*, *b3* micromechanical parameter for fiber shear according to Kabele - *f* snubbing friction coefficient - *M* exponent related to fiber unloading - *fibreOrientationVector* vector specifying orientation for CAF and SAF fibers - *fssType* type of Fiber bond Shear Strength (bond shear strength vs. crack opening) 0 - constant shear strength 1 - bond shear strength with parameter *b0* 2 - bond shear strength with parameters *b1*, *b2*, *b3* 3 - bond shear strength with parameters *b1*, *b2*, *b3* which leads to smooth traction-separation law

	- *fDamType* type of damage law for fibers 0 - no damage 1 - damage controlled by shear slip deformation of the crack (with *gammaCrack*), linear law 2 - damage controlled by shear slip deformation of the crack (with *gammaCrack*), exponential law - *fiberType* type of reinforcing fibers 0 - CAF (continuous aligned fibers) 1 - SAF (short aligned fibers) 2 - SRF (short randomly oriented fibers) - *gammaCrack* crack shear strain parameter applicable with fDamType = 1 or 2 (here the crack shear strain is understood as the crack slip u divided by the crack opening w) - *computeCrackSpacing* crack spacing is evaluated automatically based on provided composition - *fibreActivationOpening* crack opening at which the fibers begin transferring bridging stress - *dw0*, *dw1* applicable only if *fibreActivationOpening* $\neq 0$, then it allows to smooth the traction-separation law for fibers; lower bound is *fibreActivationOpening* - *dw0* and the upper bound is *fibreActivationOpening* - *dw1*
Supported modes	3dMat, PlaneStress, PlaneStrain

Table 43: Fixed crack model for fiber reinforced concrete – summary.

1.6.13 "Nonlocal" model for SHCC

The material parameters are summarized in Tables 42 (matrix), 43 (fiber extension), and 44 (nonlocal extension).

Description	Nonlocal fixed crack model for FRC
Record Format	**FRCFCMNL** input record of ConcreteFCM and FRCFCM $\mathrm{r}_{(\mathrm{rn})}$ # $\mathrm{wft}_{(\mathrm{in})}$ #
Parameters	- *r* nonlocal radius (reasonable value is several millimeters and its maximum is $L_f/2$ for short fibers) - *wft* nonlocal averaging function, must be set to 4 (constant function)
Supported modes	PlaneStress

Table 44: Nonlocal fixed crack model for fiber reinforced concrete – summary.

1.7 Orthotropic damage model with fixed crack orientations for composites - CompDamMat

The model is designed for transversely isotropic elastic material defined by five elastic material constants. Typical example is a carbon fiber tow. Axis 1 represents the material principal direction. The orthotropic material constants are defined as

$$\begin{aligned}
\nu_{12} &= \nu_{13},\ \nu_{21} = \nu_{31},\ \nu_{23} = \nu_{32},\ E_{22} = E_{33} && (197)\\
G_{12} &= G_{13} = G_{21} = G_{31}, G_{23} = G_{32} && (198)\\
\frac{\nu_{12} = \nu_{13}}{E_{11}} &= \frac{\nu_{21} = \nu_{31}}{E_{22}},\ \frac{\nu_{31} = \nu_{21}}{E_{33}} = \frac{\nu_{13} = \nu_{12}}{E_{11}} && (199)
\end{aligned}$$

Material orientation on a finite element can be specified with *lcs* optional parameter. If unspecified, material orientation is the same as the global coordinate system. *lcs* array contains six numbers, where the first three numbers represent a directional vector of the local x-axis, and the next three numbers represent a directional vector of the local y-axis with the reference to the global coordinate system. The composite material is extended to 1D and is also suitable for beams and trusses. In such particular case, the *lcs* has no effect and the 1D element orientation is aligned with the global xx component.

The index p, $p \in \{11, 22, 33, 23, 31, 12\}$ symbolizes six components of stress or strain vectors. The linear softening occurs after reaching a critical stress $f_{p,0}$, see Fig. 9. Orientation of cracks is assumed to be orthogonal and aligned with an orientation of material axes [3, pp.236]. The transverse isotropy is generally lost upon fracture, material becomes orthotropic and six damage parameters d_p are introduced.

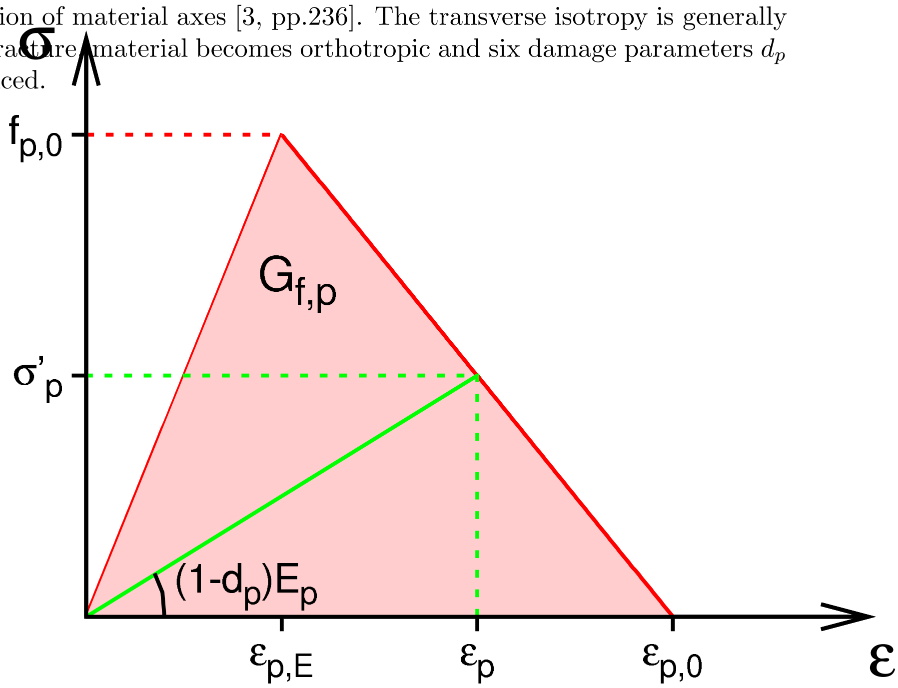

Figure 9: Implemented stress-strain evolution with damage for 1D case. Tension and compression are separated, but sharing the same damage parameter.

The compliance material matrix **H**, in the secant form and including damage parameters, reads

$$\mathbf{H} = \begin{bmatrix} \frac{1}{(1-d_{11})E_{11}} & -\frac{\nu_{21}}{E_{22}} & -\frac{\nu_{31}}{E_{33}} & 0 & 0 & 0 \\ -\frac{\nu_{12}}{E_{11}} & \frac{1}{(1-d_{22})E_{22}} & -\frac{\nu_{32}}{E_{33}} & 0 & 0 & 0 \\ -\frac{\nu_{13}}{E_{11}} & -\frac{\nu_{23}}{E_{22}} & \frac{1}{(1-d_{33})E_{33}} & 0 & 0 & 0 \\ 0 & 0 & 0 & \frac{1}{(1-d_{23})G_{23}} & 0 & 0 \\ 0 & 0 & 0 & 0 & \frac{1}{(1-d_{31})G_{31}} & 0 \\ 0 & 0 & 0 & 0 & 0 & \frac{1}{(1-d_{12})G_{12}} \end{bmatrix} \tag{200}$$

Damage occurs when any out of six stress tensor components exceeds a given strength $f_{p,0}$

$$|\sigma_p| \geq |f_{p,0}| \tag{201}$$

Positive and negative ultimate strengths can be generally different but share the same damage variable. At the point of damage initiation, see Fig. 9, one evaluates $\varepsilon_{p,E}$ and characteristic element length l_p, generally different for each damage mode. Given the fracture energy $G_{F,p}$, the maximum strain at zero stress $\varepsilon_{p,0}$ is computed

$$\varepsilon_{p,0} = \varepsilon_{p,E} + \frac{2G_{F,p}}{f_{p,0}l_p} \tag{202}$$

The point of damage initiation is never reached exactly, one needs to interpolate between the previous equilibrated step and current step to achieve objectivity.

The evolution of damage d_p is based on the evolution of corresponding strain ε_p. A maximum achieved strain is stored in the variable κ_p. If $\varepsilon_p > \kappa_p$ the damage may grow so the corresponding damage variable d_p may increase. Desired stress σ'_p is evaluated from the actual strain ε_p

$$\sigma'_p = f_{p,0}\frac{\varepsilon_{p,0} - \varepsilon_p}{\varepsilon_{p,0} - \varepsilon_{p,E}} \tag{203}$$

and the calculation of damage variables d_p stems from Eq. 200, for example

$$d_{11} = 1 - \frac{\sigma'_{11}}{E_{11}\left(\varepsilon_{11} + \frac{\nu_{21}}{E_{22}}\sigma_{22} + \frac{\nu_{31}}{E_{33}}\sigma_{33}\right)} \tag{204}$$

$$d_{12} = 1 - \frac{\sigma'_{12}}{G_{12}\varepsilon_{12}} \tag{205}$$

Damage is always controled not to decrease. Fig. 10 shows a typical performance for this damage model in one direction.

The damage initiation is based on a trial stress. It becomes necessary for higher precision to skip a few first iteration, typically 5, and then to introduce damage. A parameter *afterIter* is designed for this purpose and *MinIter* forces a solver always to proceed certain amount of iterations.

allowSnapBack skips the checking of sufficient fracture energy for each direction. If not specified, all directions are checked to prevent snap-back which dissipates incorrect amount of energy.

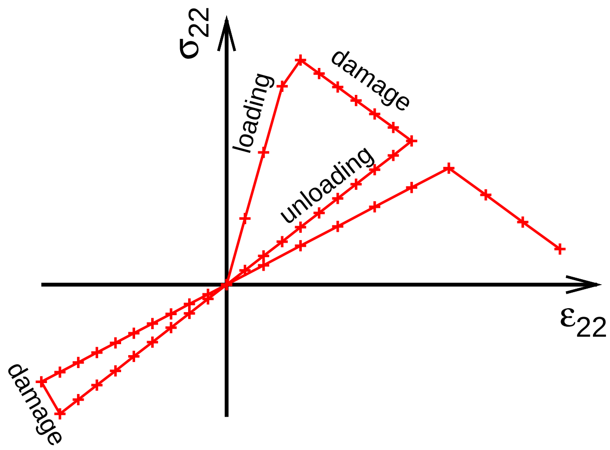

Figure 10: Typical loading/unloading material performance for homogenized stress and strain in the direction '2'. Note that one damage parameter is common for both tension and compression.

1.8 Orthotropic elastoplastic model with isotropic damage - TrabBone3d

This model combines orthotropic elastoplasticity with isotropic damage. Material orthotropy is described by the fabric tensor, i.e., a symmetric second-order tensor with principal directions aligned with the axes of orthotropy and principal values normalized such that their sum is 3. Elastic constants as well as coefficients that appear in the yield condition are linked to the principal values of the fabric tensor and to porosity. The yield condition is piecewise quadratic, with different parameters in the regions of positive and negative volumetric strain.

1.8.1 Local formulation

The basic equations include an additive decomposition of total strain into elastic (reversible) part and plastic (irreversible) part

$$\boldsymbol{\varepsilon} = \boldsymbol{\varepsilon}_{\rm e} + \boldsymbol{\varepsilon}_{\rm p}, \tag{206}$$

the stress strain law

$$\boldsymbol{\sigma} = (1-\omega)\,\bar{\boldsymbol{\sigma}} = (1-\omega)\,\boldsymbol{D} : \boldsymbol{\varepsilon}_{\rm e}, \tag{207}$$

the yield function

$$f(\bar{\boldsymbol{\sigma}},\kappa) = \sqrt{\bar{\boldsymbol{\sigma}} : \boldsymbol{F} : \bar{\boldsymbol{\sigma}}} - \sigma_Y(\kappa). \tag{208}$$

loading-unloading conditions

$$f(\bar{\boldsymbol{\sigma}},\kappa) \le 0 \qquad \dot{\lambda} \ge 0 \qquad \dot{\lambda} f(\bar{\boldsymbol{\sigma}},\kappa) = 0, \tag{209}$$

evolution law for plastic strain

$$\dot{\boldsymbol{\varepsilon}}_{\rm p} = \dot{\lambda}\frac{\partial f}{\partial \bar{\boldsymbol{\sigma}}}, \tag{210}$$

the incremental definition of cumulated plastic strain

$$\dot{\kappa} = \|\dot{\boldsymbol{\varepsilon}}_{\rm p}\|, \tag{211}$$

the law governing the evolution of the damage variable

$$\omega(\kappa) = \omega_c(1 - {\rm e}^{-a\kappa}), \tag{212}$$

and the hardening law

$$\sigma_Y(\kappa) = 1 + \sigma_H(1 - {\rm e}^{-s\kappa}). \tag{213}$$

In the equations above, $\bar{\boldsymbol{\sigma}}$ is the effective stress tensor, $\boldsymbol{D}$ is the elastic stiffness tensor, f is the yield function, λ is the consistency parameter (plastic multiplier), ω is the damage variable, σ_Y is the yield stress and s, a, σ_H and ω_c are positive material parameters. Material anisotropy is characterized by the second-order positive definite fabric tensor

$$\boldsymbol{M} = \sum_{i=1}^{3} m_i(\boldsymbol{m}_i \otimes \boldsymbol{m}_i), \tag{214}$$

normalized such that ${\rm Tr}(\boldsymbol{M}) = 3$, m_i are the eigenvalues and $\boldsymbol{m}_i$ the eigenvectors. The eigenvectors of the fabric tensor determine the directions of material orthotropy and the components of the elastic stiffness tensor $\boldsymbol{D}$ are linked to eigenvalues of the fabric tensor. In the coordinate system aligned with m_i, $i = 1, 2, 3$, the stiffness can be presented in Voigt (engineering) notation as

$$\boldsymbol{D} = \begin{bmatrix} \frac{1}{E_1} & -\frac{\nu_{12}}{E_1} & -\frac{\nu_{13}}{E_1} & 0 & 0 & 0 \\ -\frac{\nu_{21}}{E_2} & \frac{1}{E_2} & -\frac{\nu_{23}}{E_2} & 0 & 0 & 0 \\ -\frac{\nu_{31}}{E_3} & -\frac{\nu_{32}}{E_3} & \frac{1}{E_3} & 0 & 0 & 0 \\ 0 & 0 & 0 & \frac{1}{G_{23}} & 0 & 0 \\ 0 & 0 & 0 & 0 & \frac{1}{G_{13}} & 0 \\ 0 & 0 & 0 & 0 & 0 & \frac{1}{G_{12}} \end{bmatrix}^{-1}, \tag{215}$$

where $E_i = E_0\rho^k m_i^{2l}$, $G_{ij} = G_0\rho^k m_i^l m_j^l$ and $\nu_{ij} = \nu_0\frac{m_i^l}{m_j^l}$. Here, E_0, G_0 and ν_0 are elastic constants characterizing the compact (poreless) material, ρ is the volume fraction of solid phase and k and l are dimensionless exponents.

Similar relations as for the stiffness tensor are also postulated for the components of a fourth-order tensor $\boldsymbol{F}$ that is used in the yield condition. The yield condition is divided into tensile and compressive parts. Tensor $\boldsymbol{F}$ is different in each part of the effective stress space. This tensor is denoted $\boldsymbol{F}^+$ in tensile part, characterized by $\hat{\boldsymbol{N}} : \bar{\boldsymbol{\sigma}} \leq 0$ and $\boldsymbol{F}^-$ in compressive part, characterized by $\hat{\boldsymbol{N}} : \bar{\boldsymbol{\sigma}} \leq 0$, where

$$\hat{\boldsymbol{N}} = \frac{\sum_{i=1}^{3} m_i^{-2q}}{\sqrt{\sum_{i=1}^{3} m_i^{-4q}}}(\boldsymbol{m}_i \otimes \boldsymbol{m}_i) \tag{216}$$

$$
\boldsymbol{F}^{\pm} = \begin{bmatrix}
\frac{1}{\left(\sigma_1^{\pm}\right)^2} & -\frac{\chi_{12}^{\pm}}{\left(\sigma_1^{\pm}\right)^2} & -\frac{\chi_{13}^{\pm}}{\left(\sigma_1^{\pm}\right)^2} & 0 & 0 & 0 \\
-\frac{\chi_{21}^{\pm}}{\left(\sigma_2^{\pm}\right)^2} & \frac{1}{\left(\sigma_2^{\pm}\right)^2} & -\frac{\chi_{23}^{\pm}}{\left(\sigma_2^{\pm}\right)^2} & 0 & 0 & 0 \\
-\frac{\chi_{31}^{\pm}}{\left(\sigma_3^{\pm}\right)^2} & -\frac{\chi_{32}^{\pm}}{\left(\sigma_3^{\pm}\right)^2} & \frac{1}{\left(\sigma_3^{\pm}\right)^2} & 0 & 0 & 0 \\
0 & 0 & 0 & \frac{1}{\tau_{23}} & 0 & 0 \\
0 & 0 & 0 & 0 & \frac{1}{\tau_{13}} & 0 \\
0 & 0 & 0 & 0 & 0 & \frac{1}{\tau_{12}}
\end{bmatrix}. \tag{217}
$$

In the equation above $\sigma_i^{\pm} = \sigma_0^{\pm}\rho^p m_i^{2q}$ is uniaxial yield stress along the i-th principal axis of orthotropy, $\tau_{ij} = \tau_0\rho^p m_i^q m_j^q$ is the shear yield stress in the plane of orthotropy and $\chi_{ij}^{\pm} = \chi_0^{\pm}\frac{m_i^{2q}}{m_j^{2q}}$ is the so-called interaction coefficient, p and q are dimensionless exponents and parameters with subscript 0 are related to a fictitious material with zero porosity. The yield surface is continuously differentiable if the parameters values are constrained by the condition

$$
\frac{\chi_0^- + 1}{(\sigma_0^-)^2} = \frac{\chi_0^+ + 1}{(\sigma_0^+)^2}. \tag{218}
$$

The model description and parameters are summarized in Tab. 46.

1.8.2 Nonlocal formulation - TrabBoneNL3d

The model is regularized by the over-nonlocal formulation with damage driven by a combination of local and nonlocal cumulated plastic strain

$$
\hat{\kappa} = (1-m)\kappa + m\bar{\kappa}, \tag{219}
$$

where m is a dimensionless material parameter (typically $m > 1$) and

$$
\bar{\kappa}(x) = \int\limits_V \alpha(x,s)\kappa(s)\,\mathrm{d}s \tag{220}
$$

is the nonlocal cumulated plastic strain. The nonlocal weight function is defined as

$$
\alpha(x,s) = \frac{\alpha_0(\|x-s\|)}{\int\limits_V \alpha_0(\|x-t\|)\,\mathrm{d}t} \tag{221}
$$

where

$$
\alpha_0(r) = \begin{cases} \left(1-\frac{r^2}{R^2}\right)^2 & \text{if } r \le R \\ 0 & \text{if } r > R \end{cases} \tag{222}
$$

Parameter R is related to the internal length of the material. The model description and parameters are summarized in Tab. 47.

Description	CDPM2
Record Format	**con2dpm** d$_{(rn)}$ # E$_{(rn)}$ # n$_{(rn)}$ # tAlpha$_{(rn)}$ # ft$_{(rn)}$ # fc$_{(rn)}$ # wf$_{(rn)}$ # [stype$_{(in)}$ #] [ft1$_{(rn)}$ #] [wf1$_{(rn)}$ #] [efc$_{(rn)}$ #] [ecc$_{(rn)}$ #] [kinit$_{(rn)}$ #] [Ahard$_{(rn)}$ #] [Bhard$_{(rn)}$ #] [Chard$_{(rn)}$ #] [Dhard$_{(rn)}$ #] [Asoft$_{(rn)}$ #] [helem$_{(rn)}$ #] [dilation$_{(rn)}$ #] [hp$_{(rn)}$ #] [isoflag$_{(in)}$ #] [rateflag$_{(in)}$ #] fcZero$_{(in)}$ # [yieldtol$_{(rn)}$ #] [newtoniter$_{(in)}$ #]
Parameters	- *d* material density - *E* Young modulus - *n* Poisson ratio - *tAlpha* thermal dilatation coefficient - *ft* uniaxial tensile strength - *fc* uniaxial compressive strength - *wf* parameter that controls the slope of the softening branch to be used - *stype* allows to choose different types of softening laws, default value 1: 0 - linear softening 1 - bilinear softening 2 - exponential softening - *ft1* parameter for the bilinear softening law (stype = 1) defining the ratio between intermediate stress and tensile strength, optional, default value 0.3 - *wf1* parameter for the bilinear softening law (stype = 1) defining the intermediate crack opening, optional, default value 0.15 - *efc* parameter for exponential softening law in compression, optional, default value 100×10^{-6} - *ecc* eccentricity parameter, optional, default value 0.525 - *kinit* initial value of hardening law, optional, default value 0.3 - *Ahard* hardening parameter, optional, default value 0.08 - *Bhard* hardening parameter, optional, default value 0.003 - *Chard* hardening parameter, optional, default value 2 - *Dhard* hardening parameter, optional, default value 1×10^{-6} - *Asoft* softening parameter, optional, default value 15 - *helem* element size h, optional (if not specified, the actual element size is used) - *dilation* dilation factor, optional, default value 0.85 - *hp* hardening modulus, optional, default value 0.5 - *isoflag* flag which allows for the use of only one damage parameter if set to 1, default value 0 - *rateflag* flag which allows for the consideration of the effect of strain rates if set to 1, default value 0 - *fcZero* Input parameter for modelling the effect of strain value. Recommended value 10 MPa. Only if rateflag=1, *fcZero* has to be specified. - *yieldtol* tolerance for the implicit stress return algorithm, optional, default value 1×10^{-6} - *newtoniter* maximum number of iterations in the implicit stress return algorithm, optional, default value 100
Supported modes	3dMat, PlaneStrain

Table 41: CDPM2 – summary.

Description	Orthotropic damage model with fixed crack orientations for composites
Record Format	**CompDamMat** num$_{(in)}$ # d$_{(rn)}$ # Exx$_{(rn)}$ # EyyEzz$_{(rn)}$ # nuxynuxz$_{(rn)}$ # nuyz$_{(rn)}$ # GxyGxz$_{(rn)}$ # Tension_f0_Gf$_{(ra)}$ # Compres_f0_Gf$_{(ra)}$ # [afterIter$_{(in)}$ #] [allowSnapBack$_{(()}$ #ia)]
Parameters	- *num* material model number - *d* material density - *Exx* Young's modulus for principal direction xx - *EyyEzz* Young's modulus in orthogonal directions to the principal direction xx - *nuxynuxz* Poisson's ratio in xy and xz directions - *nuyz* Poisson's ratio in yz direction - *GxyGxz* shear modulus in xy and xz directions - *Tension_f0_Gf* array with six pairs of positive numbers. Each pair describes maximum stress in tension and fracture energy for each direction (xx, yy, zz, yz, zx, xy) - *Compres_f0_Gf* array with six pairs of numbers. Each pair describes maximum stress in compression (given as a negative number) and positive fracture energy for each direction (xx, yy, zz, yz, zx, xy)
Supported modes	3dMat, 1dMat - *afterIter* how many iterations must pass until damage is computed from strains, zero is default. User must ensure that the solver proceeds the minimum number of iterations. - *allowSnapBack* array to skip checking for snap-back. The array members are 1-6 for tension and 7-12 for compression components.

Table 45: Orthotropic damage model with fixed crack orientations for composites – summary.

Description	Anisotropic elastoplastic model with isotropic damage
Record Format	**TrabBone3d** (in) # d(rn) # eps0(rn) # nu0(rn) # mu0(rn) # expk(rn) # expl(rn) # m1(rn) # m2(rn) # rho(rn) # sig0pos(rn) # sig0neg(rn) # chi0pos(rn) # chi0neg(rn) # tau0(rn) # plashardfactor(rn) # expplashard(rn) # expdam(rn) # critdam(rn) #
Parameters	- material number - *d* material density - *eps0* Young modulus (at zero porosity) - *nu0* Poisson ratio (at zero porosity) - *mu0* shear modulus of elasticity (at zero porosity) - *m1* first eigenvalue of the fabric tensor - *m2* second eigenvalue of the fabric tensor - *rho* volume fraction of solid phase - *sig0pos* yield stress in tension - *sig0neg* yield stress in compression - *tau0* yield stress in shear - *chi0pos* interaction coefficient in tension - *plashardfactor* hardening parameter - *expplashard* exponent in hardening law - *expdam* exponent in damage law - *critdam* critical damage - *expk* exponent k in the expression for elastic stiffness - *expl* exponent l in the expression for elastic stiffness - *expq* exponent q in the expression for tensor $\boldsymbol{F}$ - *expp* exponent p in the expression for tensor $\boldsymbol{F}$
Supported modes	3dMat

Table 46: Anisotropic elastoplastic model with isotropic damage - summary.

Description	Nonlocal anisotropic elastoplastic model with isotropic damage
Record Format	**TrabBoneNL3d** (in) # d(rn) # eps0(rn) # nu0(rn) # mu0(rn) # expk(rn) # expl(rn) # m1(rn) # m2(rn) # rho(rn) # sig0pos(rn) # sig0neg(rn) # chi0pos(rn) # chi0neg(rn) # tau0(rn) # plashardfactor(rn) # expplashard(rn) # expdam(rn) # critdam(rn) # m(rn) # R(rn) #
Parameters	- material number - *d* material density - *eps0* Young modulus (at zero porosity) - *nu0* Poisson ratio (at zero porosity) - *mu0* shear modulus (at zero porosity) - *m1* first eigenvalue of the fabric tensor - *m2* second eigenvalue of the fabric tensor - *rho* volume fraction of the solid phase - *sig0pos* yield stress in tension - *tau0* yield stress in shear - *chi0pos* interaction coefficient in tension - *chi0neg* interaction coefficient in compression - *plashardfactor* hardening parameter - *expplashard* exponent in the hardening law - *expdam* exponent in the damage law - *critdam* critical damage - *expk* exponent k in the expression for elastic stiffness - *expl* exponent l in the expression for elastic stiffness - *expq* exponent q in the expression for tensor $\boldsymbol{F}$ - *expp* exponent p in the expression for tensor $\boldsymbol{F}$ - m over-nonlocal parameter - R nonlocal interaction radius
Supported modes	3dMat

Table 47: Nonlocal formulation of anisotropic elastoplastic model with isotropic damage – summary.

1.9 Material models for interfaces

Interface elements have to be used with material models describing the constitutive behavior of interfaces between two materials (e.g. between steel reinforcement and concrete), or between two bodies in contact. Such interface laws are formulated in terms of the traction vector t and the displacement jump vector δ.

1.9.1 Cohesive interface material - cohInt

A simple interface material with generally different stiffness in compression, tension and shear. It is intended for simulating a contact with low stiffness in tension and high in compression. The parameter *transitionOpening* specifies initial gap embedded in an element which causes transition from tension to compression. For example, *transitionOpening*=0.01 m means that there exists the embedded gap which needs displacement jump 0.01 m to close. Traction-separation law for normal direction takes the following form:

$$
\begin{aligned}
t_n &= \left(\frac{\pi}{2}+\arctan(s_m\bar{\delta})\right)\frac{k_t}{\pi}\bar{\delta}+\left(\frac{\pi}{2}-\arctan(s_m\bar{\delta})\right)\frac{k_n}{\pi}\bar{\delta} && (223)\\
s_m &= \mathit{smoothMag} && (224)\\
\delta_0 &= \mathit{transitionOpening} && (225)\\
\bar{\delta} &= \delta_n+\delta_0 && (226)\\
k_t &= k_n\cdot \mathit{stiffCoeffKn} && (227)
\end{aligned}
$$

where *smoothMag* controlls smoothing magnitude. Tangential stiffness for normal direction is found by differentiating Eq. (223)

$$
\begin{aligned}
k_{nn} &= \left(\frac{\pi}{2}+\arctan(s_m\bar{\delta})\right)\frac{k_t}{\pi}+\left(\frac{\pi}{2}-\arctan(s_m\bar{\delta})\right)\frac{k_n}{\pi}+ && (228)\\
&+ \frac{s_m\cdot k_t\bar{\delta}}{\pi(s_m^2\bar{\delta}^2+1)}-\frac{s_m\cdot k_n\bar{\delta}}{\pi(s_m^2\bar{\delta}^2+1)} && (229)
\end{aligned}
$$

Shear stiffness remains constant during all possible loadins and there is no influence of normal direction.

Description	Cohesive interface material
Record Format	**cohInt** (in) # kn(rn) # ks(rn) # [stiffCoeffKn(rn) #] [smoothMag(rn) #] [transitionOpening(rn) #]
Parameters	- material number - *kn* (penalty) stiffness in compression - *ks* stiffness in shear - *stiffCoeffKn* ratio (tensile stiffness / compression stiffness) - *smoothMag* smoothing parameter for transition between tensile/compressive behavior - *transitionOpening* embedded gap in the element
Supported modes	_1dInterface,_2dInterface,_3dInterface

Table 48: Cohesive interface material – summary.

1.9.2 Isotropic damage model for interfaces

This model is described in Section 1.5.9.

1.9.3 Simple interface material - obsolete

This model provides a simple interface law with penalty-type contact and friction. In the normal direction, the response is linear elastic, but with different stiffnesses in tension and in compression (stiffness *kn* in compression, *kn***stiffcoeff* in tension). By setting *kn* to a high value, the penetration (overlap) can be reduced, in the sense of the penalty approach. By setting *stiffcoeff* to 0, free opening of the gap can be allowed. The shear response is elastoplastic, with the yield limit dependent on the normal traction. Crosssection's width, height or area have no influence on the results. The magnitude of the shear traction $\boldsymbol{\sigma}_T$ must not exceed the yield limit computed according to a Coulomb-like friction law as the product of the (negative part of) normal traction σ_N and a dimensionless coefficient of friction fc:

$$||\boldsymbol{\sigma}_T|| \leq \langle -\sigma_N \cdot fc \rangle \tag{230}$$

σ_N is computed multiplying a known normal strain and a known stiffness in tension or in compression.

The shear elastic stiffness is assumed to be *kn* (i.e., equal to the normal stiffness). If the normal traction is tensile or zero, no shear traction can be transmitted by the interface. In the future, this law will be enriched by a cohesion-like term.

If used in connection of two nodes with `interface1delement`, the element-level parameter *normal* determines what is compression and what is tension (from the 1st node to the 2nd node in *normal* direction it is tension). If *normalClearance* is defined, the element has tensile stiffness until the gap within the element is closed. This feature allows simulating two faces with a gap. When the gap is smaller than *normalClearance*, the element stiffness changes to compression, see Figure 11.

The model description and parameters are summarized in Tab. 49.

Description	Simple interface material
Record Format	**simpleintermat** $_{\text{(in)}}$ # kn$_{\text{(rn)}}$ # [fc$_{\text{(rn)}}$ #] [stiffcoeff$_{\text{(rn)}}$ #] [normalClearance$_{\text{(rn)}}$ #]
Parameters	- material number - *kn* (penalty) stiffness in compression - *fc* friction coefficient - *stiffcoeff* ratio (tensile stiffness / compression stiffness) - *normalClearance* free distance within element
Supported modes	_1dInterface

Table 49: Simple interface material – summary.

1.9.4 Bond-slip model for reinforced concrete - BondCEB

The complex steel/concrete interaction can be modelled with a bond-slip relation, which describes the bond stress (tangential interface traction), τ, in terms

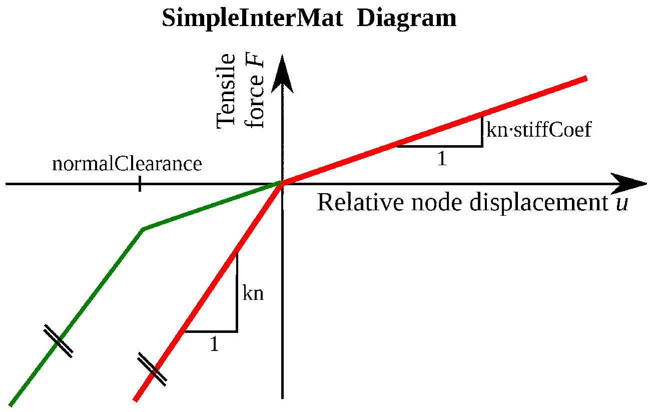

Figure 11: Working diagram of SimpleInterfaceMat.

of the relative reinforcement slip (tangential interface jump), s. This interface material model is based on the local bond–slip relationship for reinforced concrete under good bond conditions outlined in the the *fib* Model Code for Concrete Structures 2010 [31]. In general, the model is formulated in terms of the interface traction vector $\boldsymbol{t}$ and the interface jump vector $\boldsymbol{\delta}$. In the model, the interface is assumed to have only elastic stiffness k_n in the normal direction. The normal interface traction is then evaluated elastically from the normal interface jump, i.e. $t_\mathrm{n} = k_\mathrm{n}\delta_\mathrm{n}$. The tangential traction $t_\mathrm{t} = \tau$ is evaluated from the user-specified function $\tau(s)$, see Figure 12:

$$\tau(s) = \begin{cases} \tau_\mathrm{max}\left(\dfrac{s}{s_1}\right)^\alpha & \text{for } 0 \leq s \leq s_1, \\ \tau_\mathrm{max} & \text{for } s_1 < s \leq s_2, \\ \tau_\mathrm{max} - \dfrac{(\tau_\mathrm{max} - \tau_\mathrm{f})\,(s - s_2)}{(s_3 - s_2)} & \text{for } s_2 < s \leq s_3, \\ \tau_\mathrm{f} & \text{for } s > s_3. \end{cases} \tag{231}$$

For an exponent α smaller than 1 (default value 0.4), the initial tangential stiffness of the interface, k_s, is undefined and cannot be used in numerical computations. Therefore, this stiffness needs to be specified manually. Should the provided stiffness be smaller than $k_\mathrm{n} = \dfrac{\tau_\mathrm{max}}{s_1}$, it will be automatically adjusted to this value. Note that only elastic tangent stiffness is supported. Hence, in 2D the tangent stiffness matrix takes the form

$$\frac{\partial \boldsymbol{t}}{\partial \boldsymbol{\delta}} = \begin{bmatrix} \dfrac{\partial t_\mathrm{n}}{\partial \delta_\mathrm{n}} & \dfrac{\partial t_\mathrm{n}}{\partial s} \\ \dfrac{\partial \tau}{\partial \delta_\mathrm{n}} & \dfrac{\partial \tau}{\partial s} \end{bmatrix} = \begin{bmatrix} k_\mathrm{n} & 0 \\ 0 & k_\mathrm{s} \end{bmatrix} \tag{232}$$

Model description and the input parameters are summarized in Tab. 50.

1.10 Material models for lattice elements

Lattice elements have to be used with material models describing the constitutive behavior in the form of vector of tractions and strains determined from

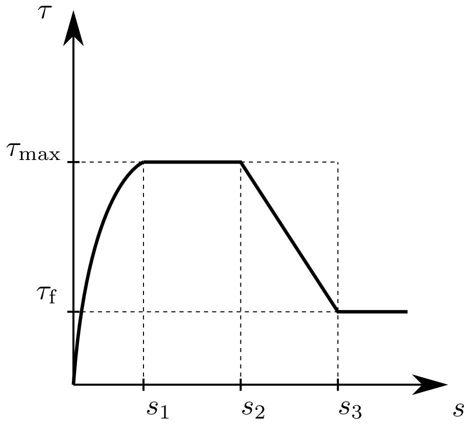

Figure 12: Bond stress (τ) - reinforcement slip (s) diagram for BondCEB model.

Description	Bond-slip model for reinforced concrete
Record Format	**bondceb** $_{\text{(in)}}$ # kn$_{\text{(rn)}}$ # ks$_{\text{(rn)}}$ # s1$_{\text{(rn)}}$ # s2$_{\text{(rn)}}$ # s3$_{\text{(rn)}}$ # taumax$_{\text{(rn)}}$ # [tauf$_{\text{(rn)}}$ #] [alpha$_{\text{(rn)}}$ #]
Parameters	- material number - *kn* interface elastic normal stiffness - *ks* interface elastic tangential (shear) stiffness - *s1* characteristic slip value - *s2* characteristic slip value - *s3* characteristic slip value - *taumax* maximum bond stress - *tauf* residual bond stress at reinforcement pull-out - *alpha* bond-slip curve parameter (exponent)
Supported modes	_2dInterface, _3dInterface

Table 50: Bond-slip model for reinforced concrete – summary.

displacement jumps smeared out over the element length.

1.10.1 Latticedamage2d

This is a damage lattice material used together with latticedamage2d elements. It uses a scalar damage relationship of the form

$$\boldsymbol{\sigma} = (1 - \omega)\,\mathbf{D}_{\mathrm{e}}\boldsymbol{\varepsilon} \tag{233}$$

where $\boldsymbol{\sigma} = (\sigma_{\mathrm{n}}, \sigma_{\mathrm{t}}, \sigma_{\phi})^T$ is a vector of tractions and $\boldsymbol{\varepsilon} = (\varepsilon_{\mathrm{n}}, \varepsilon_{\mathrm{t}}, \varepsilon_{\phi})^T$ is a vector of strains obtained from displacement jumps smeared over the element length. Furthermore, ω is the damage variable varying from 0 (undamaged) to 1 (fully damaged). Also, $\mathbf{D}_{\mathrm{e}}$ is the elastic stiffness matrix which is based on the elastic modulus of the lattice material E, and a parameter γ which is the ratio of the modulus of the shear and normal direction. The strength envelope is elliptic (Figure 13) and determined by three parameters, f_{t}, f_{q} and f_{c}. The evolution of the damage variable ω is controlled by normal stress-normal crack opening law. The three possible laws are linear, bilinear and exponential (Figure 14).

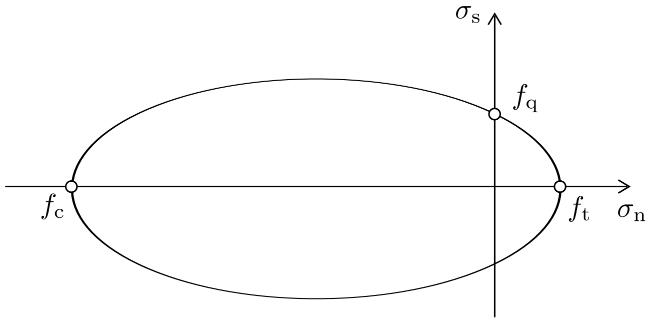

Figure 13: Strength envelope of LatticeDamage2d.

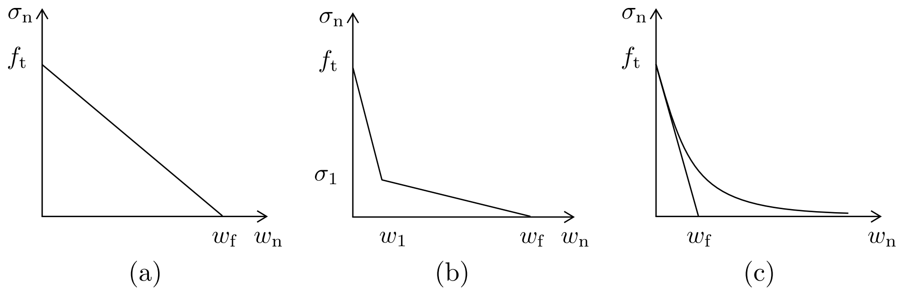

Figure 14: Softening types of LatticeDamage2d: (a) linear softening, (b) bilinear softening, (c) exponential softening.

The model parameters are summarised in Tab. 51.

Description	Saclar damage model for lattice2d
Record Format	**latticedamage2d** (in) # d(rn) # talpha(rn) # e(rn) # a1(rn) # a2(rn) # e0(rn) # coh(rn) # ec(rn) # stype(rn) # wf(rn) # wf1(rn) #
Parameters	- material number - *d* material density - *talpha* Thermal exansion coefficient - *e* normal modulus of lattice material - *a1* ratio of shear and normal modulus - *a2* ratio of rotational and normal modulus. Optional parameter. Default is 1. - *e0* strain at tensile strength: f_t/E - *coh* ratio of shear and tensile strength: f_q/f_t - *ec* ratio of compressive and tensile strength: f_c/f_t - *stype* softening types: 1-linear, 2-bilinear and 3-exponential - *wf* displacement threshold related to fracture energy used in all three softening types.
Supported modes	2dlattice

Table 51: Scalar damage model for 2d lattice elements – summary.

1.11 Material models for steel relaxation

1.11.1 Model for relaxation of prestressing steel - SteelRelaxMat

This section describes the implementation of the material model for steel relaxation given in Eurocode 2 (the same as in Model Code 2010) and in Bažant and Yu (J. of Eng. Mech, 2013) which reduces to the first model under constant strain. At variable strain history the first model uses the approach employing the so-called *equivalent time* approach described in Annex D in the Eurocode 2.

The current implementation takes into account only prestress losses due to steel relaxation, other losses (e.g. slip at anchorage, thermal dilation, friction, etc.) need to be treated separately. The same holds for the stress transfer from prestressing reinforcement to concrete in the region called *transmission length*. On the other hand, losses due to sequential prestressing, elastic deformation and both short-time and long-time creep and shrinkage are taken into account automatically provided that a suitable material model is chosen for concrete.

In the first approach the stress on the end of the time step is explicitly given by the current stress, prestressing level and the cumulative value of prestress losses. On the other hand, in Bažant's approach it is necessary to iterate on the material point level in order to reach equilibrium.

As a simplification the stress-strain diagram is in the current implementation assumed to be linear (no yielding), this should be sufficient for most cases.

Under a constant strain, the evolution of prestress loss is defined as

$$\Delta\sigma = \sigma_{init} k_1 \rho_{1000} \exp(k_2 \mu)(t/1000)^{0.75(1-\mu)} \times 10^{-5} \tag{234}$$

where σ_{init} is the initial value of prestress reduced for losses during prestressing, t is time after prestressing in **hours**, $\mu = \sigma_{init}/f_{pk}$, f_{pk} is the characteristic strength of prestressing steel in tension, and finally k_1, k_2, and ρ_{1000} are material parameters determined by the relaxation properties of the reinforcement. For wires or cables with **normal relaxation** (class 1) $k_1 = 5.39$, $k_2 = 6.7$ and $\rho_{1000} = 8.0$, for cables or wires with **reduced relaxation** (class 2) $k_1 = 0.66$, $k_2 = 9.1$ and $\rho_{1000} = 2.5$, and for **hot-rolled** and modified rods (class 3) $k_1 = 1.98$, $k_2 = 8.0$ and $\rho_{1000} = 4.0$.

The prestress σ_{init} is not specified in the input record. It is initialized automatically at the time instant when stress differs from zero.

The material model has one internal variable which has a meaning of cumulative prestress loss when *equivalent time* approach is employed; otherwise its meaning is a cumulative strain caused by relaxation.

Description	SteelRelaxMat model for relaxation of prestressing reinforcement
Record Format	**SteelRelaxMat** d(rn) # E(rn) # reinfClass(in) # [timeFactor(rn) #] charStrength(rn) # approach(in) # [k1(rn) #] [k2(rn) #] [rho1000(rn) #] [tolerance(rn) #] [relRelaxBound(rn) #]
Parameters	- *num* material model number - *d* specific weight - *E* Young's modulus - *reinfClass* class of prestressing reinforcement (1, 2, 3) - *timeFactor* scaling factor transforming the actual time into appropriate units needed by the formulae of the eurocode. For analysis in days timeFactor = 1, for analysis in seconds timeFactor = 86,400. - *charStrength* characteristic strength of prestressing steel in appropriate units (not necessarily MPa) - *approach* 0 = approach according to Bažant and Yu, 1 = equivalent time approach according to Eurocode 2 and *fib* Model Code 2010 - *k1* possibility to overwrite default value given by the reinforcement class - *k2* possibility to overwrite default value given by the reinforcement class - *rho1000* possibility to overwrite default value given by the reinforcement class - *tolerance* applicable only for *approach* = 0; tolerance specifying the residual in the stress evaluation algorithm, default value is 10^{-6} - *relRelaxBound* ratio of stress to characteristic strength under which the relaxation is zero (typically 0.4–0.5); default value is zero
Supported modes	1dMat

Table 52: SteelRelaxMat material model – summary.

2 Material Models for Transport Problems

2.1 Isotropic linear material for heat transport – IsoHeat

Linear isotropic material model for heat transport problems described by the linear diffusion equation

$$c\frac{\partial T}{\partial t} = \nabla \cdot (k\nabla T) \tag{235}$$

where T is the temperature, c is the specific heat capacity, and k is the conductivity. The model parameters are summarized in Tab. 53.

Description	Linear isotropic elastic material
Record Format	**IsoHeat** num$_{\text{(in)}}$ # d$_{\text{(rn)}}$ # k$_{\text{(rn)}}$ # c$_{\text{(rn)}}$ #
Parameters	- *num* material model number
	- *d* material density
	- *k* Conductivity
	- *c* Specific heat capacity
	- *maturityT0* Baseline value for material maturity, default 0
Supported modes	_2dHeat

Table 53: Linear isotropic material for heat transport - summary.

2.2 Isotropic linear material for moisture transport – IsoLinMoisture

Linear isotropic material model for moisture transport problems described by the linear diffusion equation[3]

$$k\frac{\partial h}{\partial t} = \nabla \cdot (c\nabla h) \tag{236}$$

where h is the pore relative humidity (dimensionless, between 0 and 1), k is the moisture capacity [kg/m^3], and c is the moisture permeability [kg/m·s]. The model parameters are summarized in Tab. 54.

2.3 Isotropic material for moisture transport based on Bažant and Najjar – BazantNajjarMoisture

This is a specific model for nonlinear moisture transport in isotropic cementitious materials, based on [2]. The governing equation

$$\frac{\partial h}{\partial t} = \nabla \cdot (C(h)\nabla h) \tag{237}$$

[3]Note that the symbols k and c in Eq. (236) have a different meaning than in Eq. (235). The reason is that the nonlinear model for moisture transport described in Section 2.4 traditionally uses c for permeability and Eq. (236) should be obtained as a special case of Eq. (239). On the other hand, the heat conduction model from Section 2.1 was implemented earlier and the input parameters are directly called k and c, so changing this notation now could lead to confusion for some older input files.

Description	Linear isotropic material for moisture transport
Record Format	**IsoLinMoistureMat** num$_{(in)}$ # d$_{(rn)}$ # perm$_{(rn)}$ # capa$_{(rn)}$ #
Parameters	- *num* material model number - *d* material density - *perm* moisture permeability - *capa* moisture capacity
Supported modes	_2dHeat

Table 54: Linear isotropic material for moisture transport - summary.

is a special case of Eq. (239), valid under the assumption that the slope of the sorption isotherm is linear, i.e. the moisture capacity is constant. In Eq. (237), h is the relative humidity and $C(h)$ is the humidity-dependent diffusivity approximated by

$$C(h) = C_1 \left(\alpha_0 + \frac{1-\alpha_0}{1+\left(\frac{1-h}{1-h_c}\right)^n} \right) \tag{238}$$

where C_1 is the diffusivity at saturation (typical value for concrete $\approx 30\ \mathrm{mm}^2/\mathrm{day}$), α_0 is the dimensionless ratio of diffusivity at low humidity to diffusivity at saturation (typical value ≈ 0.05), h_c is the humidity "in the middle" of the transition between low and high diffusivity (typical value ≈ 0.8), and n is dimensionless exponent (high values of n, e.g. 12, lead to a rapid transition between low and high diffusivity). Optionally, it is possible to specify the moisture capacity. This property is not needed for solution of the diffusion equation (237), but it is needed if the computed change of relative humidity is transformed into water content loss (mass of lost water per unit volume).

The model parameters are summarized in Tab. 55.

Description	Nonlinear isotropic material for moisture transport
Record Format	**BazantNajjarMoistureMat** num$_{(in)}$ # d$_{(rn)}$ # c1$_{(rn)}$ # n$_{(rn)}$ # alpha0$_{(rn)}$ # hc$_{(rn)}$ # [capa$_{(rn)}$ #]
Parameters	- *num* material model number - *d* material density - *c1* moisture diffusivity at full saturation [$\mathrm{m}^2\ \mathrm{s}^{-1}$] - *n* exponent [-] - *alpha0* ratio between minimum and maximum diffusivity [-] - *hc* relative humidity at which the diffusivity is exactly between its minimum and maximum value [-] - *capa* moisture capacity (default value is 1.0)
Supported modes	_2dHeat

Table 55: Nonlinear isotropic material for moisture transport - summary.

2.4 Nonlinear isotropic material for moisture transport – NlIsoMoisture

This is a more general model for nonlinear moisture transport in isotropic porous materials, based on a nonlinear sorption isotherm (relation between the pore relative humidity h and the water content w) and on a humidity-dependent moisture permeability. The governing differential equation solves water mass balance in a unit volume [kg/m^3/s] and reads

$$k(h)\frac{\partial h}{\partial t} = \nabla \cdot [c(h)\nabla h] + w_n \frac{\mathrm{d}\alpha}{\mathrm{d}t} \tag{239}$$

where $k(h)$ [kg/m^3] is the humidity-dependent moisture capacity ($k(h) = \frac{\partial w}{\partial h}$ which is derivative of the moisture content $w(h)$ [kg/m^3] with respect to the relative humidity), $c(h)$ [kg/m/s] is the moisture permeability and the sink term $w_n \frac{\mathrm{d}\alpha}{\mathrm{d}t}$ corresponds to non-evaporable water loss due to hydration. w_n is non-evaporable water content for complete hydration per m^3 [kg/m^3] and α is degree of hydration [-]. For the majority of cements, 1 kg of cement consumes approximately 0.23 kg of non-evaporable water at complete hydration.

So far, six different functions for the **sorption isotherm** have been implemented (in fact, what matters for the model is not the isotherm itself but its derivative—the moisture capacity):

1. **Linear** isotherm ($isothermType$ = 0) is characterized only by its slope given by parameter $moistureCapacity$.

2. **Piecewise linear** isotherm ($isothermType$ = 1) is defined by two arrays with the values of pore relative humidity *iso_h* and the corresponding values of moisture content *iso_w*(h). The arrays must be of the same size.

3. **Ricken** isotherm [15] ($isothermType$ = 2), which is widely used for sorption of porous building materials. It is expressed by the equation

$$w(h) = w_0 - \frac{\ln(1-h)}{d} \tag{240}$$

   where w_0 [kg/m^3] is the water content at $h = 0$ and d [m^3/kg] is an approximation coefficient. In the input record, only d must be specified (w_0 is not needed). Note that for $h = 1$ this isotherm gives an infinite moisture content.

4. Isotherm proposed by **Kuenzel** [15] ($isothermType$ = 3) in the form

$$w(h) = w_f \frac{(b-1)h}{b-h} \tag{241}$$

   where w_f [kg/m^3] is the moisture content at free saturation and b is a dimensionless approximation factor greater than 1.

5. Isotherm proposed by **Hansen** [13] ($isothermType$ = 4) in the form

$$u(h) = u_h \left(1 - \frac{\ln h}{A}\right)^{-1/n} \tag{242}$$

characterizes the amount of adsorbed water by the moisture ratio u [kg/kg]. To obtain the moisture content w, it is necessary to multiply the moisture ratio by the density of the solid phase. In (242), u_h is the maximum hygroscopically bound water by adsorption, and A and n are constants obtained by fitting of experimental data.

6. The **BSB** isotherm [4] ($isothermType = 5$) is an improved version of the famous BET isotherm. It is expressed in terms of the moisture ratio

$$u(h) = \frac{CkV_m h}{(1-kh)(1+(C-1)kh)} \tag{243}$$

where V_m is the monolayer capacity, and C depends on the absolute temperature T and on the difference between the heat of adsorption and condensation. Empirical formulae for estimation of the parameters can be found in [27]. Note that these formulae hold quite accurately for cement paste only; a reduction of the moisture ratio is necessary if the isotherm should be applied for concrete.

The present implementation covers three functions for **moisture permeability**:

1. **Piecewise linear** permeability ($permeabilityType = 0$) is defined by two arrays with the values of pore relative humidity *perm_h* and the corresponding values of moisture content *perm_c*(h). The arrays must be of the same size.

2. The **Bažant-Najjar** permeability function ($permeabilityType = 1$) is given by the same formula (238) as the diffusivity in Section 2.3. All parameters have a similar meaning as in (238) but $c1$ is now the moisture permeability at full saturation [kg/m·s].

3. Permeability function proposed by **Xi et al.** [27] ($permeabilityType = 2$) reads

$$c(h) = \alpha_h + \beta_h \left[1 - 2^{-10^{\gamma_h(h-1)}}\right] \tag{244}$$

where α_h, β_h and γ_h are parameters that can be evaluated using empirical mixture-based formulae presented in [27]. However, if those formulae are used outside the range of water-cement ratios for which they were calibrated, the permeability may become negative. Also the physical units are unclear.

Note that the Bajant-Najjar model from Section 2.3 can be obtained as a special case of the present model if $permeabilityType$ is set to 1 and $isothermType$ is set to 0. The ratio $c1/moistureCapacity$ then corresponds to the diffusivity parameter C_1 from Eq. (237).

The model parameters are summarized in Tab. 56.

2.5 Material for cement hydration - CemhydMat

CemhydMat represents a hydrating material based on CEMHYD3D model version 3.0, developed at NIST [5]. The model represents a digital hydrating microstructure, driven with cellular automata rules and combined with cement chemistry. Ordinary Portland cement is treated without any difficulties, blended cements are usually decomposed into hydrating Portland contribution and intert secondary cementitious material. The microstructure size can be from $10 \times 10 \times 10$ to over $200 \times 200 \times 200$ μm. For standard computations the size $50 \times 50 \times 50$ suffices.

Each material instance creates an independent microstructure. It is also possible to enforce having different microstructures in each integration point. The hydrating model is coupled with temperature and averaging over shared elements within one material instance occurs during the solution. Such approach allows domain partitioning to many CemhydMat instances, depending on expected accuracy or computational speed. A more detailed description with engineering examples was published [25]. Tab. 57 summarizes input parameters.

The input XML file specifies the details about cement and concrete composition. It is possible to start all simulations from the scratch, i.e. with the reconstruction of digital microstructure. Alternatively, the digital microstructure can be provided directly in two files; one for chemical phases, the second for particle's IDs. The XML input file can be created with the CemPy package, obtainable from http://mech.fsv.cvut.cz/~smilauer/index.php?id=software. The CemPy package alleviates tedious preparation of particle size distribution etc.

The linear solver (specified as NonStationaryProblem) performs well when the time integration step is small enough (order of minutes) and heat capacity, conductivity and density remain constant. If not so, use of nonlinear solver is strongly suggested (specified as NlTransientTransportProblem).

Description	Nonlinear isotropic material for moisture transport
Record Format	**NlIsoMoistureMat** num$_{(in)}$ # d$_{(rn)}$ # isothermType$_{(in)}$ # permeabilityType$_{(in)}$ # [rhodry$_{(rn)}$ #] [capa$_{(rn)}$ #] [iso_h$_{(ra)}$ #] [iso_w(h)$_{(ra)}$ #] [dd$_{(rn)}$ #] [wf$_{(rn)}$ #] [b$_{(rn)}$ #] [uh$_{(rn)}$ #] [A$_{(rn)}$ #] [nn$_{(rn)}$ #] [c$_{(rn)}$ #] [k$_{(rn)}$ #] [Vm$_{(rn)}$ #] [perm_h$_{(ra)}$ #] [perm_c(h)$_{(ra)}$ #] [c1$_{(rn)}$ #] [n$_{(rn)}$ #] [alpha0$_{(rn)}$ #] [hc$_{(rn)}$ #] [alphah$_{(rn)}$ #] [betah$_{(rn)}$ #] [gammah$_{(rn)}$ #] [wn$_{(rn)}$ #] [alpha$_{(expr)}$ #]
Parameters	- *num* material model number - *d* material density - *isothermType* isotherm function as listed above (0, 1, ...5) - *permeabilityType* moisture permeability function as listed above (0, 1, 2) - *rhodry* [kg/m^3] density of dry material (for $isothermType = 4$ and 5) - *capa* [kg/m^3] moisture capacity (for $isothermType = 0$) - *iso_h* [-] humidity array (for $isothermType = 1$) - *iso_w(h)* [kg/m^3] moisture content array (for $isothermType = 1$) - *dd* [-] parameter (for $isothermType = 2$) - *wf* [kg/m^3] is the moisture content at free saturation (for $isothermType = 3$) - *b* [-] parameter (for $isothermType = 3$) - *uh* [kg/kg] maximum hygroscopically bound water by adsorption (for $isothermType = 4$) - *A* [-] parameter (for $isothermType = 4$) - *n* [-] parameter (for $isothermType = 4$) - *Vm* (for $isothermType = 5$) - *k* (for $isothermType = 5$) - *C* (for $isothermType = 5$) - *perm_h* [-] humidity array (for $permeabilityType = 0$) - *perm_c(h)* [kg m^{-1} s^{-1}] moisture permeability array (for $permeabilityType = 0$) - *c1* [kg m^{-1} s^{-1}] moisture permeability at full saturation (for $permeabilityType = 1$) - *n* [-] exponent (for $permeabilityType = 1$) - *alpha0* [-] ratio between minimum and maximum diffusivity (for $permeabilityType = 1$) - *hc* [-] relative humidity at which the diffusivity is exactly between its minimum and maximum value (for $permeabilityType = 1$) - *alphah* [kg m^{-1} s^{-1}] (for $permeabilityType = 2$) - *betah* [kg m^{-1} s^{-1}] (for $permeabilityType = 2$) - *gammah* [-] (for $permeabilityType = 2$) - *wn* [kg m^{-3}] nonevaporable water content per m^3 of concrete, default 0.23 kg/kg of cement - *alpha* [-] function of degree of hydration
Supported modes	_2dHeat

Table 56: Nonlinear isotropic material for moisture transport - summary.

Description	Cemhyd - hydrating material
Record Format	**CemhydMat** num$_{(in)}$ # d$_{(rn)}$ # k$_{(rn)}$ # c$_{(rn)}$ # file$_{(s)}$ # [eachGP$_{(in)}$ #] [densityType$_{(in)}$ #] [conductivityType$_{(in)}$ #] [capacityType$_{(in)}$ #] [castingtime$_{(rn)}$ #] [nowarnings$_{(ia)}$ #] [scaling$_{(ra)}$ #] [reinforcementDegree$_{(rn)}$ #]
Parameters	- *num* material model number - *d* material density - *k* Conductivity - *c* Specific heat capacity - *file* XML input file for cement microstructure and concrete composition - *eachGP* 0 (default) no separate microstructures in each GP, 1 assign separate microstructures to each GP - *densityType* 0 (default) get density from OOFEM input file, 1 get it from XML input file - *conductivityType* 0 (default) get constant conductivity from OOFEM input file, 1 compute as $\lambda = \mathrm{k}(1.33 - 0.33\alpha)$ [21] - *capacityType* 0 (default) get capacity, 1 according to Bentz, 2 according to XML and CEMHYD3D routines - *castingtime* optional casting time of concrete, from which hydration takes place. Absolute time is used. - *nowarnings* supresses warnings when material data are out of standard ranges. The array of size 4 represent entries for density, conductivity, capacity, temperature. Nonzero values mean supression. - *scaling* components in the array scale density, conductivity, capacity in this order. *nowarnings* are checked before scaling. - *reinforcementDegree* specifies the area fraction of reinforcement. Typical values is 0.015. Steel reinforcement slightly increases concrete conductivity and slightly decreases its capacity. Thermal properties of steel are considered 20 W/m/K and 500 J/kg/K.
Supported modes	_2dHeat, _3dHeat

Table 57: Cemhydmat - summary.

2.6 Material for cement hydration - HydratingConcreteMat

Simple hydration models based on chemical affinity are implemented. The models calculate degree of hydration of cement, α, which can be scaled to the level of concrete when providing corresponding amount of cement in concrete. Blended cements can be considered as well, either by separating supplementary cementitious materials from pure Portland clinker or by providing parameters for the evolution of hydration degree and potential heat. Released heat from cement paste is obtained from

$$Q(t) = \alpha Q_{pot}, \tag{245}$$

where potential hydration heat, Q_{pot}, is expressed in kJ/kg of cement and for pure Portland cement is around 500 kJ/kg.

Evolution of hydration degree under isothemal curing conditions is approximated by several models. Scaling from a reference temperature to arbitrary temperature is based on Arrhenius equation, which coincides with the maturity method approach. The equivalent time, t_e, is defined as time under constant reference (isothermal) temperature

$$t_e(T_0) = t(T)k_{rate}, \tag{246}$$

$$k_{rate} = \exp\left[\frac{E_a}{R}\left(\frac{1}{T_0} - \frac{1}{T}\right)\right], \tag{247}$$

where t is real time, T is the arbitrary constant temperature of hydration, T_0 is a reference temperature, R is the universal gas constant (8.314 $\mathrm{Jmol^{-1}K^{-1}}$) and E_a is the apparent activation energy. Due to varying history of temperature, incremental solution is adopted. Linear and nonlinear nonstationary solvers are supported for all *hydrationmodeltype*'s. Hydration models are evaluated at intrinsic time in each time step. Usually, intrinsic time is in the middle of the time step.

The *hydrationmodeltype* = 1 is based on exponential approximation of hydration degree [23]. Equivalent time increment is added in each time step. Thus all the thermal history is stored in the equivalent time

$$\alpha(t_e) = \alpha_\infty \exp\left(-\left[\frac{\tau}{t_e}\right]^\beta\right) \tag{248}$$

where three parameters τ, β and α_∞ are needed. Some meaningful parameters are provided in [23], e.g. $\tau = 26 \cdot 3600 = 93600$ s, $\beta = 0.75$ and $\alpha_\infty = 0.90$.

The *hydrationmodeltype* = 2 is inspired by Cervera et al. [6], who proposed an analytical form of the normalized affinity which was refined in [7]. A slightly modified formulation is proposed here. The affinity model is formulated for a reference temperature 25°C

$$\frac{\mathrm{d}\alpha}{\mathrm{d}t} = \tilde{A}_{25}(\alpha)k_{rate} = B_1\left(\frac{B_2}{\alpha_\infty} + \alpha\right)(\alpha_\infty - \alpha)\, f_s \exp\left(-\bar{\eta}\frac{\alpha}{\alpha_\infty}\right) k_{rate} \tag{249}$$

$$\alpha > DoH_1 \Rightarrow f_s = 1 + P_1(\alpha - DoH_1) \text{ else } f_s = 1 \tag{250}$$

where B_1, B_2 are coefficients to be calibrated, α_∞ is the ultimate hydration degree and $\bar{\eta}$ represents microdiffusion of free water through formed hydrates.

The function f_s adds additional peak which may occur in slag-rich blended cements with two parameters DoH_1, P_1. The solution proceeds incrementally, where α is the unknown. During one macroscopic time step, Eq. (249) needs to be integrated in finer inner steps. This is controlled with two optional variables; *maxmodelintegrationtime* specifies maximum integration time in the loop while *minmodeltimestepintegrations* specifies minimum number of integration steps.

Description	HydratingConcreteMat
Record Format	**HydratingConcreteMat** num$_{\rm (in)}$ # d$_{\rm (rn)}$ # k$_{\rm (rn)}$ # c$_{\rm (rn)}$ # hydrationmodeltype$_{\rm (in)}$ # Qpot$_{\rm (rn)}$ # masscement$_{\rm (rn)}$ # [activationenergy$_{\rm (rn)}$ #] reinforcementdegree$_{\rm (rn)}$ #] [densitytype$_{\rm (in)}$ #] [conductivitytype$_{\rm (in)}$ #] [capacityType$_{\rm (in)}$ #] [minModelTimeStepIntegrations$_{\rm (in)}$ #] [maxmodelintegrationtime$_{\rm (rn)}$ #] [castingTime$_{\rm (rn)}$ #]
Parameters	- *num* material model number - *d* material density about 2300 kg/m^3 - *k* Conductivity about 1.7 W/m/K - *c* Specific heat capacity about 870 J/kg/K - *hydrationmodeltype* 1 is exponential model from Eq. (248), 2 is affinity model from Eq. (249) - *Qpot* Potential heat of hydration, about 500 kJ/kg of cement - *masscement* Cement mass per 1m^3 of concrete, about 200-450 - *activationenergy* Arrhenius activation energy, 38400. (default) - *DoHinf* degree of hydration at infinite time - *B1,B2,eta,DoH1,P1* parameters from Eq. (249)-Eq. (250) - *reinforcementDegree* specifies the area fraction of reinforcement. Typical values is 0.015. Steel reinforcement slightly increases concrete conductivity and slightly decreases its capacity. Thermal properties of steel are considered 20 W/m/K and 500 J/kg/K. - *densityType* 0 (default) - *conductivityType* 0 (default), 1 compute as λ = k$(1.33 - 0.33\alpha)$ [21] - *capacityType* 0 (default) - *minModelTimeStepIntegrations* Minimum integrations per time step in affinity model 30 (default) - *maxmodelintegrationtime* Maximum integration time step in affinity model 36000 s (default) - *castingtime* optional casting time of concrete, from which hydration takes place, in s - *scaling* components in the array scale density, conductivity, capacity in this order. *nowarnings* are checked before scaling.
Supported modes	_2dHeat, _3dHeat

Table 58: HydratingConcreteMat - summary of affinity hydration models.

Fig. (15) shows mutual comparison of three hydration models implemented in OOFEM. Parameters for exponential model according to Eq. (248) are $\tau = 26 \cdot 3600 = 93600$ s, $\beta = 0.75$, $\alpha_\infty = 0.90$. Parameters for affinity model according to Eq. (249) are $B_1 = 3.519e-4$ s^{-1}, $B_2 = 8.0e-7$, $\eta = 7.4$, $\alpha_\infty = 0.85$.

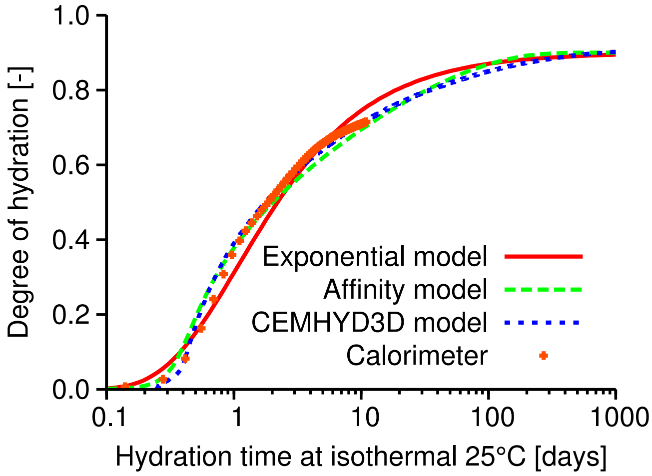

Figure 15: Performance of implemented hydration models: exponential model from Eq. (248), affinity model from Eq. (249), CEMHYD3D model from Subsection 2.5.

2.7 Coupled heat and mass transport material model - HeMotk

Coupled heat and mass transfer material model. Source: T. Krejci doctoral thesis; Bazant and Najjar, 1972; Pedersen, 1990. Assumptions: water vapor is the only driving mechanism; relative humidity is from range 0.2 - 0.98 (I and II regions). The model parameters are summarized in Tab. 59.

Description	Coupled heat and mass transfer material model
Record Format	**HeMotk** num(in) # d(rn) # a_0(rn) # nn(rn) # phi_c(rn) # delta_wet(rn) # w_h(rn) # n(rn) # a(rn) # latent(rn) # c(rn) # rho(rn) # chi_eff(rn) # por(rn) # rho_gws(rn) #
Parameters	- *num* material model number - *d*, *rho* material density - *a_0* constant (obtained from experiments) a_0 [Bazant and Najjar, 1972] - *nn* constant-exponent (obtained from experiments) n [Bazant and Najjar, 1972] - *phi_c* constant-relative humidity (obtained from experiments) phi_c [Bazant and Najjar, 1972] - *delta_wet* constant-water vapor permeability (obtained from experiments) delta_wet [Bazant and Najjar, 1972] - *w_h* constant water content (obtained from experiments) w_h [Pedersen, 1990] - *n* constant-exponent (obtained from experiments) n [Pedersen, 1990] - *a* constant (obtained from experiments) A [Pedersen, 1990] - *latent* latent heat of evaporation - *c* thermal capacity - *chi_eff* effective thermal conductivity - *por* porosity - *rho_gws* saturation volume density
Supported modes	_2dHeMo

Table 59: Coupled heat and mass transfer material model - summary.

2.8 Coupled heat and mass transport material model - HeMoKunzel

The presented formulation is based on the work of Kuenzel [15]. The model is suitable for problems with dominating water diffusion and negligible water convection. The governing equations for temperature and humidity reads

$$\frac{\partial Q}{\partial t} = \frac{\partial Q}{\partial T}\frac{\partial T}{\partial t} = C_v \frac{\partial T}{\partial t} = -\nabla q_T = \nabla\left(\lambda \nabla T\right) + h_v \nabla\left(\delta_p \nabla (H p_{sat})\right) \tag{251}$$

$$\frac{\partial w}{\partial t} = \frac{\partial w}{\partial H}\frac{\partial H}{\partial t} = -\nabla q_H = \nabla\left(D_H \nabla H + \delta_p \nabla (H p_{sat})\right) \tag{252}$$

T	(K)	Temperature
H	(-)	Relative humidity 0-1
$\frac{\partial Q}{\partial T} \approx C_v$	J/K/m^3	Heat storage capacity per volume
$\frac{\partial w}{\partial H}$	kg/m^3	Moisture storage capacity - sorption isotherm
Q	J/m^3	Total amount of heat in unit volume
q_T	W/m^2	Heat flux
λ	W/m/K	Thermal conductivity
h_v	J/kg	Evaporation enthalpy of water
δ_p	kg/m/s/Pa	Water vapour permeability
p_{sat}	Pa	Water vapour saturation pressure
w	kg/m^3	Moisture content
D_H	kg/m/s	Liquid conduction coefficient
D_w	m^2/s	Water diffusivity

Table 60: Parameters from Kunzel's model.

Numerical solution leads to the system of equations

$$\begin{bmatrix} \boldsymbol{K}_{TT} & \boldsymbol{K}_{TH} \\ \boldsymbol{K}_{HT} & \boldsymbol{K}_{HH} \end{bmatrix} \begin{Bmatrix} \boldsymbol{r}_T \\ \boldsymbol{r}_H \end{Bmatrix} + \begin{bmatrix} \boldsymbol{C}_{TT} & \boldsymbol{C}_{TH} \\ \boldsymbol{C}_{HT} & \boldsymbol{C}_{HH} \end{bmatrix} \begin{Bmatrix} \dot{\boldsymbol{r}}_T \\ \dot{\boldsymbol{r}}_H \end{Bmatrix} = \begin{Bmatrix} \boldsymbol{q}_T \\ \boldsymbol{q}_H \end{Bmatrix}, \tag{253}$$

where

$$\boldsymbol{K}_{TT} = \int_\Omega \boldsymbol{B}^T k_{TT} \boldsymbol{B} \mathrm{d}\Omega, \qquad \boldsymbol{K}_{TH} = \int_\Omega \boldsymbol{B}^T k_{Th} \boldsymbol{B} \mathrm{d}\Omega, \tag{254}$$

$$\boldsymbol{K}_{HT} = \int_\Omega \boldsymbol{B}^T k_{hT} \boldsymbol{B} \mathrm{d}\Omega, \qquad \boldsymbol{K}_{HH} = \int_\Omega \boldsymbol{B}^T k_{hh} \boldsymbol{B} \mathrm{d}\Omega, \tag{255}$$

$$\boldsymbol{C}_{TT} = \int_\Omega \boldsymbol{N}^T c_{TT} \boldsymbol{N} \mathrm{d}\Omega, \qquad \boldsymbol{C}_{TH} = \int_\Omega \boldsymbol{N}^T c_{Th} \boldsymbol{N} \mathrm{d}\Omega, \tag{256}$$

$$\boldsymbol{C}_{HT} = \int_\Omega \boldsymbol{N}^T c_{hT} \boldsymbol{N} \mathrm{d}\Omega, \qquad \boldsymbol{C}_{HH} = \int_\Omega \boldsymbol{N}^T c_{hh} \boldsymbol{N} \mathrm{d}\Omega, \tag{257}$$

$$\boldsymbol{q}_T = \int_{\Gamma_2} \boldsymbol{N}^T \overline{q}_T \mathrm{d}\Gamma, \qquad \boldsymbol{q}_H = \int_{\Gamma_2} \boldsymbol{N}^T \overline{q}^h \mathrm{d}\Gamma, \tag{258}$$

where

$$k_{TT} = \lambda(w) + h_v \cdot \delta_p(T) \cdot H \cdot \frac{\Delta p_{sat}}{\Delta T}(T), \tag{259}$$
$$k_{TH} = h_v \cdot \delta_p(T) \cdot p_{sat}(T), \tag{260}$$
$$k_{HT} = \delta_p(T) \cdot H \cdot \frac{\Delta p_{sat}}{\Delta T}(T), \tag{261}$$
$$k_{HH} = D_w(H) \cdot \frac{\Delta w}{\Delta H}(H) + \delta_p(T) \cdot p_{sat}(T), \tag{262}$$
$$c_{TT} = C_s \cdot \rho + C_w \cdot w, \tag{263}$$
$$c_{TH} = 0, \tag{264}$$
$$c_{HT} = 0, \tag{265}$$
$$c_{HH} = \frac{\Delta w}{\Delta H}(H). \tag{266}$$

Note, that conductivity matrix $\boldsymbol{K}$ is unsymmetric hence unsymmetric matrix storage needs to be used (smtype).

The model parameters are summarized in Tab. 61.

Description	Coupled heat and mass transfer material model
Record Format	**HeMoKunzel** num$_{(in)}$ # d$_{(rn)}$ # iso_type$_{(in)}$ # iso_wh$_{(rn)}$ # mu$_{(rn)}$ # permeability_type$_{(in)}$ # A$_{(rn)}$ # lambda0$_{(rn)}$ # b$_{(rn)}$ # cs$_{(rn)}$ # [pl$_{(rn)}$ #] [rhoH2O$_{(rn)}$ #] [cw$_{(rn)}$ #] [hv$_{(rn)}$ #]
Parameters	-*num* material model number -*d* bulk density of dry building material [kg/m^3] -*iso_type*=0 is isotherm from Hansen needing *iso_n*, *iso_a*, =1 is Kunzel which needs *iso_b* -*iso_wh* maximum adsorbed water content [kg/m^3] -*mu* water vapor diffusion resistance [-] -*permeability_type* =0 is Multilin_h needing *perm_h*, *perm_Dw(h)*, =1 is Multilin_wV needs *perm_wV*, *perm_DwwV*, =2 is Kunzelperm needs A as water absorption coefficient [kg/m/s^0.5] -*lambda0*rn thermal conductivity [W/m/K] -*b* thermal conductivity supplement [-] -*cs* specific heat capacity of the building material [J/kg/K] -[*pl*] ambient air pressure [Pa], default = 101325 -[*rhoH2O*] water density [kg/m3], default = 1000 -[*cw*] specific heat capacity of liquid water, default = 4183 -[*hv*] latent heat of water phase change [J/kg], default = 2.5e+6
Supported modes	_2dHeMo, _3dHeMo

Table 61: Coupled heat and mass transfer material model Kunzel - summary.

2.9 Material for unsaturated flow in lattice models – LatticeTransMat

Lattice transport elements have to be used with this material model. A positive sign is assumed for liquid tension, unlike the convention of soil mechanics which assumes compression positive.

These transport elements are idealised as one-dimensional conductive pipes. The gradient of hydraulic head, which governs flow rate along each transport element, is determined from the capillary pressures P_c at the two nodes.

The mass balance equation describes the change in moisture inside a porous element as a consequence of liquid flow and solid-liquid retention. It leads to the following partial differential equation

$$c\frac{\partial P_c}{\partial t} + k\mathrm{div}(\nabla(\frac{P_c}{g} - \rho z)) = 0 \tag{267}$$

where P_c is the capillary pressure, c is the mass capacity function(s^2m^{-2}), k is the Darcy hydraulic conductivity (ms^{-1}), ρ is the fluid mass density, g is the acceleration of gravity, z is the capillary height and t is the time.

The hydraulic conductivity k consists of

$$k = k_0 + k_c \tag{268}$$

where k_0 is the hydraulic conductivity of the intact material and k_c is the additional conductivity due to cracking.

Darcy hydraulic conductivity k_0 is defined as

$$k_0 = \frac{\rho g}{\mu}\kappa \tag{269}$$

where μ is the dynamic viscosity ($Pa.s$), κ is the permeability also called intrinsic conductivity(m^2), and κ_r is the relative conductivity. κ_r is a function of the effective degree of saturation.

The cracking part is

$$k_c = \xi\frac{\rho g}{\mu}\frac{w_c^3}{12h}\kappa_r \tag{270}$$

where ξ is a tortuosity factor taking into account the roughness of the crack surface, w_c is the equivalent crack opening of the dual mechanical lattice and h is the length of the dual mechanical element.

2.9.1 One-dimensional transport element

The discrete form of the differential equation for mass transport for a one-dimensional transport element is

$$\alpha_e P_c + C_e\frac{\partial P_c}{\partial t} = f_e \tag{271}$$

where P_c is a vector containing the nodal values of the capillary pressure, α_e is the conductivity matrix, C_e is the capacity matrix and f_e is the nodal flow rate vector ($kg.m^3$).

The capacity matrix is

$$C_e = \frac{Al}{12} c \begin{pmatrix} 2 & 1 \\ 1 & 2 \end{pmatrix} \tag{272}$$

where c is the capacity of the material, l is the length of the transport element and A is the cross-sectional area of the transport element.

The conductivity matrix is defined as

$$\alpha_e = \frac{A}{l} \frac{k}{g} \begin{pmatrix} 1 & -1 \\ -1 & 1 \end{pmatrix} \tag{273}$$

2.9.2 Constitutive laws

The mass transport equation is based on the constitutive laws for the capacity c and the hydraulic conductivity k.

The capacity c is defined as

$$c = -\rho \frac{\partial \theta}{\partial P_c} \tag{274}$$

where θ is the volumetric water content ($\theta = \frac{V_w}{V_T}$ with V_w the volume of water, and V_T the total volume) which is calculated by a modified version of van Genuchtens retention model. Note that the presence of a crack in an element does not influence the capacity in the present model.

The volumetric water content is

$$\theta = S_e(\theta_s - \theta_r) + \theta_r \tag{275}$$

where θ_r and θ_s are the residual and saturated water contents corresponding to effective saturation values of $S_e = 0$ and $S_e = 1$, respectively.

The effective degree of saturation S_e is defined as

$$S_e = \begin{cases} \frac{\theta_m - \theta_r}{\theta_s - \theta_r} \left(1 + \left(\frac{P_c}{a}\right)^{\frac{1}{1-m}}\right)^{-m} & \text{if } P_c \geq P_{c(aev)} \\ 1 & \text{if } P_c < P_{c(aev)} \end{cases} \tag{276}$$

where θ_m is an additional model parameter and $P_{c(aev)}$ is the air-entry value of capillary pressure which separates saturated ($P_c < P_{c(aev)}$) from unsaturated states ($P_c \geq P_{c(aev)}$). It is intuitive that the smaller the pore size of the material, the larger the value of $P_{c(aev)}$ will be.

The relative conductivity κ_r is a function of the effective degree of saturation and is defined as

$$\kappa_r = \sqrt{S_e}\left(\frac{1-\left[1-\left(\frac{S_e}{\frac{\theta_m-\theta_r}{\theta_s-\theta_r}}\right)^{\frac{1}{m}}\right]^m}{1-\left[1-\left(\frac{1}{\frac{\theta_m-\theta_r}{\theta_s-\theta_r}}\right)^{\frac{1}{m}}\right]^m}\right)^2 \tag{277}$$

If $\theta_m = \theta_s$, we have $\frac{\theta_m-\theta_r}{\theta_s-\theta_r} = 1$: the equation reduces to the expression of the relative conductivity of the original van Genuchten model.

The model parameters are summarized

Description	Material for fluid transport in lattice models
Record Format	**latticetransmat** num(in) # d(rn) # k(rn) # vis(rn) # contype(in) # thetas(rn) # thetar(rn) # paev(rn) # m(rn) # a(rn) # thetam(rn) # [ctor(rn) #]
Parameters	- *num* material model number - *d* fluid mass density - *k* permeability (m^2) - *vis* dynamic viscosity ($Pa.s$) - *contype* unsaturated flow allowed when contype=1 - *thetas* saturated water content - *thetar* residual water content - *paev* air-entry value of capillary pressure - *m* van Genuchten parameter - *a* van Genuchten parameter - *thetam* additional model parameter for the modified version of van Genuchtens retention model - *ctor* coefficient of tortuosity ($ctor = \frac{1}{\tau} \leq 1$)
Supported modes	2dMassLatticeTransport

Table 62: Material for unsaturated flow in lattice models - summary.

3 Material Models for Fluid Dynamic

3.1 Newtonian fluid - NewtonianFluid

Constitutive model of Newtonian fluid. The model parameters are summarized in Tab. 63.

Description	Newtonian Fluid material
Record Format	**NewtonianFluid** num$_{(in)}$ # d$_{(rn)}$ # mu$_{(rn)}$ #
Parameters	- *num* material model number
	- *d* material density
	- *mu* viscosity
Supported modes	2d, 3d flow

Table 63: Newtonian Fluid material - summary.

3.2 Bingham fluid - BinghamFluid

Constitutive model of Bingham fluid. This is a constitutive model of non-Newtonian type. The model parameters are summarized in Tab. 64.

In the Bingham model the flow is characterized by following constitutive equation

$$\boldsymbol{\tau} = \boldsymbol{\tau}_0 + \mu\dot{\boldsymbol{\gamma}} \quad \text{if } \dot{\tau} \geq \tau_0 \tag{278}$$
$$\dot{\gamma} = \mathbf{0} \quad \text{if } \dot{\tau} \leq \tau_0 \tag{279}$$

where $\boldsymbol{\tau}$ is the shear stress applied to material, $\dot{\tau} = \sqrt{\boldsymbol{\tau} : \boldsymbol{\tau}}$ is the shear stress measure, $\dot{\boldsymbol{\gamma}}$ is the shear rate, $\boldsymbol{\tau}_0$ is the yield stress, and μ is the plastic viscosity. The parameters for the model can be in general determined using two possibilities: (i) stress controlled rheometer, when the stress is applied to material and shear rate is measured, and (ii) shear rate controlled rheometer, where concrete is sheared and stress is measured. However, most of the widely used tests are unsatisfactory in the sense, that they measure only one parameter. These one-factor tests include slump test, penetrating rod test, and Ve-Be test. Recently, some tests providing two parameters on output have been designed (BTRHEOM, IBB, and BML rheometers). Also a refined version of the standard slump test has been developed for estimating yield stress and plastic viscosity. The test is based on measuring the time necessary for the upper surface of the concrete cone in the slump to fall a distance 100 mm. Semi-empirical models are then proposed for estimating yield stress and viscosity based on measured results. The advantage is, that this test does not require any special equipment, provided that the one for the standard version is available.

In order to avoid numerical difficulties caused by the existence of the sharp angle in material model response at $\tau = \tau_0$, the numerical implementation uses following smoothed relation for viscosity

$$\mu = \mu_0 + \frac{\tau_0}{\dot{\gamma}}(1 - e^{-m\dot{\gamma}}) \tag{280}$$

where m is so called stress growth parameter. The higher value of parameter m, the closer approximation of the original constitutive equation (278) is obtained.

Description	Bingham fluid material
Record Format	**BinghamFluid** num$_{(in)}$ # d$_{(rn)}$ # mu0$_{(rn)}$ # tau0$_{(rn)}$ #
Parameters	- *num* material model number - *d* material density - *mu0* viscosity - *tau0* Yield stress
Supported modes	2d, 3d flow

Table 64: Bingham Fluid material - summary.

3.3 Two-fluid material - TwoFluidMat

Material coupling the behaviour of two particulat materials based on rule of mixture. The weighting factor is VOF fraction. The model parameters are summarized in Tab. 65.

Description	Two-Fluid material
Record Format	**TwoFluidMat** num$_{(in)}$ # mat$_{(ia)}$ #
Parameters	- *num* material model number - *mat* integer array containing two numbers representing numbers of material models of which the receiver is composed. Material with index 0 is a material, that is fully active in a cell with VOF=0, material with index 1 is a material fully active in a cell with VOF=1.
Supported modes	2d flow

Table 65: Two-Fluid material - summary.

3.4 FE^2 fluid - FE2FluidMaterial

Constitutive model of multiscale fluids. The macroscale fluid behavior is determined by a Representative Volume Element (RVE) which is solved for in each integration point. Some requirements are put on the RVE, such as the it must use the MixedGradientPressure boundary condition along its outer boundary. This boundary condition is equivalent to that of Dirichlet boundary condition in classical homogenization, only adjusted for a mixed control; deviatoric gradient + pressure, instead of the full gradient only. Worth noting is that the macroscale (and microscale) behavior can still be compressible, in particular is the RVE contains pores. The triangular and tetrahedral Stokes' flow elements both support compressible behavior, but it perhaps be applicable other types of flow, as long as the extended mixed control option is used when calling the material routine (the function with gradient and pressure as input). If the RVE doesn't contain any pores (such that the response turns out to be incompressible) then material should work for all problem classes. This could for example be the case of a oil-water mixture. The model parameters are summarized in Tab. 66.

Description	FE^2 Fluid material
Record Format	**FE2FluidMaterial** num$_{(in)}$ # d$_{(rn)}$ # inputfile$_{(s)}$ #
Parameters	- *num* material model number
	- *d* unused
	- *inputfile* input file for RVE problem
Supported modes	2d, 3d flow

Table 66: FE^2 fluid material - summary.

References

[1] H.D. Baehr and K. Stephan: Heat and Mass Transfer, Springer, 2006.

[2] Z.P. Bažant, L.J. Najjar. Nonlinear water diffusion in nonsaturated concrete. *Materials and Structures*, 5:3–20, 1972.

[3] Z.P. Bažant, J. Planas: Fracture and Size Effect in Concrete and Other Quasibrittle Materials, CRC Press, 1998.

[4] S. Brunauer, J. Skalny, E.E. Bodor: J. Colloid Interface Sci, 30, 1969.

[5] D.P. Bentz: CEMHYD3D: A Three-Dimensional Cement Hydration and Microstructure Development Modeling Package. Version 3.0., NIST Building and Fire Research Laboratory, Gaithersburg, Maryland, Technical report, 2005.

[6] M. Cervera, J. Oliver, and T. Prato: Thermo-chemo-mechanical model for concrete. I: Hydration and aging. *Journal of Engineering Mechanics ASCE*, 125(9):1018–1027, 1999.

[7] D. Gawin, F. Pesavento, and B. A. Schrefler: Hygro-thermo-chemo-mechanical modelling of concrete at early ages and beyond. Part I: Hydration and hygro-thermal phenomena. *International Journal for Numerical Methods in Engineering*, 67(3):299–331, 2006.

[8] P. Grassl and M. Jirásek. Damage-plastic model for concrete failure. *International Journal of Solids and Structures*, 43:7166–7196, 2006.

[9] P. Grassl and M. Jirásek. CDPM2: A damage-plasticity approach to modelling the failure of concrete. *International Journal of Solids and Structures*, 50:3805–3816, 2013.

[10] P. Grassl and M. Jirásek. Meso-scale approach to modelling the fracture process zone of concrete subjected to uniaxial tension. *International Journal of Solids and Structures*, 47: 957–968, 2010.

[11] P. Grassl, D. Xenos, M. Jirásek and M. Horák. Evaluation of nonlocal approaches for modelling fracture near nonconvex boundaries. *International Journal of Solids and Structures*, 51: 3239-3251, 2014.

[12] M. Jirásek, Z.P. Bažant: Inelastic analysis of structures, John Wiley, 2001.

[13] P.F. Hansen: Coupled Moisture/Heat Transport in Cross Sections of Structures, Beton og Konstruktionsinstituttet, 1985.

[14] E. Hoek and Z.T. Bieniawski: Brittle Rock Fracture Propagation In Rock Under Compression, International Journal of Fracture Mechanics 1(3), 137-155, 1965.

[15] H.M. Künzel, H.M.: Simultaneous heat and moisture transport in building components, Ph.D. thesis, IRB-Verlag, 1995.

[16] M. Jirásek: Comments on microplane theory, Mechanics of Quasi-Brittle Materials and Structures, ed. G. Pijaudier-Cabot, Z. Bittnar, and B. Gérard, Hermès Science Publications, Paris, 1999, pp. 57-77.

[17] B. Lourenco, J.G. Rots: Multisurface Interface Model for Analysis of Masonry Structures, Journal of Engng Mech, vol. 123, No. 7, 1997.

[18] M. Ortiz, E.P. Popov: Accuracy and stability of integration algorithms for elasto-plastic constitutive relations, Int. J. Numer. Methods Engrg, 21, 1561-1576, 1985.

[19] B. Patzák: OOFEM home page, http://www.oofem.org, 2003.

[20] J.C. Simo, T.J.R. Hughes: Computational Inelasticity, Springer, 1998.

[21] J. Ruiz, A. Schindler, R. Rasmussen, P. Kim, G. Chang: Concrete temperature modeling and strength prediction using maturity concepts in the FHWA HIPERPAV software, 7th international conference on concrete pavements, Orlando (FL), USA, 2001.

[22] J.C. Simo, J.G. Kennedy, S. Govindjee: Non-smooth multisurface plasticity and viscoplasticity. Loading/unloading conditions and numerical algorithms, Int. J. Numer. Methods Engrg, 26, 2161-2185, 1988.

[23] A. K. Schindler and K. J. Folliard: Heat of Hydration Models for Cementitious Materials, ACI Materials Journal, 102, 24 - 33, 2005.

[24] J.C. Simo, K.S. Pister: Remarks on rate constitutive equations for finite deformation problems: computational implications, Comp Methods in Applied Mech and Engng, 46, 201-215, 1984.

[25] V. Šmilauer and T. Krejčí, Multiscale Model for Temperature Distribution in Hydrating Concrete, International Journal for Multiscale Computational Engineering, 7 (2), 135-151, 2009.

[26] J.H.P. de Vree, W.A.M. Brekelmans, and M.A.J. van Gils: Comparison of nonlocal approaches in continuum damage mechanics. Computers and Structures 55(4), 581588, 1995.

[27] Y. Xi, Z.P. Bažant, H.M. Jennings: Moisture Diffusion in Cementitious Materials, Advn Cem Bas Mat, 1994.

[28] Z.P. Bažant, S. Prasannan: Solidification theory for concrete creep. I: Formulation. Journal of Engineering Mechanics 115(8), 16911703, 1989.

[29] Z.P. Bažant, A.B. Hauggaard, F. Ulm: Microprestress-solidification theory for concrete creep. I: Aging and drying effects. Journal of Engineering Mechanics 123(11), 11881194, 1997.

[30] M. Jirásek, P. Havlásek: Microprestress-Solidification Theory of Concrete Creep: Reformulation and Improvement. Cement and Concrete Research 60, 5162, 2014.

[31] International Federation for Structural Concrete (*fib*): The *fib* Model Code for Concrete Structures 2010.